SYNTHESIS OF DISTILLATION-BASED SEPARATION SYSTEMS

Arthur W. Westerberg and Oliver Wahnschafft*

Department of Chemical Engineering and the Engineering Design Research Center Carnegie Mellon University Pittsburgh, Pennsylvania

*Currently as AspenTech, Cambridge, Massachusetts.

ADVANCES IN CHEMICAL ENGINEERING, VOL. 23

This tutorial paper is a review of recent advances in the synthesis of ideal and nonideal distillation-based separation systems. We start by showing that the space of alternative separation processes is enormous. We discuss simple methods to classify a mixture either as nearly ideal or as nonideal, in which case it displays azeotropic and possibly liquid/liquid behavior.

For nearly ideal mixtures, insights based on marginal vapor flows permit the development of a simple screening criterion computed using only relative volatilities and component feed flowrates to find the better column sequences from among the many possible. This criterion explains several of the traditional heuristics.

We ask how one can invent alternative structures to separate nonideal mixtures. We present and illustrate an approach with three examples: separating n*-butanol and water; separating acetone, chloroform, and benzene; and separating* n*-pentane, acetone, methanol, and water. We find that these processes always contain recycles because we are unable to obtain the sharp separations possible for ideal mixtures.*

Next, we explore more advanced methods to assess the behavior of complex mixtures. We discuss two algorithms to find all azeotropes for a mixture; we also discuss the problem of finding the regions for liquid/liquid behavior.

Example problems are included to highlight the need to estimate the entire set of products that can be reached for a given feed when using a particular type of separation unit. We show that readily computed distillation curves and pinch point curves allow us to identify the entire reachable region for simple and extractive distillation for ternary mixtures. This analysis proves that finite reflux often permits increased separation; we can compute exactly how far we can cross so-called "distillation boundaries." For extractive distillation, we illustrate how to find minimum solvent rates, minimum reflux ratios, and, interestingly, maximum reflux ratios.

I. Introduction

The goal of this paper is to discuss a methodology for the *preliminary design* of separation processes for liquid mixtures using distillation- and extraction-based technologies. We define the preliminary design step to be the one in which we *discover* the alternative overall system structures that might be reasonable for solving the problem. Choosing which alternative to use among those pro-

posed in this step and adjusting the operating conditions to their best values is a follow-up step not covered by the preliminary design step; it will not be covered here to any significant extent. If the vapor/liquid equilibrium behavior of the species is reasonably ideal, we shall, however, present a simple method to screen among the distillation-based alternatives to find the likely better ones. The selection of the better sequences for relatively ideal mixtures is the subject of several past reviews (Westerberg, 1980, 1985; Nishida *et al.,* 1981; Hlavacek, 1978; Hendry *et al.,* 1973).

We use the word "discover" in the previous paragraph very carefully. In artificial intelligence the discovery step is the one in which we identify the building blocks we have to use when solving a problem. For well behaved mixtures, discovery is simple: we can quickly sketch likely alternatives built from such building blocks. It is the search among those alternatives—of which there can be a large number—that is the problem. Often, especially when the species display azeotropic behavior, the problem is to discover which types of separation steps can be used—a process that requires us to conjecture a method and then to carry out significant computer calculations (e.g., column or flash unit simulations) to find if the conjectured method is useful. Proposing any solution for these harder problems, much less enumerating a number of alternatives, is a difficult task.

The following illustrates the type of problem we would like to be able to solve:

Design a separation process to split a (liquid) mixture of 25% methanol, 40% water, and 35% ethanol into the three relatively pure products of methanol, water, and ethanol.

This particular problem is not a simple one to solve because water and ethanol form an azeotrope. In this paper, we concentrate first on selecting the better alternative processes for ideal (or near ideal) mixtures, and then we present a prototypical method for generating alternatives for nonideal mixtures such as the one above.

Distillation processes are large consumers of hot and cold utilities. It is often useful to consider their heat integration (Rathore *et al.,* 1974; Andrecovich and Westerberg, 1985) where the heat expelled from one column supplies part or all of the heat needed by another. While important, we shall not consider such issues here.

This paper assumes the reader is familiar with the standard textbook presentation for staged processes such as that in McCabe and Smith (1976). More extensive texts on distillation include King (1980), Henley and Seader (1981), and Holland (1981). We shall build on the standard background to develop needed insights for designing separation systems and to understand less conventional single-unit configurations which are often a part of such designs.

II. The Richness of the Solution Space

As a first step in design, we must be aware that many more alternatives may be available for solving a problem than at first seem likely (Westerberg, 1985), even for well-behaved mixtures. To confirm this statement, we show that many alternative structures are available first for a single distillation step and then for a system of steps. The intent of this section is simply to expand our thinking about this problem.

We start by sketching a simple two-product distillation column, as shown in Fig. 1. This column is the unit operation most likely to be considered as a building block for these problems. The two-product distillation column splits its feed into two essentially disjoint product sets. The distillate contains species A, B, and C (plus, of course, a small amount of D and generally only traces of the other species) while the bottom product contains predominantly D and E. Heat is injected at the bottom into the reboiler, the hottest point in the column, and removed from the condenser at the top, the coldest point in the column. Liquid flows downward against a flow of vapor upward, with the more volatile species enriching as one moves up the column.

Typically, we put a specification onto such a column of the following form: recover 99.8% of the species C in the distillate while recovering 99% of species D in the bottoms. From a practical point of view, then, the *light* and *heavy keys* for this split are C and D, respectively. In this case, 0.2% of C will make it to the bottom product and will be the lightest species to make it to the bottom in more than trace amounts. Similarly, 1% of D will make it to the top along with at most a trace of E.

Columns can be run differently from the one shown above. For example, we may remove heat from or add it to trays within a column. We can add heat by removing part of the liquid from a tray, vaporizing it, and returning the vapor

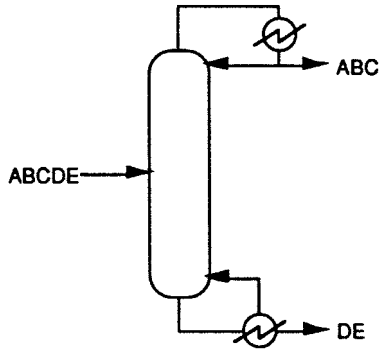

FIG. 1. A simple two-product column.

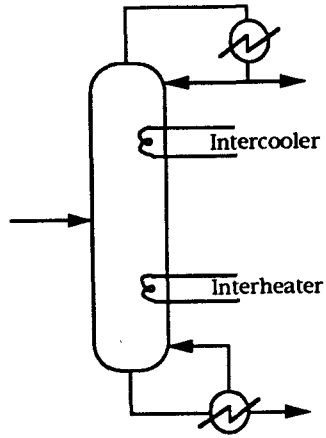

FIG. 2. Columns with interheating and/or intercooling.

just below the tray from which it was removed; or we can remove heat by withdrawing some vapor, condensing it, and placing it back into the column. Such a configuration is called an intercooled and/or interheated column, as shown in Fig. 2. When there are three or more species in the feed, we can alter the set of product compositions a column can produce by using interheating or intercooling, as we shall note later.

Another commonly used configuration is a column with a side enricher or a side stripper. As illustrated in Fig. 3, the column with a side stripper can separate

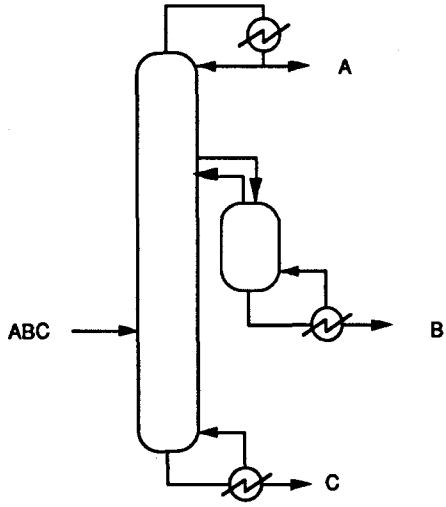

FIG. 3. Column with a side stripper.

three species, each to a desired purity. This column has one condenser and two reboilers. At first glance, it looks as if it is the equivalent of one and one-half columns; but it is really more like two.

We next consider separating a mixture of ethane, propane, *n*-butane, and *n*-pentane. Two evident alternative solutions are shown in Fig. 4. Three more, equally "evident" solutions exist, as well as many more less obvious solutions. There is, however, a problem with these two (and the remaining three) sequences. The top of the column in which ethane is a product is very cold. The column is pressurized to elevate its temperature, but, even so, it cannot be brought up to anywhere near ambient temperatures. Thus, we will have to cool the condenser using refrigeration, which is very expensive.

Is there any way we might reduce the amount of refrigeration required for the sequence on the left of Fig. 4? One possibility is to recycle some of the *n*-pentane produced back to the top of the first column, thus providing part or all of the liquid required for reflux instead of condensing ethane. The normal boiling point for *n*-pentane is about 310 K, which means it can be liquefied easily at ambient temperatures and very slightly elevated pressures. Running the column at several atmospheres pressure can reduce but cannot eliminate the loss of *n*-pentane with the ethane. If this loss cannot be allowed, we can add a few trays above where *n*-pentane is fed into the column and use a much reduced amount of ethane as reflux, significantly reducing rather than eliminating the need for refrigeration. Economics will, of course, indicate whether such designs are a good idea.

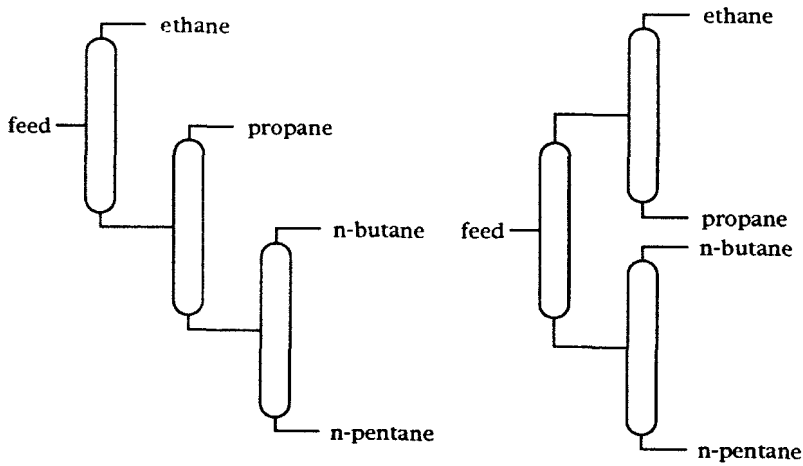

FIG. 4. Two alternative separation sequences for separating a mixture of four species.

III. Assessing the Behavior of a Mixture

It does little good to assume ideal vapor/liquid equilibrium behavior for a mixture that is highly nonideal. The design proposed assuming ideal behavior has little to do with the design actually required. There is, in fact, no reason even to assume it represents a lower cost bound. For example, suppose we wish to separate water from toluene. Assuming ideal behavior would lead us to design a distillation column. But in fact, toluene and water "hate" each other, and can be separated by using a simple decanter. Therefore, the first step in designing a separation process is often to assess the vapor/liquid/liquid equilibrium behavior of the species to be separated. We start with an approach that is useful for this activity, given today's plethora of excellent computer-based physical-properties packages. Having experimental data is the only assured way to know the behavior, and many such data are currently available. Horsley (1973), for example, has compiled a listing of known azeotropes.

Assume we can have a reliable flash computation available to us and that the physical property options to be used for the species can be reasonably selected (a step for which help from an expert consultant within the company may be necessary). Then the following is a first step we can use to discover if the mixture displays highly nonideal behavior.

A. Azeotropic Behavior: Infinite-Dilution *K*-Values

We will examine a quick method based on performing two flash computations to determine the existence of azeotropic behavior for binary mixtures. The hydrogen-bonding classes for the species in a mixture are also a clue that the mixture might exhibit liquid/liquid behavior. Indeed, we have used these classes to find mixtures that display nonideal behavior as illustrative examples.

1. Infinite-Dilution K-Values

We can predict azeotropic behavior as follows from infinite-dilution *K*-values. Using a flowsheeting system, we perform a bubble-point calculation for each species in the mixture. Assuming a mixture contains the species A, B, C, and D, we wish to compute the infinite-dilution *K*-values for three of the species in the remaining one. For example, we perform a flash calculation where A is dominant and B, C, and D are in trace amounts, using something like a feed composition of 0.99999, 0.000003333, 0.000003333, 0.000003334. It does not

matter what type of flash computations we do: bubble point, dew point, or a 50/50 split. We do these at the pressure intended for the separation device to be considered and repeat for all species. Then from each we tabulate the K-values for the trace species. The K-value for the abundant species is always unity at infinite dilution. The ratio of the vapor composition to the liquid composition for each of the trace species gives its infinite-dilution K-value. As we shall discuss later when considering liquid/liquid behavior, these same flash computations should also allow us to retrieve infinite-dilution activity coefficients.

Given infinite-dilution K-values, we want next to examine each species pair where one is plentiful and the other is in trace amount. As an example, Fig. 5 shows how K-values vary for a binary mixture of acetone and chloroform versus composition. We see that the K-value for a drop of chloroform (far left) is less than unity. The vapor composition y_C is less than that for the liquid, x_C. The K-value for a drop of acetone in chloroform is also less than unity. The mixture displays a maximum-boiling azeotrope.

An interpretation of these K-values is as follows:

$$\text{For} \quad K_{12}^{\infty} = \left.\frac{y_1}{x_1}\right]_{1 \text{ in } 2}; \qquad K_{21}^{\infty} = \left.\frac{y_2}{x_2}\right]_{2 \text{ in } 1}$$

$$\text{Maximum-boiling azeotrope:} \quad K_{12}^{\infty} < 1 \wedge K_{21}^{\infty} < 1$$

$$\text{Minimum-boiling azeotrope:} \quad K_{12}^{\infty} > 1 \wedge K_{21}^{\infty} > 1$$

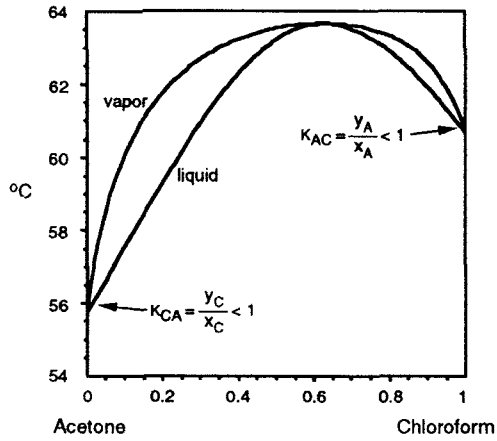

FIG. 5. Liquid and vapor mole fractions vs T at equilibrium for acetone and chloroform. Pressure is 1 atm.

Example. Table I (each row comes from one of the above flash computations) lists infinite-dilution K-values that were computed for a mixture of acetone, chloroform, and benzene. The infinite-dilution K-value for acetone in chloroform is 0.6 and for chloroform in acetone is 0.4. Both are less than 1; a maximum-boiling azeotrope must exist. For chloroform and benzene, the values are 1.5 and 0.4. These values do not suggest the existence of an azeotrope. We assume normal behavior. A similar conclusion is obtained for acetone and benzene where the K-values are 3.0 and 0.7, respectively.

2. *Hydrogen-Bonding Guidelines*

Berg (1969), in a paper on selecting agents for extractive distillation, classifies species into hydrogen-bonding classes. The deviation from ideality is then predicted depending on the classes represented in the mixture. Quoting from Berg, the classes are as follows:

> **Class I:** Liquids capable of forming 3-dimensional networks of strong hydrogen bonds—e.g., water, glycol, glycerol, amino alcohols, hydroxylamine, hydroxyacids, polyphenols, amides, etc.
>
> **Class II:** Other liquids composed of molecules containing both active hydrogen atoms and donor atoms (oxygen, nitrogen, and fluorine)—e.g., alcohols, acids, phenols, primary and secondary amines, oximes, nitro compounds with alpha-hydrogen atoms, nitriles with alpha hydrogen atoms, ammonia, hydrazine, HF, HCN (plus nitromethane, acetonitrile even though these form 3-dimensional networks; they have weaker bonds than —OH and —NH bonds in class I)
>
> **Class III:** Liquids composed of molecules containing donor atoms but no active hydrogen atoms—e.g., ethers, ketones, aldehydes, esters, tertiary amines (including pyridine type), nitro compounds and nitriles without alpha-hydrogen atoms
>
> **Class IV:** Liquids composed of molecules containing active hydrogen atoms but no donor atoms—e.g., chlorinated hydrocarbons with two or three chlorines per carbon ($CHCl_3$, CH_2Cl_2, CH_3CHCl_2, $CH_2Cl—CH_2Cl$, $CH_2Cl—CHCl—CH_2Cl$, $CH_2Cl—CHCl_2$)

TABLE I
INFINITE-DILUTION K-VALUES FOR MIXTURE

		K^∞		
		Acetone	Chloroform	Benzene
In:	Acetone	1.0	0.4 (max)	0.7 (normal)
	Chloroform	0.6	1.0	0.4 (normal)
	Benzene	3.0	1.5.	1.0

Class V: All other liquids—i.e., liquids having no hydrogen-bonding capabilities—e.g., hydrocarbons, CS_2, sulfides, mercaptans, halohydrocarbons not in class IV, nonmetallic elements such as iodine, phosphorus, sulfur.

Quoting again, their expected deviation from Raoult's Law are shown in Table II.

We can consider our example again. The classes for these species are as follows:

Acetone:	class III
Benzene:	class V
Chloroform:	class IV

The binary-pair behaviors suggested by this article are as follows:

Acetone, benzene	III+V	d: Quasi-ideal
Acetone, chloroform	III+IV	b: Always − behavior
Chloroform, benzene	IV+V	d: Quasi-ideal

As before, we see that the problem in this mixture is the acetone, chloroform pair. As we have already seen, they have a maximum boiling azeotrope.

TABLE II
EXPECTED DEVIATIONS FROM RAOLT'S LAW
(FROM BERG, 1969)

	I	II	III	IV	V
I	c	c	c	a	a
II	—	c	c	a	a
III	—	—	d	b	d
IV	—	—	—	d	d
V	—	—	—	—	d

a. Always + deviations, frequently limited solubility (min boiling azeotropes if any). Hydrogen bonds broken only.
b. Always − deviations (tendency for max boiling azeotropes). Hydrogren bonds formed only.
c. Usually + deviations; some very complicated situations. Some will give maximum azeotropes (from negative deviations). Hydrogen bonds both formed and broken, but dissocation of class I or II liquid is more important effect.
d. Quasi-ideal systems, always + deviations or ideal. Minimum azeotropes only if any. No hydrogen bonds involved.

B. Liquid/Liquid Behavior: Infinite-Dilution Activity Coefficients

Mixtures may also form two or more liquid phases at equilibrium. For example, a 50/50 mol% liquid mixture of toluene in water will partition into a water-rich liquid phase and a toluene-rich liquid phase. We just used infinite-dilution K-values as a means to predict azeotropic behavior. We can argue that we should use infinite-dilution liquid activity coefficients to alert us to the potential for liquid/liquid behavior. We do so as follows.

For a liquid mixture at constant temperature and pressure, an equilibrium state is one that minimizes the total Gibbs free energy for the system (Smith and Van Ness, 1987). Figure 6 shows a plot of the total Gibbs free energy of a binary mixture where we form the total from three terms: one that mole-fraction averages the Gibbs free energy for the two pure species, one that computes the ideal Gibbs free energy of mixing, and one that estimates the excess Gibbs free energy. We can model this last term by using an empirical relationship such as the Margules equation. We have rescaled the ordinate for this plot by dividing all terms by RT, where R is the universal gas constant and T is the absolute temperature.

Suppose the rescaled Gibbs free energy, G_1/RT, for species 1 (left side Fig. 6) is 0 while for pure species 2 it is 0.5. Then, if the Gibbs free energy simply mixed with no effect of mixing nor any effect from nonidealities, the line joining 0 on the right to 0.5 on the left would give us the mixture Gibbs free energy:

$$\frac{G_{\text{avg}}}{RT} = x_1\frac{G_1}{RT} + x_2\frac{G_2}{RT} \qquad \text{where} \quad x_1 + x_2 = 1$$

However, even for an ideal mixture, there is an effect on the Gibbs free energy from the entropy of mixing, namely,

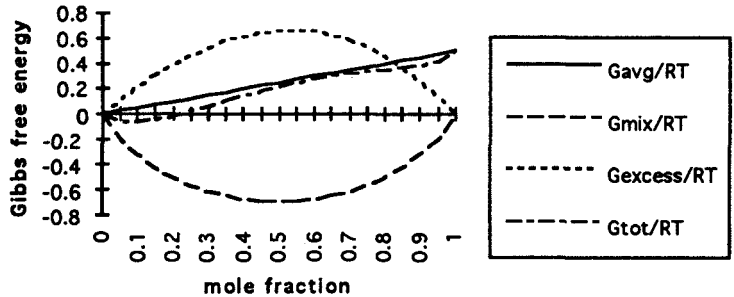

FIG. 6. Gibbs free energy for binary mixture.

$$\frac{G_{\text{mix}}}{RT} = x_1 \ln x_1 + x_2 \ln x_2$$

Note it always has this exact shape—that of an upward-opening "convex" curve that passes through zero at 0 and 1. If the mixture were ideal, this curve plus that averaging the pure species Gibbs free energies would assume this upward-opening convex shape.

The following Margules equation is one form in which we can approximately represent nonideal behavior, allowing us to estimate the excess Gibbs free energy as a function of composition:

$$\frac{G_{\text{excess}}}{RT} = x_1 x_2 (A_{21} x_1 + A_{12} x_2)$$

We would find, when taking compositions to their limiting values, that

$$A_{21} = \ln(\gamma_1^{\infty}); \qquad A_{12} = \ln(\gamma_2^{\infty})$$

where A_{12} and A_{21} are constants for this equation and γ_i^{∞} is the infinite-dilution activity coefficient of species i in the other species. This curve can assume all sorts of shapes as it is cubic in mole fraction. It too must be zero at both ends.

With a downward-opening *concave* shape as illustrated here, it starts by canceling only a part of the effect of ideal mixing; then it more than cancels this effect and takes over in making the G_{tot}/RT curve switch from convex-upward to concave-downward. It is this switch in shape that indicates liquid/liquid behavior. The mixing term approaches its endpoints with an infinite slope so the G_{tot}/RT curve always starts out in the downward direction, no matter what model we use to estimate the nonideal behavior.

If our total curve switches to a concave-downward appearance anywhere along it, as it does here between approximately 10% and 90% B in A, any mixture with compositions between these two points will break into two liquid phases at equilibrium. Suppose we compute the total Gibbs free energy for a 50/50 mixture on the G_{tot}/RT curve. We can get a lower total Gibbs free energy by breaking the mixture into two mixtures, one at approximately 10% and the other at approximately 90%. Their total Gibbs free energy is along a straight line connecting their individual Gibbs free energies. The lowest possible value would be along a support line that just touches the total curve from below. The value on this line is below that predicted for the mixture; thus the system can reduce its total Gibbs free energy by breaking into these two phases.

By carrying out numerical studies, we find that the Margules equation predicts the onset of liquid/liquid behavior if either of the following is (approximately) true:

- if either $\gamma_{1 \text{ in } 2}^{\infty}$ or $\gamma_{2 \text{ in } 1}^{\infty}$ is greater than 9;
- for $\gamma_{j \text{ in } k}^{\infty} > \gamma_{k \text{ in } j}^{\infty}$, if $\gamma_{j \text{ in } k}^{\infty} > 9(\gamma_{k \text{ in } j}^{\infty})^{1/3}$.

For example, if $\gamma^{\infty}_{1 \text{ in } 2}$ is 0.001, then we need to worry about liquid/liquid behavior if $\gamma^{\infty}_{2 \text{ in } 1}$ is greater than about $9(0.001)^{1/3} = 0.9$.

We can propose to use this guideline to alert us to the potential for liquid/liquid behavior. For example, we might consider the need to check more thoroughly for liquid/liquid behavior if we replace the 9 by a 6 and either of these test passes.

We used infinite-dilution activity coefficients of 10 and 20 to create Fig. 6. Both are greater than 9, so we should expect the Margules equations to predict liquid/liquid behavior. Water and toluene have infinite-dilution activity coefficients in the thousands. They really dislike each other and break into relatively pure phases. If we examine the total Gibbs free energy curve, we gain the impression that the curve is totally convex-upward; however, there is a slight downward move at the extremes because of the infinite downward slope of the mixing term at the extreme compositions. The two liquid phases are almost, but not quite pure.

1. Relating Infinite-Dilution K-Values and Activity Coefficients

If we have evaluated infinite-dilution K-values to test for the existence of azeotropes, we can use those numbers to get a quick estimate of the corresponding activity coefficients by noting that

$$\gamma^{\infty}_{i \text{ in } j} = \frac{\phi_i P}{f_i^0} K^{\infty}_{i \text{ in } j} \approx \frac{P_j^{\text{sat}}(T)}{P_i^{\text{sat}}(T)} K^{\infty}_{i \text{ in } j}$$

If the mixture is at 1 atm, T is the normal boiling point for the plentiful species j.

IV. Separating Nearly Ideal Systems

A. Analysis

Here, we review some techniques that are useful for analyzing nearly ideally behaving distillation columns—i.e., for predicting how these columns might perform, given certain specifications. The first topic will be minimum reflux calculations so we can determine the required internal flowrates in a column. However, to really understand this topic, we should first examine the concept of a *pinch point* in a column. Using our understanding of a pinch point on a McCabe–Thiele diagram, we shall see that a pinch point occurs when the compositions passing each other between two trays (thus satisfying the operating line equations) are also in equilibrium with each other (King, 1980).

1. Pinch

We follow the development in Terranova and Westerberg (1989) to explain a pinch point. The material balance and equilibrium relationships for the top section of a column are as shown in Fig. 7.

The species material balance is

$$Vy_i = Lx_i + Dx_{D,i}$$

We can express equilibrium as follows:

$$y_i = K_i x_i \equiv \frac{\alpha_{ik}}{\sum_j \alpha_{jk} x_j} x_i = \frac{\alpha_{ik}}{\bar{\alpha}_k} x_i$$

where α_{ik} is the *relative volatility* of species i relative to an arbitrarily selected key species k—e.g., the heaviest species in the mixture or the most plentiful (or the lightest, etc.). Note that

$$\bar{\alpha}_k \equiv \sum_j \alpha_{jk} x_j$$

is a *mole-fraction–averaged relative volatility*. It will lie somewhere between the largest and the smallest relative volatility for the mixture.

Using Raoult's law

$$y_i = K_i x_i \approx \frac{P_i^{\text{sat}}(T)}{P} x_i$$

we can estimate relative volatility as

$$\alpha_{ik} \equiv \frac{K_i}{K_k} \approx \frac{P_i^{\text{sat}}(T)/P}{P_k^{\text{sat}}(T)/P} = \frac{P_i^{\text{sat}}(T)}{P_k^{\text{sat}}(T)}$$

The ratio of K-values is an exact definition for relative volatility. The ratio of vapor pressures is an approximate one that assumes Raoult's law holds, thereby assuming that the K-values are not composition-dependent. *The advan-*

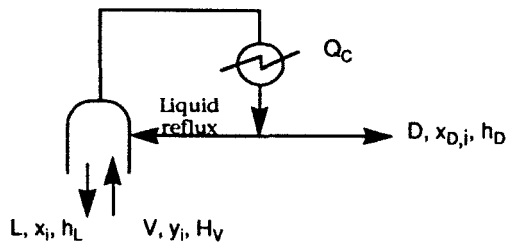

FIG. 7. Top section of a column showing flows and compositions.

tage to relative volatilities are that they are much less temperature- and pressure-sensitive than are K-values.

A pinch point occurs when the vapor and liquid compositions for the operating relationships are also in equilibrium with each other. For such a situation, the operating point of streams flowing against each other between stages is also on the equilibrium surface for the problem. To step through a pinch point requires an infinite number of stages. Substituting equilibrium into the species material balance equation for species i, we get

$$\left(\frac{\alpha_{ik}V}{\overline{\alpha}_k} - L\right)x_i = Dx_{D,i}$$

which, when solved for x_i, gives

$$x_i = \frac{Dx_{D,i}}{\dfrac{\alpha_{ik}V}{\overline{\alpha}_k} - L}$$

We multiply both sides by the relative volatility α_{ik} and sum over all species to get

$$\sum_i \alpha_{ik}x_i = \overline{\alpha}_k = \sum_i \frac{Dx_{D,i}}{\dfrac{\alpha_{ik}V}{\overline{\alpha}_k} - L}$$

If we are given

- all the relative volatilities,
- the mole fractions and total flow for the distillate product, and
- the vapor and liquid flows in the column at the pinch point (i.e., the reflux ratio defined at the pinch point),

this equation is a single equation in the one unknown $\overline{\alpha}_k$. It has to be solved numerically, using something like Newton's method. Once we have $\overline{\alpha}_k$, we can use the previous equation to solve for each of the mole fractions x_i at the pinch point.

If the relative volatilities are composition-, temperature-, and pressure-dependent, we can use this composition as input to a bubble point computation. When solved, we will have new estimates for the relative volatilities. Then we can iterate the computation until all the numbers are consistent.

We can also compute the condenser duty with a heat balance around this part of the column:

$$Q_C = H_V V - (h_L L + h_D D),$$

where H_V, h_L, and h_D are molar enthalpies for the given mixtures and Q_C is the condenser heat duty. Note that there is nothing approximate about this computation. We can compute the molar enthalpies given the temperature, pressure, and stream composition using a rigorous physical property package and obtain as accurate a number as the property computations allow.

2. *Underwood's Method*

It is possible to derive—roughly—the equations underlying the Underwood method (Underwood, 1946) from the above. The variable R represents the reflux ratio defined in terms of the liquid flow *at the pinch point* relative to the distillate top product flow; i.e.,

$$R \equiv L/D.$$

We again write the equation giving x_i at the pinch point, and then do some rearrangements and variable transformations.

$$x_i = \frac{x_{D,i}D}{\frac{\alpha_{ik}V}{\bar{\alpha}_k} - L} = \frac{x_{D,i}}{\frac{\alpha_{ik}V/D}{\bar{\alpha}_k} - \frac{L}{D}} = \frac{x_{D,i}}{\frac{\alpha_{ik}(R_{\min}+1)}{\bar{\alpha}_k} - R_{\min}}$$

$$= \frac{\frac{1}{R_{\min}}\frac{R_{\min}\bar{\alpha}_k}{R_{\min}+1}x_{D,i}}{\alpha_{ik} - \frac{R_{\min}\bar{\alpha}_k}{R_{\min}+1}} = \frac{\frac{1}{R_{\min}}\phi x_{D,i}}{\alpha_{ik} - \phi}$$

Summing over all species, we get

$$R_{\min} = \sum_i \frac{\phi x_{D,i}}{\alpha_{ik} - \phi}$$

Adding $1 = \sum_i x_{D,i}$ to both sides gives

$$R_{\min} + 1 = \sum_i \frac{\phi + \alpha_{ik} - \phi}{\alpha_{ik} - \phi} x_{D,i} = \sum_i \frac{\alpha_{ik}}{\alpha_{ik} - \phi} x_{D,i}$$

Finally, multiplying both sides by D gives the form

$$(R_{\min} + 1)D = \sum_i \frac{\alpha_{ik}}{\alpha_{ik} - \phi} x_{D,i}D = \sum_i \frac{\alpha_{ik}}{\alpha_{ik} - \phi} d_i = V_{\min} \qquad (1)$$

which is one of the familiar equations from the Underwood method. A similar relationship exists for the bottom of the column (note the minus sign):

$$\bar{R}_{\min}B = -\sum_i \frac{\alpha_{ik}}{\alpha_{ik} - \phi} x_{B,i}B = -\sum_i \frac{\alpha_{ik}}{\alpha_{ik} - \phi} b_i = \bar{V}_{\min} \tag{2}$$

We can now write a relationship between the vapor flows in the top and bottom of the column:

$$V = \bar{V} + (1 - q)F$$

Then assuming the roots ϕ for the top and the bottom are both the same and using this equation, we derive the remaining Underwood equation:

$$\sum_i \frac{\alpha_{ik}}{\alpha_{ik} - \phi} d_i + \sum_i \frac{\alpha_{ik}}{\alpha_{ik} - \phi} b_i = \sum_i \frac{\alpha_{ik}}{\alpha_{ik} - \phi} f_i = (1 - q)F \tag{3}$$

The assumption that the ϕ values are the same is quite an assumption. It takes a good deal of arguing to make that plausible. We shall not go into that here, however.

Use of Underwood's Method. Table III presents an example that illustrates a computation we might do to compute the minimum reflux flows for a column. In this example, species C distributes between the top and bottom product in the column. Underwood's method permits us to compute how it distributes. The approach for using Underwood's equations to compute minimum reflux is as follows:

- Write Eq. (3) for each of the roots ϕ lying between the species that appear in both the top and bottom products—here B, C, and D. So we write it twice. There will be a root between α_{BE} and α_{CE} and between α_{CE} and α_{DE}. Call them ϕ_{BC} and ϕ_{CD} (for the relative volatilities, E is arbitrarily selected to be the key species).

TABLE III
PROBLEM FOR ILLUSTRATING UNDERWOOD'S METHOD

Species	Relative volatility	Feed (kmol/s)	Top product (kmol/s)
A	4	1	1
B (*lk*)	3	1	0.98
C	2	1	?
D (*hk*)	1.5	1	0.03
E	1	1	0

$$\frac{4 \cdot 1}{4 - \phi_{BC}} + \frac{3 \cdot 1}{3 - \phi_{BC}} + \frac{2 \cdot 1}{2 - \phi_{BC}} + \frac{1.5 \cdot 1}{1.5 - \phi_{BC}} + \frac{1 \cdot 1}{1 - \phi_{BC}} = (1 - 1)4 = 0$$

$$\frac{4 \cdot 1}{4 - \phi_{CD}} + \frac{3 \cdot 1}{3 - \phi_{CD}} + \frac{2 \cdot 1}{2 - \phi_{CD}} + \frac{1.5 \cdot 1}{1.5 - \phi_{CD}} + \frac{1 \cdot 1}{1 - \phi_{CD}} = (1 - 1)4 = 0$$

which gives $\phi_{BC} = 1.673825$ and $\phi_{CD} = 2.395209$.

- Write Eq. (1) twice, one for each root, and solve these two equations for the two unknowns d_C ($=x_{D,C}D$) and R_{min}. (Solved for these two variables, the equations will be linear.) Once d_C is known, D can be computed and then the mole fractions for the top product:

$$\frac{4 \cdot 1}{4 - 1.673825} + \frac{3 \cdot 0.98}{3 - 1.673825} + \frac{2d_C}{2 - 1.673825} + \frac{1.5 \cdot 0.03}{1.5 - 1.673825} + \frac{1 \cdot 0}{1 - 1.673825} = V_{min}$$

which gives $V_{min} = 5.664$ kmol/s and $d_C = 0.324$ kmol/s.

B. System Synthesis for Nearly Ideal Systems

We shall present our ideas in this section by example. Consider the following separations problem, for which the species should all behave relatively ideally when in a mixture.

1. Example: Separation of Five Alcohols

Table IV gives the species flows for a five-species alcohol mixture. Design a system of distillation columns to separate them.

TABLE IV
Five-Alcohol Separation

Species i	$f(i)$ (kmol/h)
Isobutanol	5
1-pentanol	10
1-hexanol	20
1-heptanol	50
1-octanol	15

We first need to assess how many different sequences we might actually invent for this problem. Using only simple columns, we can construct the alternative sequences shown in Fig. 8, where each column does a fairly sharp split between adjacent key species. As we can see, there are 14 sequences. The third sequence has two binary separations at the end for it in this "tree" of alternatives. Note that both are required, so only one sequence results in the counting.

Thompson and King (1972) developed a formula for predicting the number of simple sequences for such a problem:

$$\text{No. Seq.} = \frac{[2(N-1)]!}{[N-1]!N!} = \frac{[2(5-1)]!}{[5-1]!5!} = \frac{8!}{4!5!} = 14$$

where N is the number of species in the original mixture. We note that for a problem where the vapor/liquid equilibrium behavior of the species is relatively ideal, discovery of the alternative simple sequences is straightforward. The number of sequences grows to over 290,000 for a ten-species mixture. Separating a ten-species mixture into ten relatively pure single species products is a rather large separation problem. However, if the analysis is simple, this number of alternative sequences is not too large a problem to be investigated using a computer. We would want to do it efficiently, none the less.

2. *Separation Selection Using Marginal Costs*

In this section we present a very simple method based on marginal cost (Modi and Westerberg, 1992) to compare the different sequences. As it is a very ap-

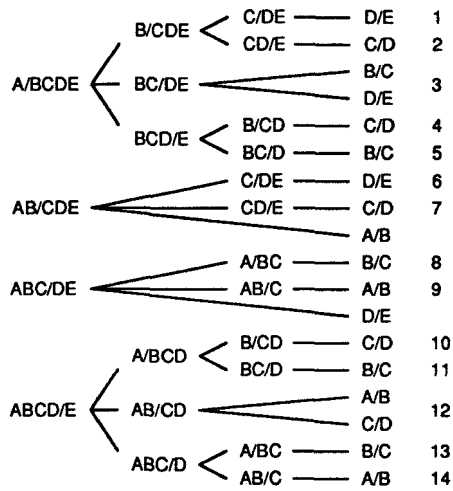

FIG. 8. All 14 "simple" separation sequences for separating a mixture of five species.

proximate method, it should be used only to remove sequences from consideration, leaving one with a (hopefully) much reduced set to investigate with more accurate methods.

We start by noting two heuristics presented a number of years ago by Hendry *et al.* (1973) that we should consider before proceeding very far into the selection of the sequences.

Dangerous Species Heuristic: *Remove dangerous and corrosive species early.*

We would wish to handle dangerous (deadly if released, toxic, carcinogenic, explosive) and corrosive species in as few pieces of equipment as possible. (Best of all, avoid handling them completely by not designing a process with such species present.) They should be removed first. If such a species is either the most or the least volatile, then we can remove it in the first column. Otherwise, it will take at least two columns (a split just above and a split just below—in either order) to remove it.

Final Product Heuristic: *Produce final products as distillate products, not as bottoms products.*

All mixtures will contain contaminants, such as heavy organics, which tend to discolor the yield if they are removed from the process with final products. That is, heavy species will exit a column with the bottoms product, contaminating it. Customers will pay more for a cleaner looking product (even when it really may not matter). However, this heuristic should not be followed blindly. Many times it is not cost-effective to follow this heuristic; at other times it may be impossible to abide by it—for example, when the heaviest species is the product to be sold. Moreover, it is possible to clean up a product in other ways: e.g., by vaporizing and then condensing the material, leaving the contaminant as a heavy residual, or by passing the product through a bed of activated carbon.

Assuming we have considered these two heuristics, we need to select among the many alternative sequences that may remain for a problem. One criterion is to select the one with the lowest annual cost in units like $/year (£/year, DM/year, etc.). Annual cost is the total of the costs per year to operate the plant and the annualized cost of the investment required to build the plant. Investments are measured in dollars. Annualizing investments means that we convert an investment cost in dollars ($) into an equivalent expense in dollars per year ($/yr).

A very simple method for annualization is to divide investment cost by the number of years over which the company wants that investment paid back by the earnings of the process; e.g., we divide by 3 years if we want the investment back in three years. Many other ways exist, such as establishing a set of equal

yearly payments over a specified lifetime of the process, say 15 years, that would have the same present value as the investment. Present value requires us to set an acceptable interest rate over the inflation rate, say 10–15% per year.

We propose finding the sequence with lowest costs by using *marginal costs.* We compute marginal costs by devising a base cost that all sequences have as a minimum, then estimating only the added costs that distinguish one sequence from another. One appealing base cost is the cost to carry out all the needed separations—such as A/B, B/C, C/D, and D/E for our earlier example—as if they were done with no other species present. Then the *incremental cost* of a task is the cost to carry out those separations with the other species present, a cost that differs from sequence to sequence. For nonideal systems, the cost may actually go down when other species are present. However, for ideal systems, the costs increase.

Returning to our previous five-species example, the sequence {A/BCDE, B/CDE, C/DE, D/E} differs from the sequence {AB/CDE, A/B, CD/E, C/D} as shown in Table V. The entries in the second and third columns indicate the extra species present for each binary separation when accomplished using these two different sequences. The binary separation B/C is done with species D and E present in the first sequence, while it is done with species A, D, and E for the second.

The particular *cost-related* quantity we shall consider here is the *marginal vapor flow* rather than the actual annual cost. It is a quantity we can more readily estimate. In fact, for nearly ideal systems, we shall show a very easy way to approximate it.

We define the symbol

$\Delta V(i/j,\text{list})$ = Marginal vapor flow for column having i and j as light and heavy key species, respectively. The list contains species other than i and j which are present in the feed.

For example, ΔV(B/C,ADE) is for the task AB/CDE: This column is splitting B from C, and the other species present are A, D, and E.

TABLE V
EXTRA SPECIES AS A FUNCTION OF THE COLUMN SEQUENCE USED

Binary Separation	Sequence 1	Sequence 2
A/B	CDE	none
B/C	DE	ADE
C/D	E	none
D/E	none	C

Marginal vapor flow is the added vapor flow required in the column because the other species—i.e., those on the list—are present. The vapor flow in a column is an indicator of the cost of purchasing and operating the column. A difficult separation will have a large vapor flow because it will require a large reflux ratio. Also, refluxed material has to be vaporized and condensed, which directly affects the utility costs for operating the column. Therefore, it makes sense to try to minimize the total of the vapor flows for a system of columns.

Formally, we can define marginal vapor flow as

$$\Delta V(i/j,\text{list}) = V(i/j,\text{list}) - V(i/j)$$

where the last term is the vapor flow in a column to split i from j with no other species present (the list is empty).

We should note that all sequences to separate a mixture will have the same set of binary splits. For example, each alternative sequence for the separation of ABCDE into five single-species pure products will have a split between A and B, another between B and C, etc. The difference among the alternative sequences is the presence or absence of other species when carrying out each of these binary splits. The total of the vapor flows for a sequence is the base set of vapor flows $V(i/j)$, where i and j are A/B, B/C, C/D, and D/E, plus its marginal vapor flows. Thus, the difference in marginal vapor flows is the difference in total vapor flows among the sequences. The sequence with the minimum marginal vapor flows is the sequence with the minimum total vapor flows.

How can we estimate a marginal vapor flow for a column? One approach is to estimate the minimum reflux required using any method that is appropriate. If the separation is among species that are acting nearly ideally, we can use Underwood's method.

3. Five-Alcohol Example Continued

For our five-alcohol example, let species A be n-butanol, B be 1-pentanol, etc. Now, let us consider the column that accomplishes the separation AB/CDE. To estimate the internal vapor flows in the column, we will have to assume recoveries for the species. Here, we shall assume that 99% of the key species go to their respective products, while everything lighter than the light key goes to the distillate and everything heavier than the heavy key ends up in the bottoms.

Applying Underwood's method gives us a minimum vapor flow of 72.5 kmol/h for a column accomplishing the separation of AB/CDE. Without species A, D, and E present, the minimum vapor flow is computed to be 44.5 kmol/h. The marginal vapor rate is therefore 38.0 kmol/h.

Let us look more closely at the Underwood equations to see if we can quickly compute an approximate answer. The minimum vapor flow for the split AB/CDE is given by

$$V_{\min} = \frac{\alpha_{AC} d_A}{\alpha_{AC} - \phi_{BC}} + \frac{\alpha_{BC} d_B}{\alpha_{BC} - \phi_{BC}} + \frac{\alpha_{CC} d_C}{\alpha_{CC} - \phi_{BC}}$$

but it is also related to the bottoms vapor flow as follows:

$$\begin{aligned} V_{\min} &= \overline{V}_{\min} + (1 - q)F \\ &= -\frac{\alpha_{BC} b_B}{\alpha_{BC} - \phi_{BC}} - \frac{\alpha_{CC} b_C}{\alpha_{CC} - \phi_{BC}} \\ &\quad - \frac{\alpha_{DC} b_D}{\alpha_{DC} - \phi_{BC}} - \frac{\alpha_{EC} b_E}{\alpha_{EC} - \phi_{BC}} + (1 - q)F \end{aligned}$$

Let us assume the root ϕ_{BC} does not move all that much if we add other species. Then these two equations would suggest that $V_{\min}$ is increased by an amount

$$\frac{\alpha_{AC} d_A}{\alpha_{AC} - \phi_{BC}}$$

because species A is present and by an amount

$$-\frac{\alpha_{DC} b_D}{\alpha_{DC} - \phi_{BC}} - \frac{\alpha_{EC} b_E}{\alpha_{EC} - \phi_{BC}}$$

because species D and E are present. The extra species are those lighter than the light key (species A) and heavier than the heavy key (species D and E). They will be essentially fully recovered in their respective products, so we should be able to substitute the feed flows for the product flows for each of them. Also in the terms for the species D and E, the denominator of the expressions is negative, so the terms are positive.

We can thus estimate the added vapor flow for each as the absolute value for the appropriate term, i.e.,

$$\left| \frac{\alpha_{ik} f_i}{\alpha_{ik} - \phi_{lk,hk}} \right|$$

where species i is in the feed when separating species lk from hk.

Figure 9 is a sketch of the relative sizes of the numerator and denominator for terms such as this for our example problem.

The amount of added vapor flow because A is present is proportional to α_{AC} divided by $\alpha_{AC} - \phi_{BC}$. We do not need a particularly accurate value for ϕ_{BC}

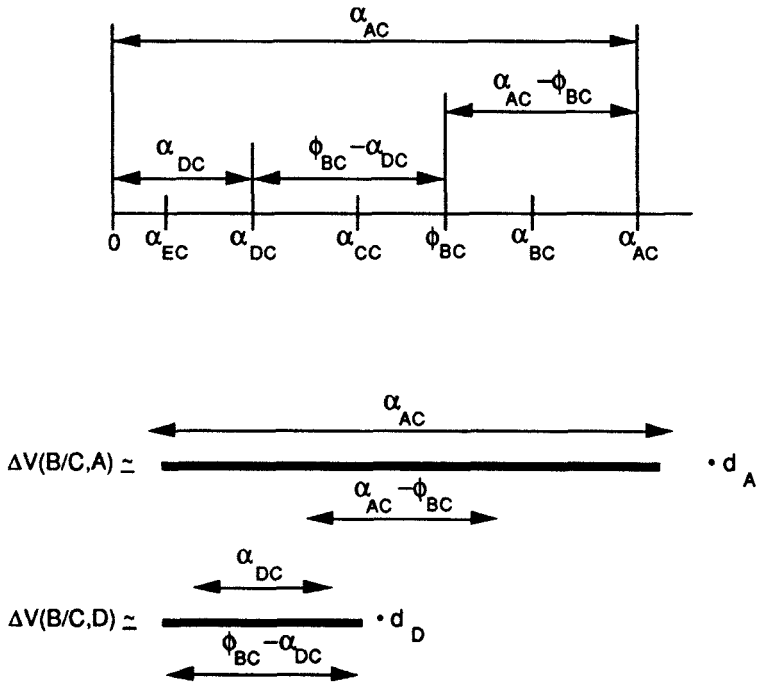

FIG. 9. Relative size of numerators and denominators in term to estimate marginal vapor flow: (a) terms relative to each other; (b) ratios.

to get a reasonable value for this term. A similar argument holds for the term when D is present and, although not shown, when E is present, too. We could, for example, let ϕ_{BC} be the average of the two surrounding relative volatilities. Our final term to approximate the increase in internal vapor flow for a column is thus

$$\left| \frac{\alpha_{ik} f_i}{\alpha_{ik} - \left(\frac{\alpha_{lk} + \alpha_{hk}}{2} \right)} \right|$$

We see that the term in front of the flow for the species in its respective product is much larger for a light species than for a heavy one. Thus, Figure 9 alerts us to the heuristic that the vapor flow is more sensitive to the presence of extra light species than the presence of extra heavy ones. This heuristic is often stated as follows:

Direct Sequence Heuristic: *Prefer removing the most volatile species first.*

Repeated application of this heuristic gives what is called the direct sequence. For example, the direct sequence for our problem is A/BCDE, B/CDE, C/DE, and D/E. (The indirect sequence—the other one with a special name—is ABCD/E, ABC/D, AB/C, A/B.)

4. Five-Alcohol Example Continued Further

The calculations were done using vapor pressure data available in Reid *et al.* (1987) for each of the species; Table VI gives the results. The temperature selected for evaluating the vapor pressure is the bubble point at 1 atm for the feed mixture, i.e., at 434.21 K. Using the relative volatilities and feed flows shown in Table VI, we can estimate the marginal vapor rates shown in Table VII using the equation

$$\left| \frac{\alpha_{ik} f_i}{\alpha_{ik} - \left[\frac{\alpha_{lk} + \alpha_{hk}}{2} \right]} \right|$$

For example, with C present for the A/B split, we get

$$\Delta V(\text{A/B,C}) = \left| \frac{1.0000 \cdot 20 \text{ kmol/h}}{1.0000 - \left(\frac{3.3199 + 1.7735}{2} \right)} \right| = 12.9 \text{ kmol/h}$$

To read Table VII, the marginal rate for AB/CDE, ΔV(B/C, ADE), is computed by adding the terms for the B/C split (second row) with A, D, and E

TABLE VI
VAPOR PRESSURE AND RELATIVE VOLATILIES FOR EXAMPLE PROBLEM

Species	Vapor pressure (bars)	Relative volatility	$f(i)$ (kmol/h)
Isobutanol	3.8279	3.3199	5
1-pentanol	2.0449	1.7735	10
1-hexanol	1.1530	1.0000	20
1-heptanol	0.6407	0.5557	50
1-octanol	0.3542	0.3072	15

TABLE VII
ESTIMATED MARGINAL VAPOR RATES[a]

	A	B	C	D	E
A/B	****	****	12.9	14.0	2.1
B/C	8.6	****	****	33.4	4.3
C/D	6.5	17.8	****	****	9.8
D/E	5.7	13.2	35.2	****	****

[a]Key species are listed along the left side, extra species across top.

added: namely, 8.6 + 33.4 + 4.3 = 46.3 kmol/h. This number should be compared to the more exact number, 38.0 kmol/h computed earlier. We should not expect it to be any more accurate than these numbers indicate.

We note there are two rather large numbers: one for which D is present with the B/C split and the other for which C is present with the D/E split. No doubt these should be avoided—as they can be if we split ABC/DE at the start. Then the "cost" to have A present for the AB/C split (8.6) compared to that of having C present in the A/BC split (12.9) suggests we should probably split C off next. That fixes the sequence as

ABC/DE, AB/C, A/B, D/E

The only other sequence that avoids these two high costs is A/BCDE followed by BC/DE.

We can search over all possible sequences quite quickly as follows. We sum up the marginal costs for each split possible in the problem and organize them in the following way.

		B/CDE	37.7		
A/BCDE	28.9	BC/DE	27.6		
		BCD/E	48.4	C/DE	9.8
				CD/E	35.2
AB/CDE	46.3				
				B/CD	33.4
				BC/D	17.8
ABC/DE	34.1				
				A/BC	12.9
		A/BCD	26.9	AB/C	8.6
ABCD/E	54.1	AB/CD	42.0		
		ABC/D	19.0		

To develop a solution using the least cost, we start with the total feed and compare the costs for the first splits. Here, the costs range from a low of 28.9 to a high of 54.1 kmol/h, so we select A/BCDE first. We now must complete the sequence; i.e., separate BCDE. The least-cost next step is 27.6 corresponding to BC/DE, which gives us a total of 56.5 kmol/h. That completes this sequence

because the marginal costs for the two remaining splits, B/C and D/E, are zero (there are no extra species present for them). Note that this is the second of the two solutions we spotted above. Can we find a cheaper solution? Observe that neither of the other first splits for BCDE is preferable: each has a higher-cost first step (and each requires another split, with an added cost, to finish them).

We try ABC/DE next at a first-step cost of 34.1. The AB/C split adds 8.6 for a cost of 42.7. This sequence is the first one we found intuitively above, and it is better. No sequence starting with AB/CDE (first-step cost of 46.3) or ABCD/E (54.1) can possibly be better. We are done.

The approach we just used to completely search this space is a form of branch and bound. We branched off the least expensive first steps and slowly eliminated the need to look at others as they each had a first-step cost (bound) that was too high to win.

Because errors in these numbers can occur, we might want to look at anything within 20% of the best with a more accurate analysis. If none exists, we are done with a relatively cheap analysis. If some exist, we could use Underwood's method (i.e., find the roots) to estimate the minimum reflux ratios as we did above for one of the columns.

5. *Distillation Heuristics*

The marginal cost approach explains (at least partially) many of the commonly published heuristics used to select the better sequences. We have already seen how it explains the direct sequence heuristic, which is stated as follows:

Direct Sequence Heuristic: *All other aspects of the problem being equal, remove the most volatile species first.*

For all other things to be equal, the amounts of the species must be the same and the relative volatility between all adjacent pairs of species must also be the same. For example, in the case of a four-species feed having equal amounts of each species (e.g., 1 kmol/h each) and relative volatilities of $\alpha_{AD} = 1.2^3 = 1.728$, $\alpha_{BD} = 1.2^2 = 1.44$, $\alpha_{CD} = 1.2^1 = 1.2$, and $\alpha_{DD} = 1.2^0 = 1$, "all other aspects of the problem [would be] equal." For each binary split (e.g., A/B or B/C), the McCabe–Thiele diagram would be drawn with the equilibrium curve based on a relative volatility of 1.2.

In carrying out the above search, we become aware that different sequences are associated with different numbers of extra species contributions. For example, in the sequence

{A/BCDE, B/CDE, C/DE, and D/E}

CDE, DE, and E show up as six instances of extra species, while in the sequence

{ABC/DE, A/BC, B/C, D/E}

only four instances, ABE and C, show up. The more we split the problem into halves, the fewer the number of extra species contributions we will add into the objective for the above search. We can use this observation to justify partially the following commonly stated heuristic:

50/50 Split Heuristic: *Separate the mixture into roughly equal amounts of products.*

Using marginal vapor flows, we can also explain the following heuristic fairly straightforwardly, as the approximation for the added vapor flow for a species in any mixture in which it appears is proportional to its flow in the feed:

Major Species Heuristic: *Have the major species in as few splits as possible.*

One other heuristic very commonly stated is

Save the difficult splits for last.

In other words, *do the easy splits first.* A split is easy if the relative volatility between the two key species is large. The (plausible) argument is that the hard splits should be done when no other species are present. Since the marginal vapor flow computation neither supports nor rejects this heuristic, we might draw the conclusion that this heuristic is not valid for the problem as we have posed it above. But there is some justification for this heuristic when we consider the energy integration of columns (e.g., using the heat expelled from the condenser of one column as the heat input into the reboiler of another).

All of these heuristics depend on amounts and relative volatilities for the species in the mixture. Based on precisely these quantities, the *simple* computation

$$\left| \frac{\alpha_{ik} f_i}{\alpha_{ik} - \left[\frac{\alpha_{lk} + \alpha_{hk}}{2} \right]} \right|$$

would seem to quantify their relative importance.

V. Separating Highly Nonideal Mixtures

We shall now look at the synthesis of separation systems for liquid mixtures of species that display highly nonideal behavior. We reference a small sampling

of the work on this topic: Ewell and Welch (1945), the classical text by Hoffman (1964), early work on classifying behavior by Berg (1969), a scheme for classifying vapor–liquid behavior for ternary mixtures by Matsuyama (1975), many papers on homogeneous continuous azeotropic distillation by Doherty and coworkers (Doherty and Perkins, (1978); Doherty, (1985); Doherty and Caldarola, (1985); Levy *et al.,* (1985); Van Dongen and Doherty, (1985); Knight and Doherty, (1989); Julka and Doherty, (1990); Foucher *et al.,* (1991); Fidkowski *et al.,* (1993); work by Petlyuk (1978), Stichlmair *et al.,* (1989), an expert system described by Barnicki and Fair (1990), work on multiple steady states by Bekiaris *et al.,* (1993), work by Bossen *et al.,* (1993), and our own work. Poellmann and Blass (1994) presented a review and new analysis methods for azeotropic mixtures.

Distillation remains a likely option for separating a complicated liquid mixture except for the fact that we cannot readily predict what the products will be if we do distill a given mixture. Extractive distillation is often a viable alternative. If the species display liquid/liquid behavior (e.g., hydrocarbons and water), we can consider simple decantation or liquid/liquid extraction, too.

In general, we will try simple distillation; but, when we do, we often discover that significant amounts of almost all of the species show up in either or both of the distillate and bottoms products, no matter how we run the column. The inability to effect sharp splits gives rise to the recycling of streams within the separation process itself—something we did not require earlier when we looked at the separation of ideally behaving mixtures.

A. Azeotropic Separation: Example 1

Consider the separation of water from *n*-butanol. The phase behavior for this mixture is quite complex. There is a minimum-boiling azeotrope formed as well as a liquid–liquid phase separation when the liquid is cooled enough. Figure 10 is a sketch of the general shape of the phase behavior for this system. (It is not an accurately drawn phase diagram.)

Several textbooks and reference books (e.g., the third edition of Perry's *Handbook,* 1950) use this example to illustrate azeotropic distillation. They show the solution sketched in Fig. 11 for a feed whose composition is about 60% *n*-butanol. If we analyze this configuration, we see that it separates the mixture. The same textbooks suggest that for a feed below the azeotropic composition, one should use the same configuration but put the feed into the decanter. The question that occurs immediately is: How was this configuration selected? Was it a trial-and-error procedure, or is there some way to find it directly?

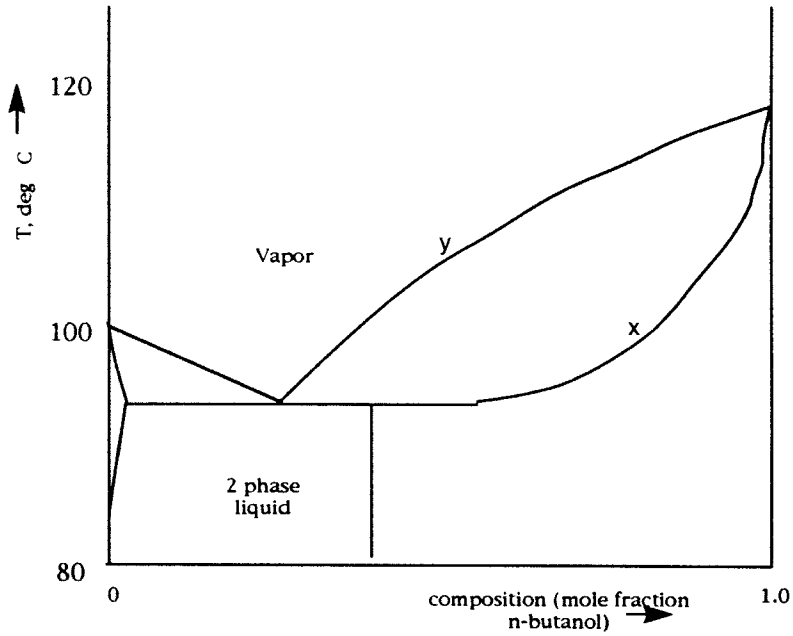

FIG. 10. Vapor/liquid equilibrium diagram for *n*-butanol/water.

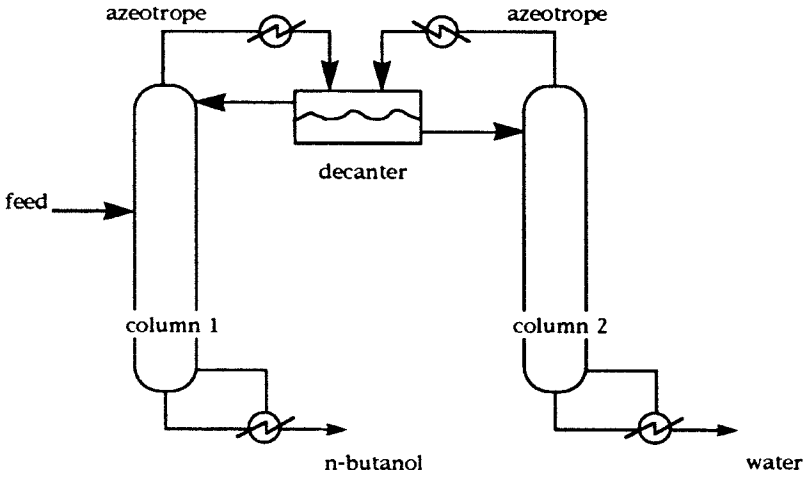

FIG. 11. Configuration presented in handbooks for separating *n*-butanol and water.

As will be true in virtually all synthesis problems, the secret to finding a solution is to find and use the right representation. For this problem, a convenient representation is shown in Fig. 12. We show a line that has the key compositions marked along it for the phase diagram for the system.

Starting with a feed at about 60% *n*-butanol, we see that we can distill it into two products: one close to the azeotropic composition as the distillate product and one, nearly pure *n*-butanol, as the bottoms product. The bottoms product is a desired product; however, we must still separate the top. We find that the top azeotrope lies in the region where it partitions into two liquid phases if we cool it. We therefore cool the azeotrope and put it into a decanter. Next, we decide to distill the water-rich phase (bottom phase in the decanter) into nearly pure water and azeotrope, again getting the azeotrope as a distillate product. We already know what to do with the azeotrope: cool it and feed it to the decanter. The only remaining stream is the upper decanter product, the one that is richer in *n*-butanol.

We could distill this upper product, getting *n*-butanol and azeotrope. However, the first column is already able to do this task, so we can choose to feed it into that column. We see that, with minor modifications, we have just invented the structure shown in the handbooks. In a similar manner, we should be able to invent two structures that can handle a feed to the water-rich side of the azeotrope. In one, the feed enters the decanter and in the other, the feed enters the second column (an alternative not mentioned in the handbooks).

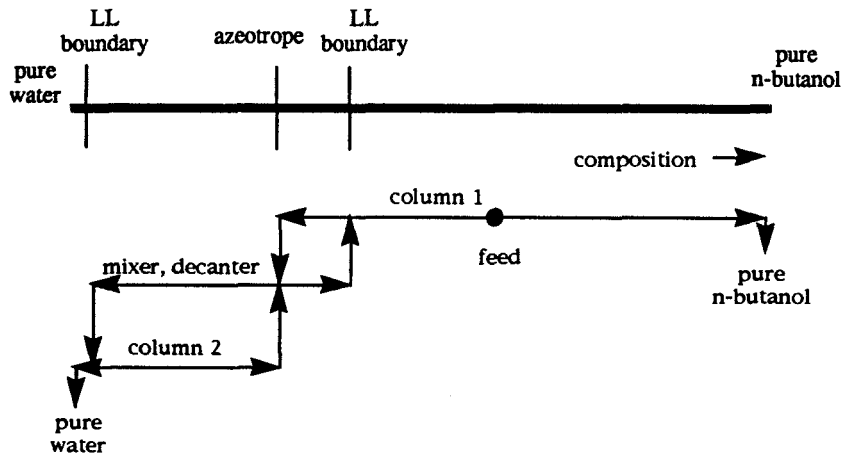

FIG. 12. Convenient diagram to synthesize a separation process for the *n*-butanol/water system.

VI. Synthesis Discussion

A. Analysis-Driven Synthesis

When the species of interest display highly nonideal behavior, the synthesis of separation processes falls into the class of synthesis problems we might call *analysis-driven synthesis.* We use that term because the real work in this synthesis problem is to establish enough information (i.e., carry out complex *pre-synthesis analysis* computations) to begin the synthesis process. We have to find out about the behavior of the mixtures of the species (e.g., are there azeotropes) before we can even propose the types of equipment we should use to carry out a separation. Then, we must also worry about how these species will behave in any equipment we suggest. Finally, we must carry out a *post-synthesis analysis* in which we design the equipment to evaluate (e.g., determine costs for) the different alternatives. At a minimum, then, column design requires us to set the column pressure and compute the reflux ratio, the number of stages, and the column diameter. For nonideal behavior, these computations can be very difficult.

We thus see a pre-synthesis analysis that characterizes the behavior of the species and a post-synthesis analysis that requires us to design equipment. Both require that we compute equilibrium phase behavior (vapor/liquid, liquid/liquid, vapor/liquid/liquid, etc.)

B. Impact of Number of Species on Representation, Analysis, and Synthesis Methods

The synthesis of distillation-based separation systems is strongly supported for two- and three-species mixtures. There is much less support for mixtures of four species, and even less for five. There are several reasons for this, some of which are fundamental.

The pre-synthesis analysis allows us to understand the topology of the phase behavior of the species when mixed. With that understanding, we find that we can conjecture reasonable process alternatives. Unfortunately, we are limited to a three-dimensional world when it comes to human visualization. Thus we can appeal to visualization of complex topologies only when we can show them in two and, with difficulty, three dimensions. The triangular composition diagram is an excellent way to visualize complex behavior among species, but it is specific to three-species mixtures. When we go to four species, we stretch the ability of people to see what is going on; when we go to five, we are approaching impossibility.

Certainly, computers can work well at higher dimensions. Unfortunately, however, when we go to higher dimensions, what were lines often become planes, then volumes, and so forth. Whereas we can search for exotic behavior along a line with a "computational sledge hammer," it currently takes enormous effort to search a plane thoroughly for complex behavior. For volumes and higher dimensional spaces, then, we must use simpler and less complete searching at this time. This is the problem we face when analyzing systems with five or more species.

Another issue is the way we can use the degrees of freedom for a column. We argue that things change qualitatively when going from systems of three to four to five and higher species. In Fig. 13, we show what we might call the "natural" degrees of freedom for a column—the ones we generally pick when we wish to compute the performance of a column. These specifications lead to the easiest column calculation to converge. Using our intuition about columns, we argue that, if we specify

- the feed to a column (flowrate, composition, pressure, and temperature),
- the column operating pressure (P),
- the number of trays in the top (n_{top}),
- the number of trays in the bottom (n_{bot}),
- the reflux ratio (R), and
- the distillate product flow rate (D),

then the column will operate as expected. That is, a typical simulation of the column would tell us the top and bottom product composition, as well as the tray-by-tray temperatures, compositions, etc. Assuming our intuition is correct, we note that, once we specify completely the feed to a column, a column provides us with five more degrees of freedom. We shall now discuss how we might use these to analyze a column in other ways, for example, in designing the column.

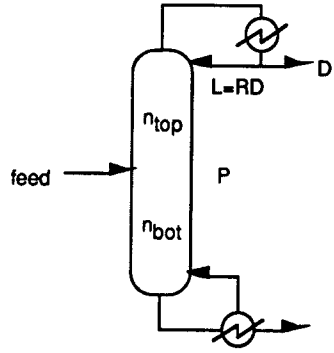

FIG. 13. "Natural" degrees of freedom for a column.

Of the five degrees of freedom, a designer typically fixes the column pressure to set the temperature of the condenser or the reboiler. Thus, we shall assume that P is not at our disposal. That leaves us with four degrees of freedom. Can we use these four degrees of freedom to fix the recoveries of four species leaving the column in the top distillate product? For example, can we design the column so that 99% of species A, 95% of species B, 1% of species C, and 0.5% of species D will leave in the distillate?

Let us carry out the following computational experiment involving the solving of a column model.

First we shall solve a column using the natural specifications—those listed above. Generally, such a model is easy to solve unless the species are highly nonideal in their behavior. We observe the recoveries for the two key species, finding that 85.1% of the light key leaves in the distillate while 74.3% of the heavy key leaves in the bottom product. We now change what we intend to compute and what we intend to specify as fixed for the model calculation. First, we decide to fix the recovery of the light key and ask the model to compute the required reflux ratio. We then alter the light key recovery to 85.0% (very slightly away from the value obtained above) and resolve the model, keeping all the other fixed variables (pressure, reflux ratio, number of trays top and bottom) at their current values. If the simulator only permits the natural specification to be made, then we can only change the reflux ratio iteratively until the recovery changes to the desired value. The reflux ratio should decrease slightly, allowing more of the heavy species to exit in the top product. Since the distillate flowrate is fixed, this will reduce the recovery of the light key.

Being more daring, we now change the recovery to 80% and then to 90%. In both cases there is no difficulty in converging to an answer. We discover that this trade is a practical one. We revert back to a recovery of 85.0%. Experience with many simulations suggests that, while it is a practical one, it is very difficult to converge with such a specification given at the start of the calculation.

Next we fix the recovery of the heavy key in the bottom product at 74.5% and ask the model to adjust the distillate top product flowrate accordingly. For this calculation we still want the light key recovery to stay at 85.0%, so the simulator adjusts the values for both the reflux ratio and the distillate top product flowrate, giving us our desired slightly altered key species recoveries. It has no difficulty in converging. We find that the larger changes also converge readily. So we can trade light and heavy key recovery specifications for distillate total flow and reflux ratio, provided we do it with a modicum of care.

We now ask if we can specify the recovery of a third species. The variable we trade is the number of trays in the top section of the column. The number

of trays is a discrete quantity so, for a tray-by-tray model, we should not be able to fix the recovery exactly for the third species while holding the recoveries of the keys fixed at 85.0% and 74.5%. However, a collocation model (Cho and Joseph, 1983; Stewart *et al.*, 1984; Seferlis and Hrymak, 1994; Huss and Westerberg, 1994) allows us to model a column approximately such that the number of trays is a continuous variable. We assume the availability of such a model. With this model, we find that the changes we can accomplish in the recovery of the third species have to be very small. For example, we might ask that the amount of a species heavier than the heavy key have its recovery in the distillate top product decrease from about 1% to about 0.5% by adjusting the number of trays in the top section. Such a change will cause changes in the distillate flowrate, the reflux rate, and the number of trays in the top section. If we try to increase the recovery to 3%, the model fails. We return it to a 1% recovery. Further testing convinces us the trade is theoretically possible, but the range for changing the specification is quite small.

Finally, we ask if we can trade the number of trays in the bottom section for the recovery of a fourth species. Our intuition tells us we could be in numerical trouble here. In principle, we can make the trade; however, very small changes lead to very large changes in the number of stages and even more often, to computational failure. The fourth specification is theoretically possible but computationally nearly impossible.

What are the implications of this experiment? First, from a theoretical point of view, we can specify the recoveries of four species at most for a column. From a practical point of view, the first two are relatively easy (if we take care in doing it) to specify, adding a third specification is difficult, and a fourth virtually impossible. We cannot, as a result, specify completely the top product of a column for more than four species in theory and more than three in practice.

C. In Summary

Any method that we develop for three species starts to run into the practical limitations we described above when we try to extend them to four species. We have difficulties in presenting them to humans for visualization; moreover, difficult searches explode in size, no longer running along lines, but extending over planes, volumes, and higher dimensional spaces. Finally, we cannot specify product compositions for more than four species separations in theory, and we have real, practical difficulty with more than three.

For these good reasons, the literature explores methods to handle three species mixtures thoroughly and hesitates to extend them to mixtures with four and more species.

VII. Pre-analysis Methods

There are two classes of analysis methods that we shall explore. The first class allows us to understand the phase behavior of the species in the problem. The second allows us to analyze the behavior or design of a piece of separation equipment.

We need to understand the behavior of the species in our problem. As we noted earlier, it is not very useful to design a separation process assuming ideal behavior when such behavior does not exist. Such a design might not represent even a lower bound on the cost of the process we might actually develop. For example, toluene and water dislike each other so much that they readily separate into two liquid phases, each with little of the other species present. That is, they behave nonideally. If the compositions for these two phases meet our specifications, we can separate these two species by a relatively inexpensive decantation procedure, which is much more effective than designing a column predicated on ideal behavior.

Some of the analysis methods we are about to discuss rely on computing residue curves, so we first need to understand what such curves are and how to compute them.

A. Equilibrium-Phase Behavior

Earlier in this paper we discussed a simple method to detect if an azeotrope will exist between two species, A and B. The method requires us to perform two bubble-point computations, one in which we have a trace of A in B and one in which we have a trace of B in A. We used the infinite-dilution K-values we computed in these bubble-point computations for the trace species to reveal where an azeotrope exists. If both infinite-dilution K-values are less than unity, there must be a maximum-boiling azeotrope between these species. (There could even be more than a single azeotrope between the species, such as two maximum-boiling azeotropes separated by a minimum-boiling azeotrope. We assume this is rare, but there must be at least one.) If the K-values are both greater than 1, by similar arguments there is at least one minimum-boiling azeotrope. Otherwise, we suggested, we could assume nonazeotropic behavior.

As we also discussed earlier, we can assess whether liquid–liquid behavior is likely by examining infinite-dilution activity coefficients.

In this section we wish to look in more detail at the nonideal behavior of mixtures of a given set of species. We shall start by examining residue and distillation trajectory plots that show the vapor/liquid behavior of mixtures when

they are being distilled. Such plots are very informative in that they depict the VLE behavior in a manner that is useful for synthesizing separation processes for such mixtures. We shall then consider methods by which we might discover all the azeotropes for a given set of species. Finally we shall discuss methods for determining the multiple-liquid phase behavior for a set of species.

1. Residue and Distillation Curves

We look first at residue curves, which correspond to batch distillation, and then to distillation curves, which correspond to separation trajectories in columns operating under total reflux conditions.

a. Residue Curves. A residue curve (Hoffman, 1964; Doherty and Perkins, 1978) traces the composition of the liquid in a batch still in composition space versus time. Along this curve the temperature always increases, the composition of the heaviest species increases, and the composition of the most volatile species decreases.

Consider the batch still shown in Fig. 14, which contains a mixture that we boil away with time. What is the composition of the liquid in the still versus time? A dynamic material balance for the species i is

$$\frac{dx_iM}{dt} = x_i \frac{dM}{dt} + M \frac{dx_i}{dt} = -y_iV$$

We note that

$$\frac{dM}{dt} = -V$$

allowing us to write

$$M \frac{dx_i}{dt} = V(x_i - y_i)$$

Defining a dimensionless time as $\theta = t/(M/V)$, this equation becomes the fol-

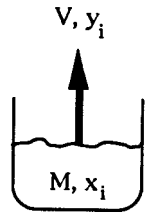

FIG. 14. Batch still.

lowing simple relationships:

$$\frac{dx_i}{d\theta} = x_i - y_i = x_i - K_i x_i$$

where setting $y_i = K_i x_i$ assumes that the vapor is in equilibrium with the liquid composition.

These equations can now be integrated versus dimensionless time. For a three-species mixture, we can plot the resulting compositions as a parametric function of θ on a triangular diagram. Note, the x_i's sum to unity so one of the equations is not independent. The last mole fraction can either be obtained by integrating the above equations or by integrating all but the last of these equations and computing the last mole fraction so the sum of mole fractions is unity.

b. Distillation curves. We can also compute a composition trajectory directly for a column by stepping from one tray to the next for a column operating at total reflux, as Fig. 15 illustrates. The material balance equations for this column are

$$V_{n+1} = L_n$$

and

$$y_{n+1,i}\, V_{n+1} = x_{n,i} L_n$$

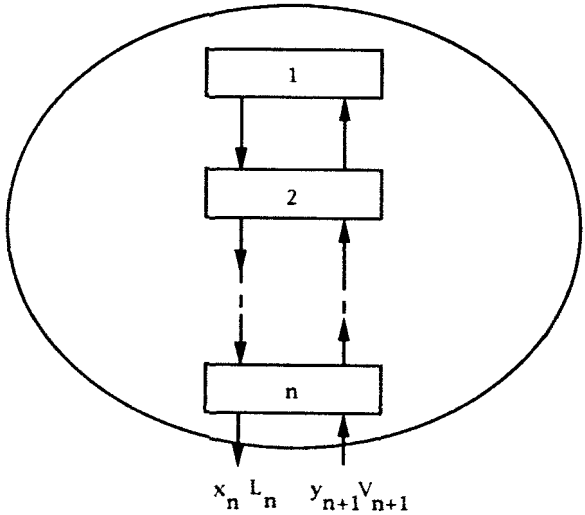

FIG. 15. Total reflux column (no feed or product).

therefore,

$$y_{n+1,i} = x_{n,i}$$

Equilibrium gives

$$y_{n+1,i} = K_{n+1,i}x_{n+1,i}$$

Propagation from one point to the next therefore combines these last two equations to give

$$x_{n,i} = K_{n+1,i}x_{n+1,i}$$

If we step down the column, we would know $x_{n,i}$ and would have to compute a dew point to find the composition $x_{n+1,i}$. Given that, we compute its dew point to step down to tray $n + 2$, etc. Stepping up the column requires that we compute a sequence of bubble points in a similar manner. Temperature increases as we step down a column, which is the same direction temperature moves when time increases for the residue curve computations.

2. *Sketching Residue Curve Plots for Ternary Systems*

Figure 16 shows a whole set of residue curve trajectories that might be computed for a stillpot containing initially a mixture of water, ethanol, and glycol.

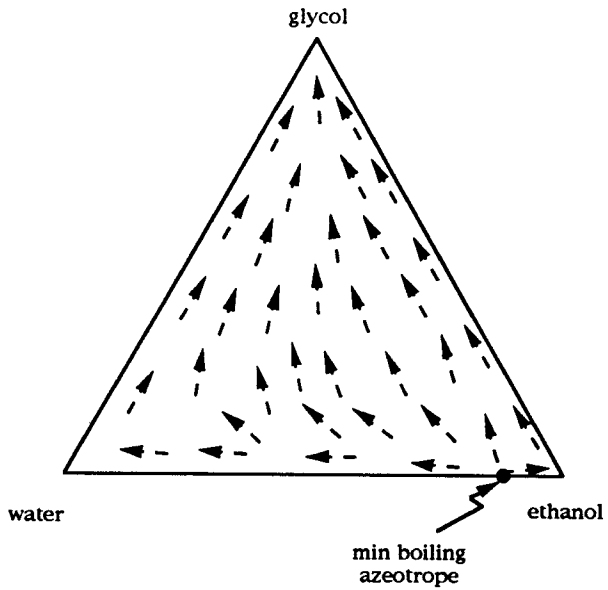

FIG. 16. Trajectories for compositions in stillpot.

(Alternatively, we could sketch distillation curve trajectories, which look very similar.) All of the residue curve trajectories move from the lowest temperature in the diagram—the ethanol and water azeotrope—and end at the highest temperature in the diagram—pure glycol. At any point in a residue plot, the equilibrium vapor composition is moving in the direction that is tangent to the curve, and in the opposite direction the trajectory is moving with time.

There are examples where the trajectories break the diagram into regions. Such a structure appears when there is more than one local minimum and/or maximum temperature in the diagram. We see such behavior in Fig. 17. The lower two species again have a minimum-boiling azeotrope between them; the third (top) species is the most volatile one. To guess the topological behavior for this diagram, we first place temperatures for the normal boiling point for the pure species and for the azeotropes onto the diagram. We then place arrows around the edges to indicate the directions for increasing temperatures, as shown. From just these few arrows, we observe that there are two local maximum temperatures in this diagram, one in the lower right and one in the lower left. Let us assume that there can be at most one ternary azeotrope and then attempt to sketch in trajectories within the diagram to expose its general structure.

Occasionally we can posit more than one structure possible, based on knowing only the temperatures for the pure species and the binary azeotropes. Since such structures can occur, care must be taken to see that all possible structures are discovered. Based on topological arguments, Zharov and Serafimov (1975; see also Serafimov, 1987) developed an equation among the number of "nodes" and "saddles" appearing in a residue curve map. Independently, Doherty and

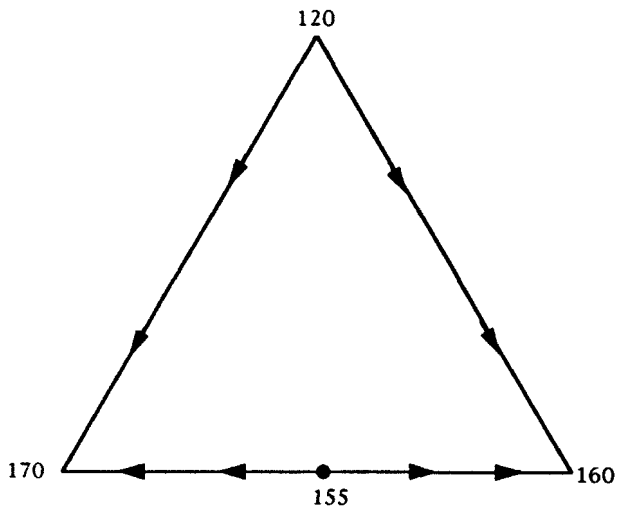

FIG. 17. Directions of increasing temperature along edges of triangular composition diagram.

Perkins (1979) developed a special version of this equation for three-species mixtures. Foucher *et al.* (1991) present detailed rules to sketch and to check the consistency of data on ternary diagrams. One version of this equation for three species mixtures is

$$4(N_3 - S_3) + 2(N_2 - S_2) + (N_1 - S_1) = 1$$

where N_i is the number of nodes and S_i is the number of saddles involving exactly i species on a ternary diagram.

A *node* is any point where all temperature trajectories enter or all leave, whereas a *saddle* is a point where some trajectories enter while others leave. The pure species in the lower left and right corners have all trajectories entering; the top pure species has all leaving. As each involves one species, each is a *single-species node.* We cannot yet classify the binary azeotrope along the lower edge. Its type will depend on whether trajectories enter it or leave it from the interior of the composition triangle. If they enter, then some trajectories will enter while those along the lower edge leave, making it a *two-species* or *binary saddle.* If they leave, all the trajectories leave, making it a *two-species node.* Points strictly inside the diagram are three-species points.

A recent review article by Fien and Liu (1994) describes how to apply this formula in some detail. Applying it for the ethanol–water–glycol example in Fig. 16, we see that $4(0 - 0) + 2(1 - 0) + (1 - 2) = 1$ satisfies this equation. If there can be only one ternary node or saddle, only $N_3 = S_3 = 0$ can satisfy this equation and the sketch must be unique.

For Fig. 17, we might ask if the azeotrope at 155° is a node or a saddle, or could it be either based on the information given. Substituting into the formula for both options, we get

If a node: $4(N_3 - S_3) + 2(1 - 0) + (3 - 0) = 1$

or $4(N_3 - S_3) = -4$

If a saddle: $4(N_3 - S_3) + 2(0 - 1) + (3 - 0) = 1$

or $4(N_3 - S_3) = 0$

The former would allow a ternary saddle (i.e., $N_3 = 0$, $S_3 = 1$) to exist while the latter permits only $N_3 = S_3 = 0$—i.e., no ternary node nor saddle—if our assumption is valid that there is at most one ternary node and/or saddle.

Figure 18 shows the diagram with the required ternary saddle where the binary azeotrope is a node. It has four *distillation regions* (labeled I to IV) separated by *distillation boundaries,* each of which has its own set of maximum and minimum temperatures within it. For example, region I has a maximum temperature of 170° and a minimum of 120°. It is this property of having its own unique minimum temperature (from which all trajectories emanate) and maximum temperature (at which all terminate) that characterizes a region.

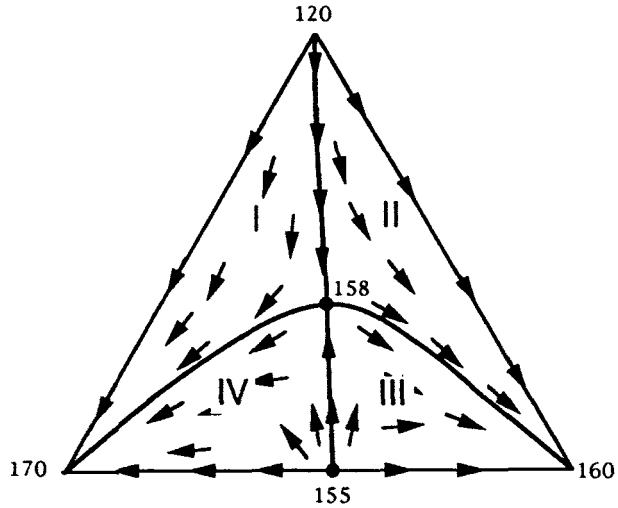

FIG. 18. Triangular composition diagram where binary azeotrope is a node.

Assuming the binary azeotrope is a saddle (as shown in Fig. 19), we note that there is a trajectory that starts at the upper vertex and passes through the minimum-boiling azeotrope on the lower edge. This trajectory is a distillation boundary that splits the diagram into two distinct distillation regions, labeled I and II. Each region has the same minimum temperature but a different maximum temperature within it.

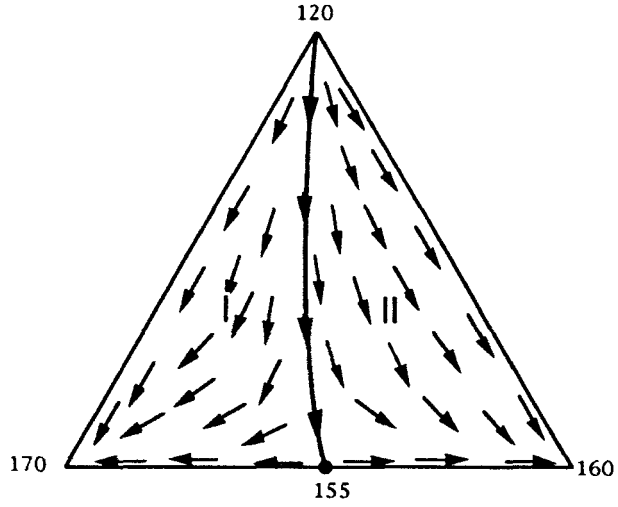

FIG. 19. Triangular composition diagram where binary azeotrope is a saddle.

The only way we can select between these two options is to obtain more information, either by computing the trajectories using a physical properties model we believe or by obtaining experimental data for the problem.

B. Distillation Column Behavior

1. Limiting Behavior

There are two limits at which we can examine the behavior of a distillation column. The first is at *total reflux* (i.e., with an infinite reflux ratio, which is often called *infinite reflux* conditions). The other extreme is to operate at *minimum reflux.* In this section we shall limit our discussion to the total reflux case; in later sections we shall look at operating columns at finite reflux (ratio) conditions. Intuitively, we tend to expect that a column will give its maximum separation when run at infinite reflux. While this is true for ideally behaving species, it does not have to be true when separating nonideally behaving species. Thus, we need to look carefully at running columns all the way from minimum to total reflux conditions.

2. Reachable Products for Total Reflux

One of the steps in developing alternative structures for a separation process is to discover the possible products for a proposed technology. There is no general method to accomplish this task for mixtures displaying complex behavior, even for distillation. For nearly ideally behaving mixtures, identifying possible products is a trivial task, sufficiently so that it is seldom recognized as a required step in posing solutions. For the special case of separating ternary mixtures using distillation columns that produce two products, Wahnschafft (1992) and Wahnschafft *et al.* (1992) show that all possible products for azeotropic mixtures can be determined with a relatively simple analysis which involves residue and distillation curves and pinch point trajectories.

To trace out these curves is to compute a sequence of flash calculations (a relatively easy task compared to computing distillation column performance). What is remarkable is the fact that we really need to use residue curves (those curves produced by solving ordinary differential equations) for a part of this analysis. Until now, we have assumed that these curves corresponded only to the time behavior of a batch still. Here, however, they become a necessary ingredient in the analysis of a staged distillation column behavior instead of a convenient approximation.

To understand the reachable-product problem, let us imagine separating an equimolar ideally behaving three-species mixture of species A, B, and C (A

being most volatile, C the least) in a two product column. We illustrate these ideas in Fig. 20. Assume the column has a very large number of trays and that it will be run at very high reflux.

We first remove only one drop of distillate top product D, letting the rest of the feed exit from the bottoms product of the column. The distillate will be pure A, while the bottoms will be virtually all of the feed. We show these two where the distillate-to-feed ratio *D/F* is zero. We then draw off 1% of the feed in the top and 99% in the bottom. We will continue to remove pure A in the top and the rest of the feed in the bottom. Material balance dictates that the feed must lie on the straight line joining the distillate and bottoms compositions. The bottoms moves directly away from the feed toward the BC edge as we remove more and more A. When we reach the point where we are removing one-third of the feed in the top, we will remove essentially all the A in the top and all the B and C in the bottoms. If we remove 50% of the feed from the top, it will be all of the A and half of the B, with the remaining half of the B leaving in the bottoms together with all the C. When the distillate is two-thirds of the feed, we have all the A and B in the top and all the C in the bottoms. At 80%, we take all the A and B and some of the C out the top, with the bottoms being the rest of the C.

We can then backmix whatever is taken off in either product with the other to reach any compositions that lie between the product compositions. Thus, we can reach any product in the shaded bow-tie region on this figure.

At total reflux, the column itself (without the backmixing) can only reach products that lie both on the same *distillation curve* (not residue curve) and on a straight line passing through the feed so as to satisfy the overall column species

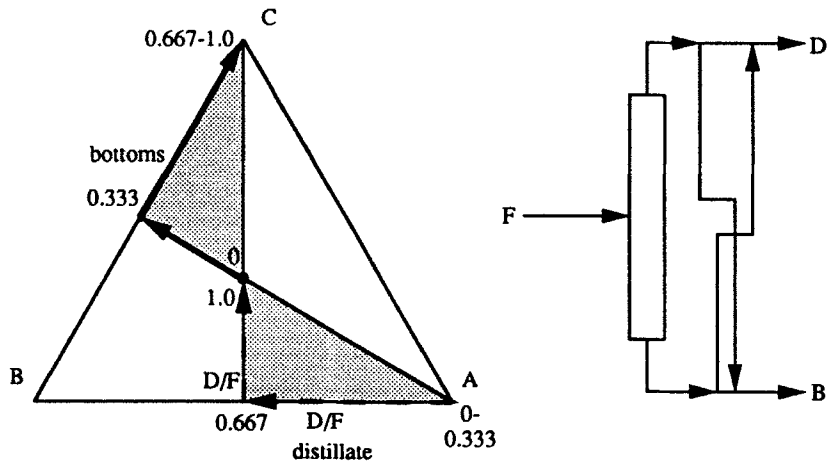

FIG. 20. Distillate and bottoms products versus *D/F* for an ideally behaving ternary mixture.

material balances. The limiting distillation curve for nearly ideal mixtures is that passing through the feed.

For this limit, think of removing one drop of top product, with the rest leaving in the bottoms while operating at near total reflux conditions. The top distillate product (one drop) will lie anywhere along the distillation curve passing through the feed, while the bottoms will be the feed. A similar argument holds for removing one drop in the bottoms at (near) total reflux conditions. Figure 21 shows the reachable region for such a column without the backmixing that we allowed before.

For nearly ideally behaving mixtures, the above completes the analysis needed to identify the reachable region at total reflux. For nonideally behaving mixtures, the shape of the distillation curves can lead to very interesting reachable-product regions. An S-shaped curve, for example, can lead to two disjoint reachable regions, a situation we shall examine later. The rule to remember for total reflux is that the column can produce any distillate product D and bottoms product B where

- the compositions for D and B lie on the same distillation curve, and
- the composition for the feed F lies on a straight line between the compositions for D and B.

VIII. Synthesis Method for Nonideal Mixtures

We now consider the separation of a nonideal mixture where the species do not display liquid/liquid behavior. Almost certainly, the technology of choice

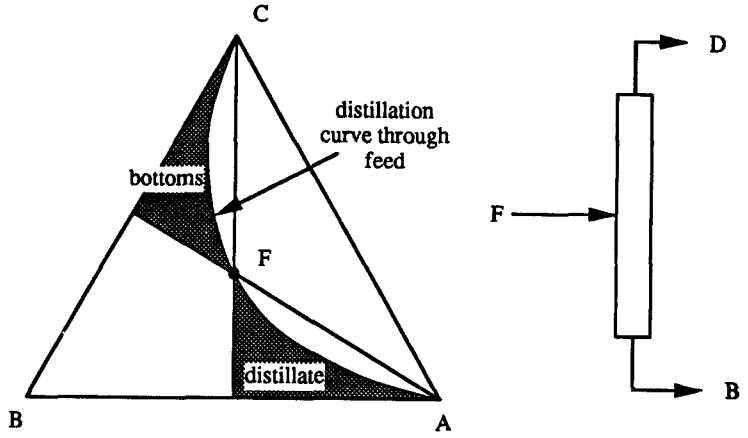

FIG. 21. Reachable region for a two-product column operating at total reflux.

will be distillation. In the following example, we examine the need to discover reachable interesting products when feeding a mixture into a distillation column. By selecting different interesting product sets, we generate design alternatives. As with the *n*-butanol/water separation example, we shall also see the need for recycle in completing the design. Here we explore two different reasons for using recycle: (1) to separate a mixture produced later in the process that is similar to an earlier one (i.e., discovering a *recursive solution*) and (2) to adjust the feeds to a column to allow it to produce two interesting products instead of one (i.e., *mixing to get better separation*, an apparent contradiction).

A. Azeotropic Separation: Example 2

Consider the separation of the mixture of acetone, chloroform, and benzene shown in Fig. 22. How do we generate alternative structures systematically for solving this problem?

We start by sketching the "binary separation tasks" for this problem, as shown in Fig. 23. As we suggest separations, we can keep track of which portions of these tasks they accomplish. We use the arrows on Fig. 23 to show the minimum separation that must be accomplished between each of the pairs of species if the product specifications are to be met. The feed composition is also illustrated. To interpret this diagram, suppose the feed is 36% acetone and 24% chloroform, yielding a

$$\text{Benzene-free composition} = \frac{36}{36 + 24} = 60\% \text{ acetone}$$

We can see this on the sketch for the acetone/chloroform pair. The chloroform product has to be at least 99% chloroform so it can contain at most 1% acetone,

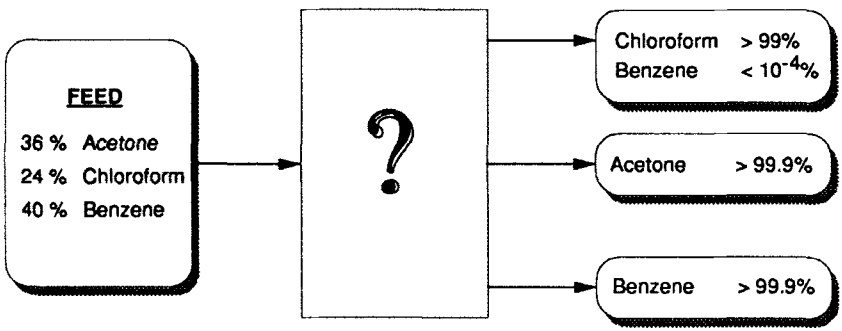

FIG. 22. Specifications for the separation of an acetone/chloroform/benzene mixture.

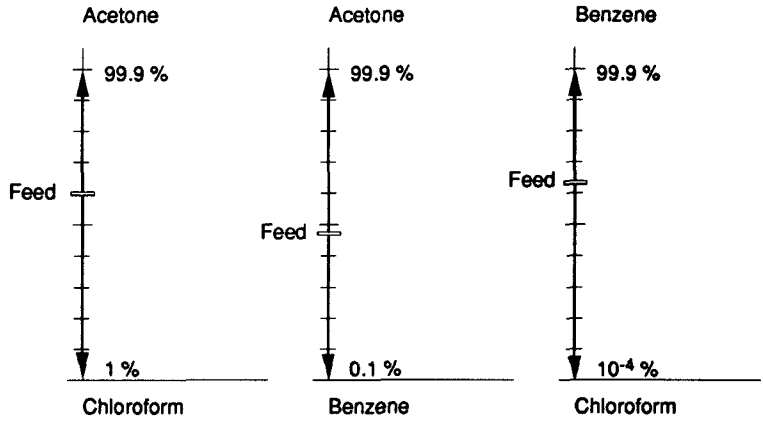

FIG. 23. Binary separation tasks and relative concentrations of the feed mixture.

while the acetone can have no more than 0.1% chloroform in it for it to be at least 99.9% pure.

We can map these tasks on the edges of our ternary composition diagram, as shown in Fig. 24. Note that a line projected from the pure acetone corner through the feed to the opposite edge has a constant ratio of benzene and chloroform all along it. Thus, the projected point on the benzene/chloroform edge

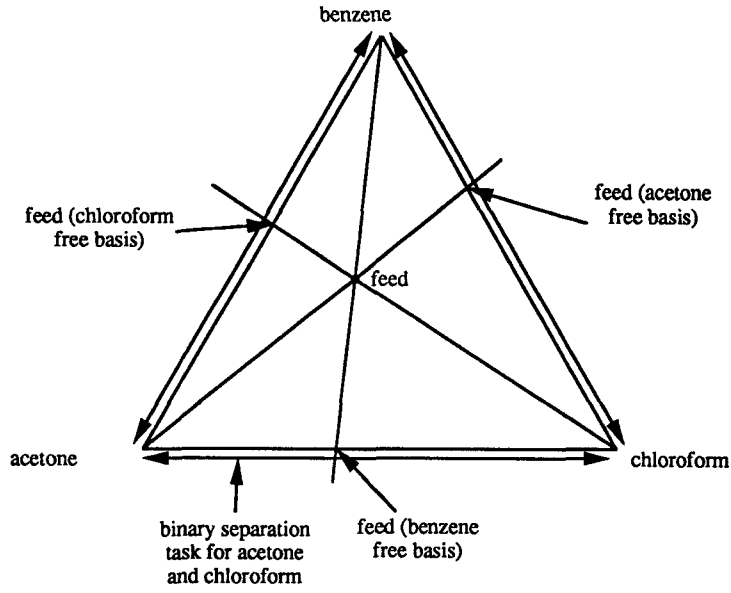

FIG. 24. Mapping separation task onto edges of triangular composition diagram.

is the composition of the feed on an acetone-free basis. Similar projections from the chloroform and benzene corners give the feed compositions on a chloroform-free and benzene-free (should be 60% acetone) basis, respectively. The mapping of the tasks is the result of similar projections. Note that the task along the bottom is to separate acetone from chloroform. Near the chloroform edge, we see a small gap, which says the chloroform product on that basis can be as much as 1% acetone.

We next need to know how these species will behave. First, their normal boiling points are 56.5°C, 61.2°C, and 80.1°C for the acetone, chloroform, and benzene, respectively. Thus, acetone is the most volatile, while benzene is the least. The lowest temperature, 56.5°C, is hot enough for cooling to be done using cooling water (i.e., above 25–30°C), so it makes sense to consider running the columns at a pressure of 1 atm.

We predicted their behavior earlier using infinite-dilution K-values, with the results at 1 atm shown in Table VIII. Only the acetone and chloroform appear to display azeotropic behavior. With this information and that for pure species boiling points at the pressure of interest, we can sketch the ternary diagram for this mixture. We can also use a computer code to generate it, which was done for Fig. 25. We see that there is one maximum-boiling azeotrope between acetone and chloroform.

Two features appear on the residue curve diagram in Fig. 25:

(1) A distillation boundary exits. We deduce this when attempting to explain the azeotropic behavior determined using infinite-dilution K-values.

(2) The boundary is curved. This, too, can be partially predicted by noting that the infinite-dilution K-values for acetone and chloroform in lots of benzene indicate that acetone is more volatile. Therefore, chloroform acts like an intermediate species in the benzene-rich end of the diagram. The residue curves start out aiming at chloroform from benzene.

What if we are dealing with a computer that does not draw or read these nice graphs, or what if we are dealing with more than three species? How might we proceed to find this behavior? We can carry out column simulations for a

TABLE VIII
INFINITE-DILUTION K-VALUES AND THEIR INTERPRETATION

		K^∞		
		Acetone	Chloroform	Benzene
In:	Acetone	1.0	0.4 (max)	0.7 (normal)
	Chloroform	0.6	1.0	0.4 (normal)
	Benzene	3.0	1.5	1.0

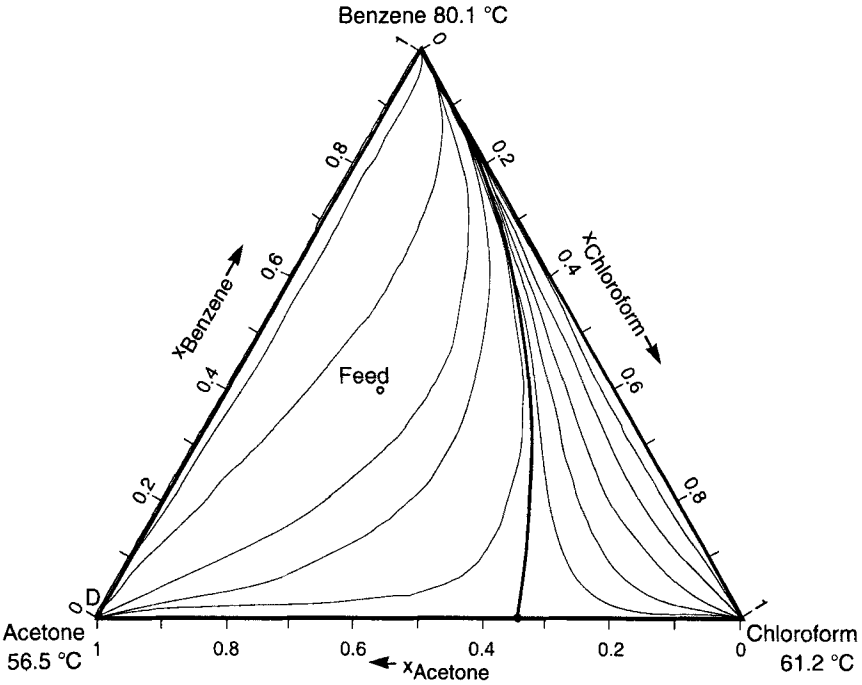

FIG. 25. Residue curve diagram for acetone/chloroform/benzene mixture. A residue curve boundary passes from the maximum-boiling azeotrope between acetone and chloroform to pure benzene.

column having lots of trays and a very high reflux ratio. The simulations can be carried out versus the amount of distillate product drawn off relative to the amount of feed, i.e., versus *D/F*. We shall assume for the moment that a column with lots of trays and a large reflux ratio will give us the maximum separations possible. That is true for ideally behaving mixtures, but (as we noted earlier and shall discuss later) it does not have to be true for azeotropic mixtures. Nonetheless, we proceed with that assumption.

Figure 26 is a sketch of the results obtained by carrying out these rigorous simulations. (It should be noted that some of these simulations can be very difficult to converge.) For small *D/F*, the top product of our column is pure acetone, the most volatile species in the region of the feed. At $D/F = 0$, the bottoms product is, in fact, the feed. As we take more and more overhead, the bottoms product moves on a trajectory away from the feed composition in the direction opposite the pure acetone vertex, continuing either until all the acetone is removed or until the bottoms product hits a distillation boundary. If we do not hit a distillation boundary, we should continue to get pure acetone until $D/F = 0.36$, the fraction of the feed that is acetone. However, at *D/F* values

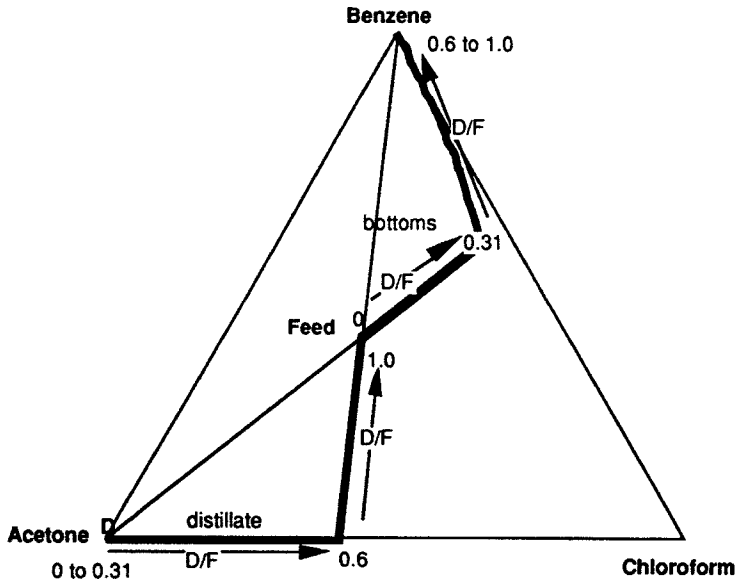

FIG. 26. Trajectories for distillate and bottoms products versus *D/F* for column.

above 0.31, the rigorously simulated column will no longer yield pure acetone in the top. We surmise we have hit a distillation boundary at the bottom of the column as the bottoms still contains acetone, and we now find chloroform showing up in the distillate.

Increasing *D/F* further causes more and more chloroform to appear in the tops while all of the benzene remains in the bottoms; it becomes purer and purer in benzene as we proceed. When *D/F* reaches 0.60, the bottoms is 40% of the feed, and it is essentially pure benzene. The feed was 40% benzene. Thus, the top must be essentially pure acetone and chloroform, which it is. Increasing *D/F* further forces some of the benzene to exit with the top product. At *D/F* = 1, the top product is the feed. The limiting composition for the bottoms is pure benzene, the point where the temperature is highest in the distillation region in which the column is operating.

We have, with this set of computations, discovered a portion of the residue curve boundary for this mixture. It is the portion that is most relevant for our feed mixture. This analysis also gives us a first estimate for the set of *reachable products* using distillation for this mixture. (The analysis is not complete, as we shall see later, because it does not discover what we might be able to reach with smaller reflux ratios.)

It is possible to show these results without using a triangular composition plot. In this form now to be proposed, we can imagine using a computer to detect the behavior we have just described.

First, we formally define the idea of a *binary separation range* for each of the binary pairs. This range is the *length* of the vectors on the plots we used earlier to indicate the part of a task that a column accomplishes. An equation to compute such a range for each value of *D/F* used in simulating the column is the following:

$$\text{separation range}_{ij} = \left| \left(\frac{f_i}{f_i + f_j} \right)_{\text{distillate}} - \left(\frac{f_i}{f_i + f_j} \right)_{\text{bottoms}} \right|$$

If both species go entirely to opposite products, the separation range is unity. If both are entirely in one product, there is no separation and the separation range has a limiting value of zero. We are looking for the maximum points in this plot, Fig. 27. (There are other useful representations we could plot, such as the molar flowrates for each of the species leaving in the distillate or bottoms or the splits on the species—e.g., 50% going into the distillate. Each of these gives a slightly different view, but all are aimed at indicating interesting products among the many possible.)

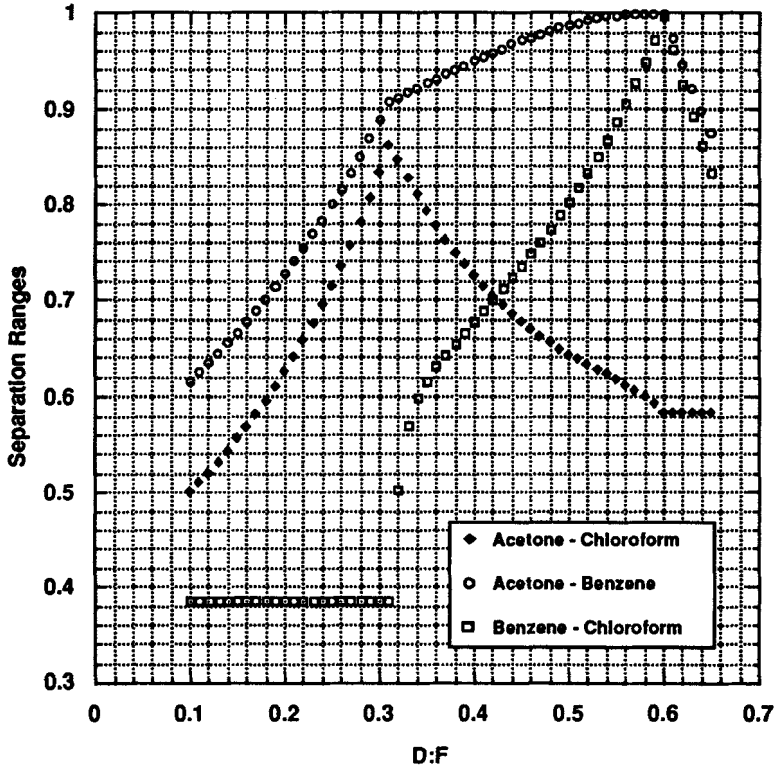

FIG. 27. Separation ranges obtained by rigorous distillation column simulation.

We would see the same interesting points we discovered before in these data:

- At ***D/F* of 0.31,** we *maximize* the separation of acetone to chloroform.
- At ***D/F* of 0.6,** both the acetone/benzene and benzene/chloroform ranges maximize at *unity*—implying that all the benzene is in one product and acetone and chloroform are in the other.
- At **just below *D/F* of 0.6,** we find a point where the amount of acetone in the bottoms product is so low that acetone can exit with the chloroform in a subsequent column while leaving the chloroform product contaminated with no more than 1% acetone, which is pure enough to meet specs.

We show these separations on a triangular composition plot in Fig. 28. The three interesting splits are as follows:

- The direct split: A top product of *pure acetone,* the bottoms being a mixture of all three species in significant amounts.
- The indirect split: A bottom product of *pure benzene,* the top being *only acetone and chloroform*—(two interesting products).
- The intermediate split: A bottom product which is a mixture of benzene and chloroform with a trace of acetone. The ratio of acetone to chloroform

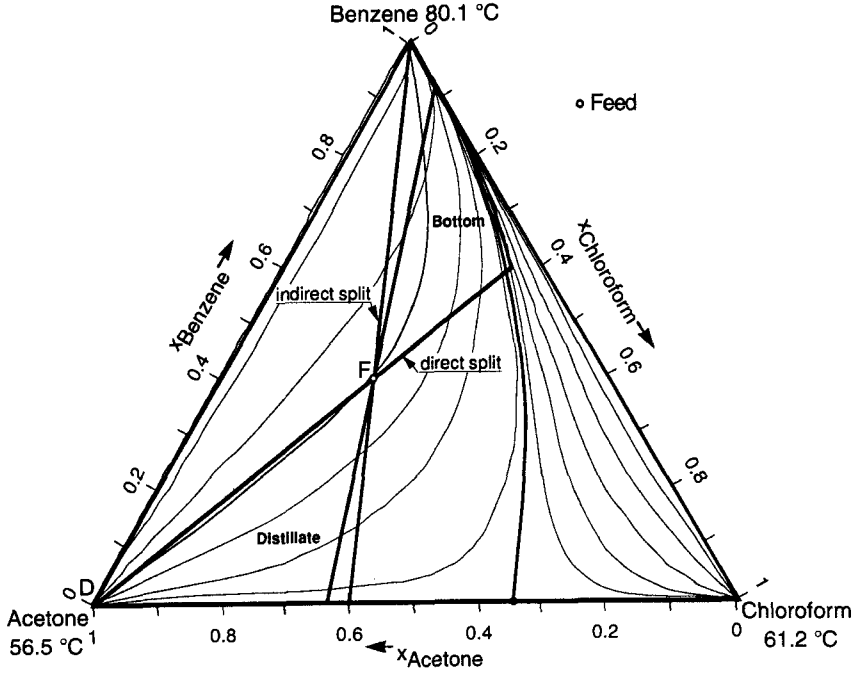

FIG. 28. The three most interesting splits for the acetone/chloroform/benzene problem.

in this bottom product is just that required for the chloroform product—1% acetone relative to the chloroform. The top is a mixture of acetone and chloroform.

1. Indirect Split: Alternative 1

The indirect split produces two interesting products in one column. However, we can quickly see that removing pure benzene as the bottom product in the first column is not a useful starting point. It leaves us with a binary mixture of acetone and chloroform to separate. A second column will give us a top product of acetone and a bottom product which is the maximum-boiling azeotrope formed by acetone and chloroform. We will need some way to break this azeotrope, which, as we shall discover, can be done using benzene. Thus removing benzene first is, in fact, counterproductive. Anticipating better success by leaving benzene in, we shall rule out considering this option.

2. Mixing to Get Two Desired Products from One Column: Alternative 2

We might be able to use mixing to get two interesting products from a single separation. We note we can mix benzene with the original feed to move the material balance line so it permits acetone to be the top product and a fairly acetone-free benzene/chloroform mixture to be the bottom product. Doing so means we can get a solution to our problem that involves only two columns. The material balance lines for the mixing task and the two columns are shown in the triangular diagram in Fig. 29, along with the corresponding process flowsheet.

First, benzene is mixed with the feed, yielding the mix point *M*. This mixture feeds column 1, yielding a pure acetone top product and a bottoms of virtually all the benzene and chloroform plus a trace of acetone. This bottom product is fed to column 2, where it is separated into benzene product and chloroform product. Part of the benzene product is then recycled to mix with the original feed.

Recycling material to alter a column feed so a single separator can produce two desired products can often be a feature of these processes. In the next alternative solution, we shall again propose a recycle, but this time it allows us to separate an intermediate product.

3. Direct Split: Alternative 3

The next alternative flowsheet we shall consider starts with the direct split, where we take pure acetone off as product from the first column. The material

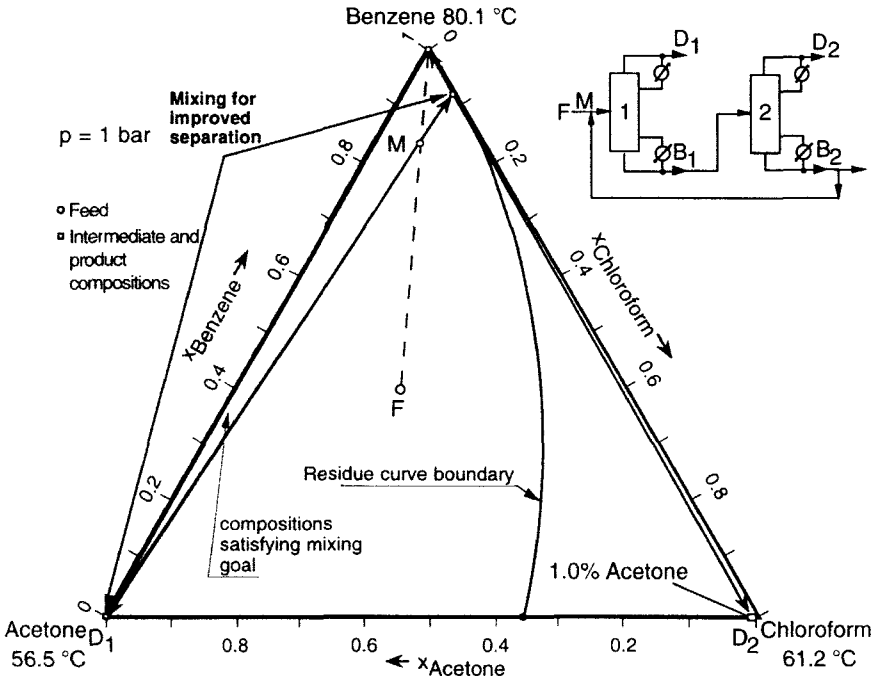

FIG. 29. Flowsheet resulting from use of recycle mixing to improve separations.

balance lines for the columns and mix points required are shown in the triangular plot in Fig. 30.

The first column produces nearly pure acetone from the top and a mixture of all three species in the bottom. This mixture is near the distillation boundary and occurs when D/F is about 0.31, as we saw earlier. We feed the bottom product to a second column, which separates benzene (bottom product) from the acetone and chloroform in its feed (top product). We find we can draw a material balance line through the mixture fed to column 2, which connects benzene to a mixture of acetone and chloroform in the other (right-hand side) region *because of the curvature of the distillation boundary*. This curvature is often important in devising separation schemes.

The top product from the second column, D_2, is separated into pure chloroform (top, D_3) and a mixture of acetone and chloroform very near the maximum-boiling azeotrope (bottom, B_3). We now seem to have an impasse, as we have an azeotrope to separate, just as we did for alternative 1. This time, however, the impasse is not "impassable."

We examine the separation ranges covered by the three columns already proposed. Figure 31 shows these ranges. To read this figure, examine the three ranges shown for column 1. The range covered by column 1 for the acetone/

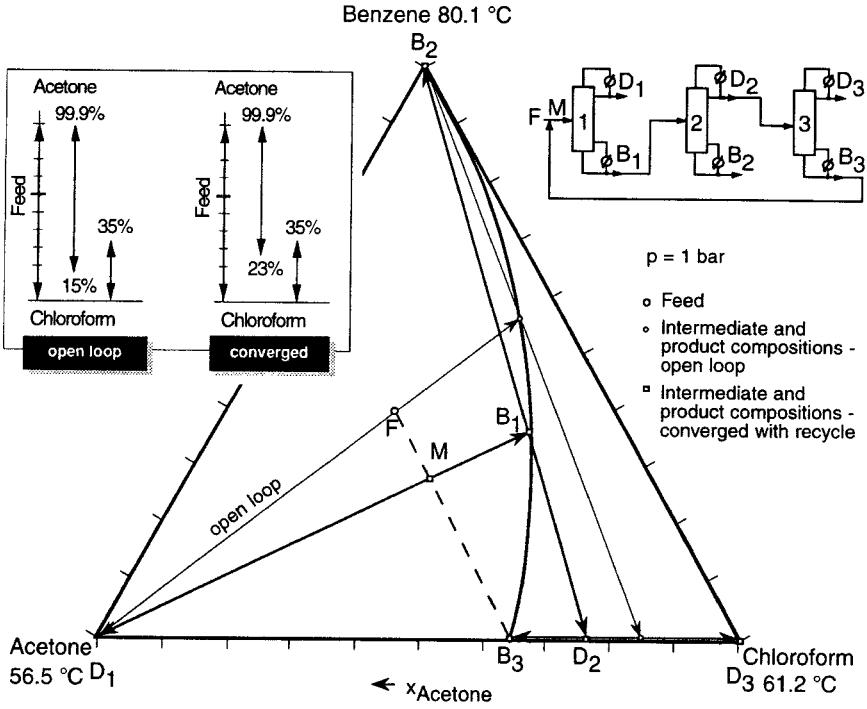

FIG. 30. Three-column alternative that starts with direct split.

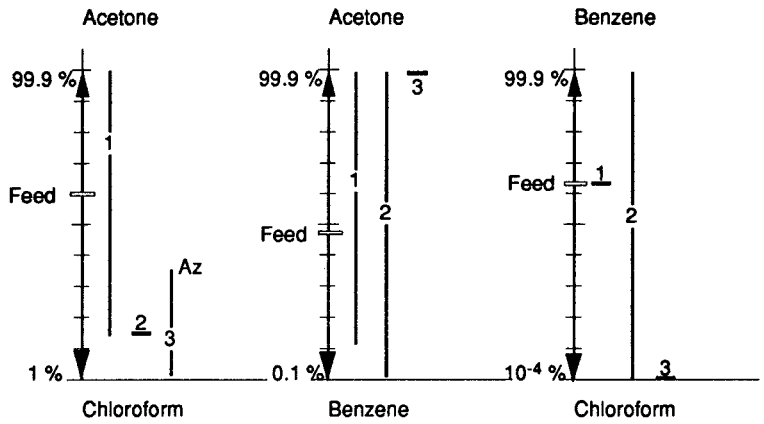

FIG. 31. Separation ranges covered by three columns for second flowsheet alternative. Column numbers are shown on their respective ranges.

chloroform binary mixture is from a top product of pure acetone to a bottom product that is about 15% acetone in chloroform—the mixture on the distillation boundary. We can discover the "15%" by projecting from pure benzene through the bottom product to the acetone/chloroform edge. This projection gives the composition of the mixture on a benzene-free basis.

Projecting from the chloroform vertex through the top and bottom products to the acetone/benzene edge gives the range covered for the acetone/benzene split by column 1. The binary range is from pure acetone (top) to a mixture of about 11% acetone in benzene (bottom).

Projecting from the acetone vertex to the benzene/chloroform edge shows that column 1 does not affect the ratio of benzene to chloroform. It is the same in all products as it is in the feed (for the pure acetone, this is a limiting condition). We show the range for column 1 for this binary mixture as being unchanged from the feed.

Figure 31 also shows the results for columns 2 and 3. Examining all these separations, we see that the entire ranges for all binary pairs are covered with the structure proposed so far. We have, in a sense, already solved the separation problem. We should therefore consider feeding the azeotropic mixture coming off the bottom of column 3 back into this process to separate it. We propose putting it back into column 1, as all three columns are needed to cover all the ranges that this feed requires for it to be separated. Figure 30 shows the flowsheet for this option with this recycle.

Feeding the azeotrope back shifts the composition of the total feed to column 1 to a point between F and B_3. We need to check that the resulting flowsheet will function as proposed. It does: the point M is the result of carrying out a rigorous simulation for the flowsheet, including the recycle. In the upper left of Fig. 30, we show the range covered by the acetone/chloroform split by the original structure (open loop—i.e., having no recycle) and by the final structure (with the recycle).

Finding that an intermediate column product can be recycled because a structure already exists to separate it is like discovering a recursive solution to our separation problem. This reason for recycling is different from the one for the previous alternative; it is a necessary part of many of these flowsheets.

4. Intermediate Split: Alternative 4

The last alternative we consider is to start with the intermediate split, where we remove a mixture of benzene, chloroform and a trace of acetone in the bottom product of the first column. (See Fig. 32.) Without a systematic approach, we would very likely miss this alternative. We separate the bottom product from the first column into benzene and chloroform in a second column. The top product from the first column is a mixture of acetone and chloroform,

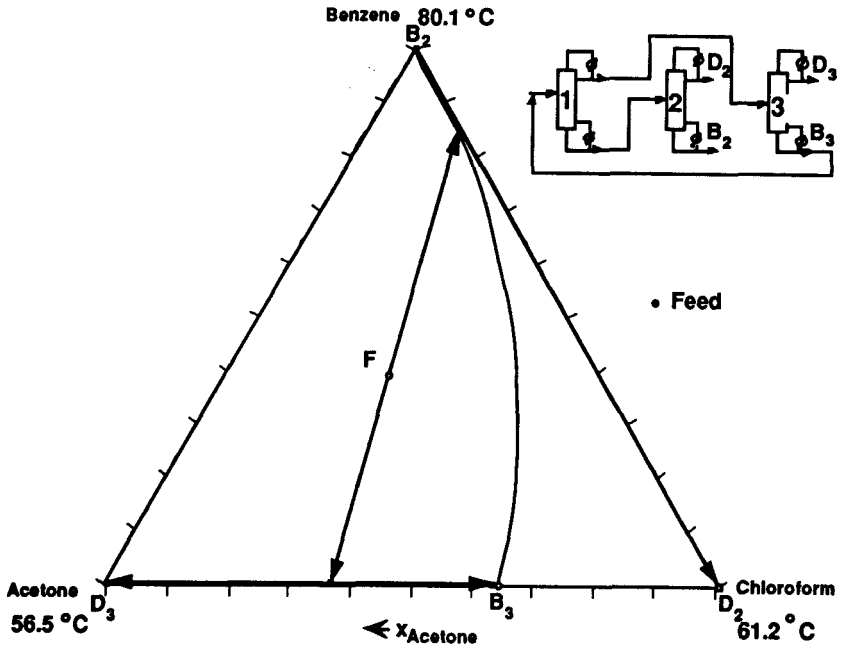

FIG. 32. Alternative three-column flowsheet. Again, note mixing of the azeotropic mixture, B_3, with the feed.

which we separate in a third column into acetone and the azeotrope between the acetone and chloroform. Using reasoning similar to that for the third alternative, we propose recycling this azeotrope back to the first column.

5. *A General Approach to Creating Alternatives*

Figure 33 summarizes the steps we take to generate alternatives for these complex separation processes. We can illustrate the approach by reviewing the steps we took for the current problem.

Starting with a feed mixture and product specifications, we analyze the feed and products to discover the binary splits required. We then place the feed onto a stack of streams to be processed. The stack is not empty, so we select the feed stream. It is not a product. We determine its binary concentrations and pass through the next two steps downward because no structure already exists that could serve as a partial structure to separate it. We select a separation method using our knowledge about the problem; here, we pick distillation. The "v" shown in this box means that several different options might be proposed here, with the different solutions branching along different paths. As we are considering ordinary distillation, we do not need to pick a separation agent.

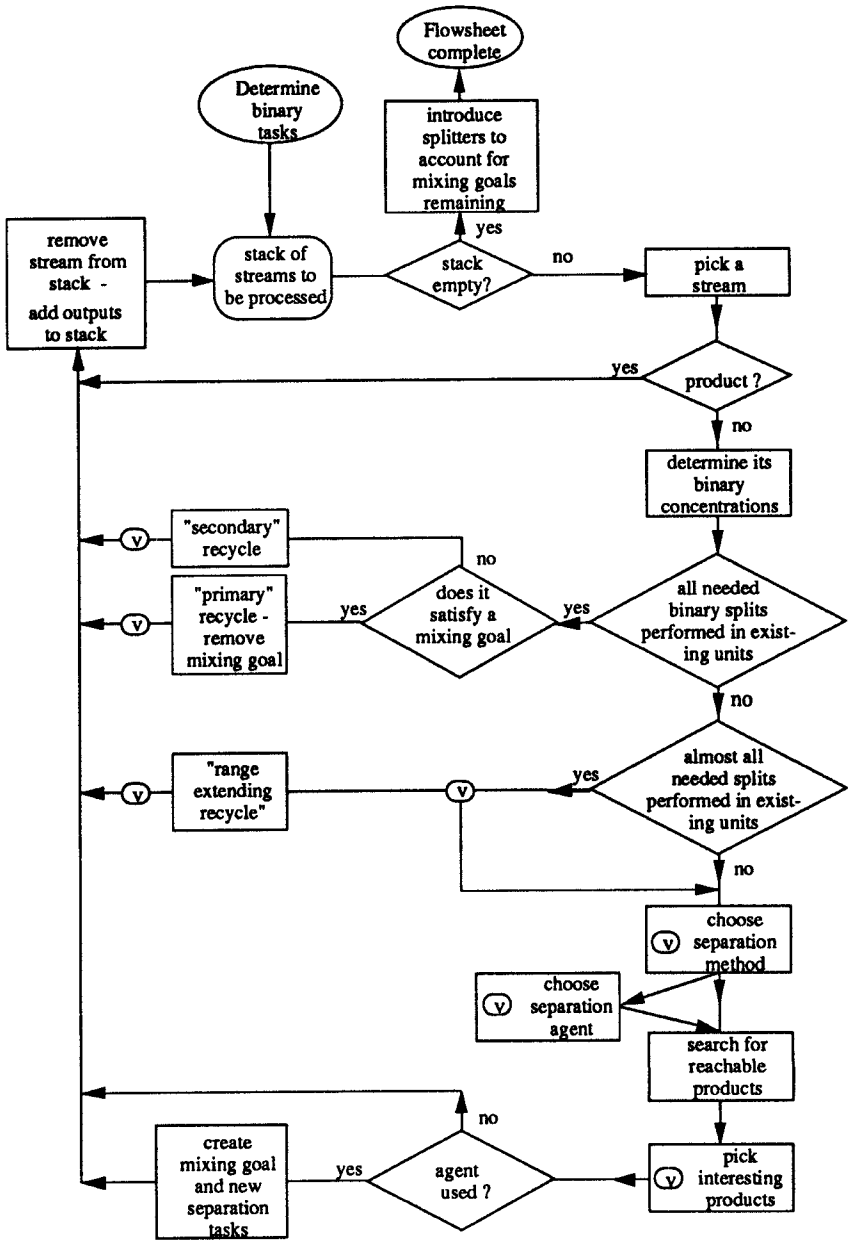

FIG. 33. Algorithm to create alternatives.

Simulations for differing *D/F* ratios sweep out the reachable separations. The interesting products among these are acetone, pure benzene, an acetone and chloroform mixture with no benzene, and a bottom mixture of benzene, chloroform, and a trace of acetone. We need to consider each of these as starting points for alternatives.

No separating agent was used, so we consider using mixing to create separation tasks that might allow two interesting products to occur in the same next step. We do see such a possibility—mixing something (which we selected to be benzene) with the feed to move it to a material balance line between acetone as a top product and the benzene/chloroform mixture with a trace of acetone as the bottom product. The need for something to mix with the feed is placed on the list as a new separation task. *Note:* Anything above the material balance line that can move the feed to that line is a legal stream for mixing. It just happens that benzene is a fairly obvious choice here.

We remove the feed from the stack and continue with the current option. We have a top product of acetone. Since acetone is a product, we cycle back from the step that tests if it is and remove it from the stack. We also have the benzene/chloroform mixture with a trace of acetone to process.

We make this mixture the stream to consider and proceed through the steps with it. The alternative flowsheets arise when we return to steps where we created alternatives, such as the one in the lower right where we have a number of interesting products not yet considered.

There are three recycle decision steps shown in the middle of the diagram. An instance of a primary recycle is the use of another stream (we used benzene) to move the feed to the material balance line between two interesting products so that both may be produced by one separator. Benzene, being a product, would be discovered in the step before last (introduce splitter to account for mixing goals remaining) rather than here, however. The recycling of the azeotropic mixture of chloroform and acetone back to the first column is an example of a secondary recycle. We have not seen the third case for recycle—a range extending recycle. There are times when a downstream separator does not have some of the species in its feed which, if they were there, it would separate to some extent. Thus we might still propose recycling a stream if the flowsheet proposed so far almost covers all the splits needed to process that stream.

We now consider a more complex example where liquid/liquid extraction and extractive distillation are among the processes to appear in the solution.

B. Azeotropic Separation: Example 3

We wish to devise a separation process based on distillation, liquid/liquid extraction, and extractive distillation for the mixture of solvents shown in Fig.

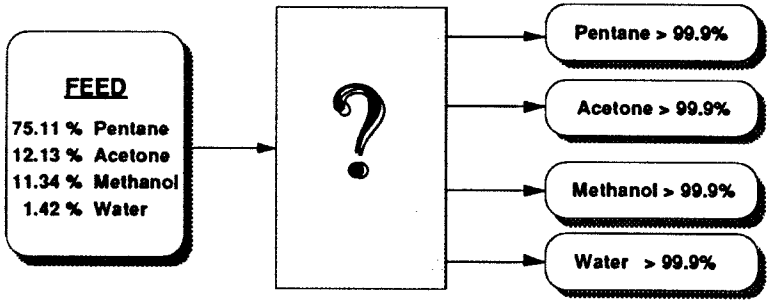

FIG. 34. Specifications for feed and products for Example 3.

34. Solvent recovery systems are often very complex systems to design, as they need to separate very different molecules.

We start by computing the infinite-dilution binary data shown in Table IX. The upper values are K-values at the boiling point of the more plentiful species. We will also need liquid activity coefficients if we wish to consider extraction processes; the lower values in each entry are infinite-dilution binary liquid activity coefficients at ambient conditions.

We now need to think of all the reasonable ways we might separate this very complex mixture. We shall use insights from the above data as well as any insights we have as chemical engineers. This step is a knowledge-intensive one.

Since pentane and water exhibit immiscibility, we might consider *decantation* as the first step. If it worked, it would be an inexpensive one to carry out. But a rigorous three-phase equilibrium calculation predicts that, in the presence of acetone and methanol, the small water fraction in the feed does not form a second liquid phase; so we reject this idea. The calculation also reveals that the feed mixture is almost at the azeotropic composition for the pentane/methanol binary pair.

TABLE IX
INFINITE-DILUTION PAIRWISE K-VALUES AND ACTIVITY COEFFICIENTS FOR EXAMPLE 3

$C_j \setminus C_i$	Pentane	Acetone	Methanol	Water
Pentane	1.0	3.0 (min)	5.9 (min)	71.4 (het)
	1.0	6.6	23.1	1537
Acetone	7.9	1.0	1.3 (min)	1.05 (min)
	4.7	1.0	2.0	7.4
Methanol	29.6	2.4	1.0	0.4 (ok)
	14.4	2.0	1.0	1.6
Water	8106	38.5	7.8	1.0
	3213	11.5	2.2	1.0

Next, we consider *distillation;* but, with the exception of water and methanol, all other pairs exhibit azeotropic behavior. Also, water is present in very a small amount here. We should be trying to get rid of the pentane first. Thus, distillation does not seem an appropriate first step.

If distillation is rejected, we might consider *extractive distillation.* The K-values of acetone and methanol at infinite-dilution (38.5 and 7.8, respectively) in water indicate that water could be used as an extractive distillation agent for the separation of these species. However, adding water would almost certainly introduce a second phase with the pentane.

If used, we would create two liquid phases in view of the calculations we did above to see if decantation is a good first step.

If water will force us to have a second phase, we might then consider using *liquid/liquid extraction.* We shall see that this is a good suggestion. Before evaluating it, however, we need to review some important ideas associated with liquid/liquid extraction.

Liquid/liquid extraction is typically used to remove small amounts of heavier species mixed with a large amount of a light species. Conventional distillation would require a large amount of the lighter species to be condensed overhead and would tend to be uneconomic. An example would be to remove a small amount of ethanol from a lot of diethylethyl ether. As a bulk separation method, liquid/liquid extraction is also suitable for isolating fractions of species with similar molecular structure from other species, as is the case when separating alkanes from aromatics. The extraction is done, for example, by finding a solvent such as acrylonitrile that likes the aromatics and forms a separate liquid phase with the alkanes. Extraction is usually performed at temperatures well below the boiling points of the species involved, which makes activity coefficients, γ, a better means of evaluation than vapor–liquid K-values.

The composition of species distributing between two liquid phases, I and II, is determined by equating their respective fugacities:

$$x_i^{\mathrm{I}}\gamma_i^{\mathrm{I}}f_i^{\circ\mathrm{I}} = x_i^{\mathrm{II}}\gamma_i^{\mathrm{II}}f_i^{\circ\mathrm{II}}$$

where x_i are mole fractions, γ_i are activity coefficients, and f_i° are standard-state fugacities. Assuming that the same standard-state fugacities are used for both phases (for example, pure liquid i at the temperature and pressure of the mixture), we see that the ratio of mole fractions is the inverse of the ratio of activity coefficients; i.e.,

$$\frac{x_i^{\mathrm{I}}}{x_i^{\mathrm{II}}} = \frac{\gamma_i^{\mathrm{II}}}{\gamma_i^{\mathrm{I}}}$$

To separate two species, we need to know how well the two phases differentiate between them in this ratio. Separability factors, $S_{ilk}^{\mathrm{I/II}}$, are frequently used to indicate potential for separation:

$$S_{i/k}^{\mathrm{I/II}} = \frac{x_i^{\mathrm{I}} / x_i^{\mathrm{II}}}{x_k^{\mathrm{I}} / x_k^{\mathrm{II}}} = \frac{\gamma_i^{\mathrm{II}} / \gamma_i^{\mathrm{I}}}{\gamma_k^{\mathrm{II}} / \gamma_k^{\mathrm{I}}} = \frac{(\gamma_i/\gamma_k)^{\mathrm{II}}}{(\gamma_i/\gamma_k)^{\mathrm{I}}}$$

Returning to our example solvent-separation problem, let us consider using liquid/liquid extraction to remove pentane from methanol and/or acetone. A suitable solvent is one that is immiscible with the bulk species, pentane. If at all possible, we would like the solvent to be present in the mixture so we do not have to introduce any other species into our separations problem. For our example problem, water is present. Noting the infinite-dilution K-values for water and pentane, we see that water will be highly immiscible with pentane.

Aside from being immiscible with the pentane, the solvent, water, has to effect a reasonably different distribution of the species to be separated, methanol and/or acetone and pentane.

We consider methanol first. For a quick estimate of the separation factors that water can produce, we consider the limiting selectivity that would be obtained if the methanol and pentane were infinitely dilute in both the extract phase (water-rich) and the raffinate (pentane-rich) phases if we were to use liquid/liquid extraction:

$$S_{\text{methanol/pentane}}^{\text{water-rich/pentane-rich}^{\infty}} = \frac{(\gamma_{\text{methanol}}^{\infty} \gamma_{\text{pentane}}^{\infty})^{\text{pentane-rich}}}{(\gamma_{\text{methanol}}^{\infty} / \gamma_{\text{pentane}}^{\infty})^{\text{water-rich}}} = \frac{(23.1/1.0)}{(2.2/3213)} = 33{,}740$$

Selectivity is excellent.

Although selectivity between acetone and pentane (using water and pentane as the extract and raffinate, respectively) is not quite as high ($\approx$ 1850), it still suggests that we could separate these species, too.

We use rigorous simulation to determine feasible separations using water as a solvent. For a theoretical ten-stage liquid/liquid extraction process, we find that rather little water is needed to recover virtually all methanol from the pentane. At higher solvent flowrates the water-rich extract contains more and more acetone, but it cannot produce a complete separation of acetone and pentane. Thus, we select the solvent flow at which the methanol–pentane separation is sufficiently sharp. Figure 35 gives the separation selected.

As shown, the raffinate stream, F_{11}, leaving such an extractor essentially contains pentane and acetone plus a trace of water. This pentane-rich mixture can be separated in a distillation column, producing pentane as bottoms and a distillate which is limited to the minimum-boiling azeotrope between pentane and acetone. (The infinite-dilution K-values of 7.9 and 3.0 indicate that such an azeotrope exists.) Figure 36 gives the flowrates and relative concentrations between the major species of the streams entering and leaving the distillation column (labeled DI-2) that carries out this separation for the raffinate (pentane-rich) stream.

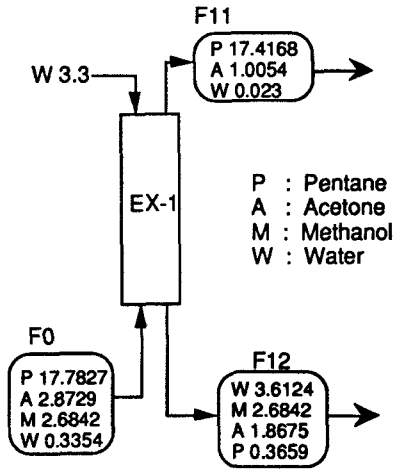

FIG. 35. Liquid/liquid extraction step to recover methanol.

It is evident that we have produced one of our desired products here, nearly pure pentane. We now have to separate the near-azeotropic stream, F_{21}. An ideal situation occurs if we can recycle it back to the liquid/liquid extractor. If its composition is close to that of the original feed to the process, we could simply mix it with the feed. Our two separation devices then would process this feed, giving us a pure pentane product and, by material balance, a second stream which is the feed but with this same amount of pentane missing.

How might we decide if the stream F_{21} coming from the top of the second column is close enough in composition of the extractor feed to be recycled back and processed with it? Two characteristics of the stream F_{21}—its composition and its flowrate—must be important in this decision. If the compositions of the two streams are really close, we assume there should be no problem, no matter the flowrate. On the other hand, if there is very little flow in F_{21} relative to the feed (for example, only one drop), then we should almost always be able to

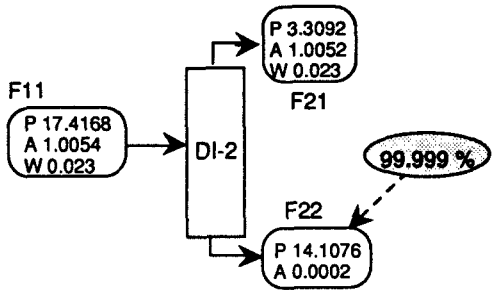

FIG. 36. Distillation column to remove acetone from pentane.

recycle it, no matter its composition. The total flowrate for the distillate stream F_{21} is 16% of that of the original total feed to the process. It is modest, but not negligible. It contains essentially only pentane and acetone, which are in the ratio of 3.3 to 1, while the feed has these same species in the ratio of 6.2 to 1.

We can perform approximate material balance calculations to see what happens to the process if we were to recycle the distillate and process it with the feed. We model each separator as a set of constant split factors for each species. For example, we see that 97.94% of the pentane, 35.00% of the acetone, and none of the methanol leave in the top stream from the extractor. Water enters as the extraction agent and also as a small part of the feed; 0.63% of the total water entering leaves with this top stream. We capture these results in the first three rows of numbers in Table X. We denote molar flow for species k in stream j leaving unit i by $\mu_{ij}[k]$, and the fraction of the flow of species k in the feed to unit i leaving in stream j by $\xi_{ij}[k]$.

Examining the distillation column, we find that 19.00% of the pentane entering it leaves in its distillate product. Similarly, 99.98% of the acetone and 10% of the water entering leave in the distillate. We assume these numbers do not change even if we recycle the distillate product from the second column. We capture these numbers in Table X, too.

The following equation gives the material balance for the total flow $\mu'_{0*}(k)$ of a species k entering into the extractor when we recycle stream F_{21}.

$$\mu'_{0*}(k) = \mu_{01}(k) + \mu_{02}(k) + \xi_{11}(k)\xi_{21}(k)\mu'_{0*}(k)$$

For example, the total flow of pentane into the extractor equals the pentane in the original feeds plus that which recycles, which is $0.9794 \cdot 0.1900$ times the total flow of total pentane into the extractor. Solving for the total flow of species k into the extractor, we get

$$\mu'_{0*}(k) = [\mu_{01}(k) + \mu_{02}(k)] \frac{1}{1 - \xi_{11}(k)\xi_{21}(k)}$$

TABLE X

APPROXIMATE MATERIAL BALANCES FOR FIRST TWO UNITS TO ESTIMATE IMPACT OF RECYCLING DISTILLATE PRODUCT BACK TO EXTRACTOR

	Pentane	Acetone	Methanol	Water
Total original feed, $\mu_{01} + \mu_{02}$	17.7827	2.8729	2.6842	3.654
Top product from extractor	17.4168	1.0054	0	0.0230
Fraction of feed in top product, ξ_{11}	0.979	0.350	0	0.0063
Distillate product from column	3.309	1.0052		0.0023
Fraction column feed in distillate, ξ_{21}	0.1900	0.9998		0.1000
$\frac{1}{1 - \xi_{11}(k)\xi_{21}(k)}$	1.229	1.538	1	1.0006
New feed (original feed times above factor)	21.9	4.42	2.68	3.64
Composition original feed	0.659	0.106	0.100	0.135
Composition of extractor input with recycle	0.670	0.136	0.082	0.112

which, when applied to pentane, gives

Total flow of pentane into the extractor = $17.7827/(1 - 0.1861) = 21.9$

In a similar manner, we can compute the total flows for the other species, getting the results shown in the third line from the bottom of Table X. Finally, we compute the compositions for the original feed and for the feed after adding the recycle so we can compare them. We see that these compositions are surprisingly close to each other. The net result of recycling here is to increase the flow of the feed to the extractor unit by approximately 20% but with little impact on its composition. We therefore elect to recycle the distillate.

We now return to consider the extract stream F_{12}, from our first separation step. It still contains all species in nonnegligible fractions. We propose that this mixture be distilled. We check if distillation is reasonable by using rigorous simulation. While we do not show the details of these runs here, they were carried out by varying *D/F* ratios over a range of values as we did when we were investigating the acetone/chloroform/benzene example earlier. These runs indicate two interesting product sets. One allows for the complete removal of water. However, because water is a candidate separating agent for the acetone/methanol split, we put it aside and consider the other option—namely, to recover all the pentane.

Figure 37 shows the results from carrying out a rigorous simulation for this option. Because pentane forms azeotropes with acetone and methanol, these species appear in both products. Noting that although F_{31} is a much smaller stream than F_{21}, it has similar compositions, we decide to recycle it back to the extractor feed also. The bottom product of column DI-3 consists of acetone, methanol, and water–with *no pentane.*

Let us examine what we have accomplished with the liquid/liquid extraction step followed by the two distillation columns. The "upper" column, DI-2, produces essentially a pure pentane product, which we remove. The "lower" column, DI-3, produces a product with no pentane. We recycle all the other streams

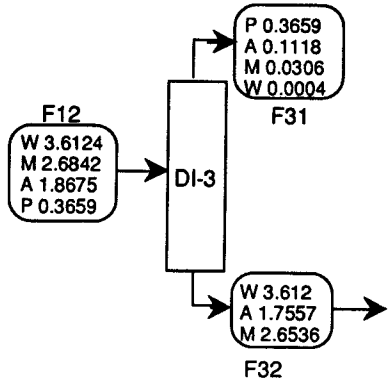

FIG. 37. Distillation column to remove pentane from methanol and water.

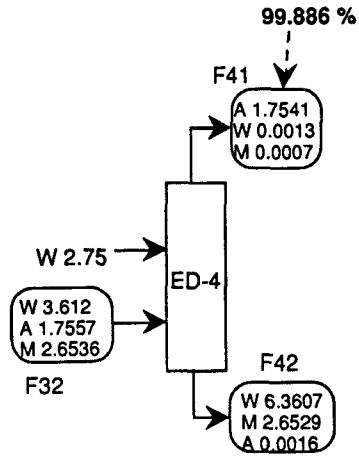

FIG. 38. Extractive distillation column to separate methanol from acetone.

so these three units, collectively, are there to remove pentane from the original feed.

So what do we do with the mixture coming off the bottom of the lower column, DI-3? Looking at our earlier data, we see that water boils at a higher temperature than the two remaining species and does not form an azeotrope with either of them. The *K*-values of acetone and methanol at infinite-dilution in water (38.5 and 7.8, respectively) suggest that water could be used as an extractive distillation agent for the separation of these species. In such a column, acetone, being decidedly more volatile, is recovered as a pure distillate product. It should be noted that, because of the tangent pinch between acetone and water, this column might best be operated below ambient pressure to exploit the improved vapor–liquid equilibrium near this tangent pinch. The results shown in Fig. 38 are from simulating such a column.

Finally, the bottom product of the extractive distillation column, ED-4, can be separated in a simple column since it contains the nonazeotropic species methanol and water only. This column is shown is Fig. 39, again based on a rigorous simulation.

The process produces all the desired pure species products. The water product from our last column, DI-5, also has to provide the water used as the extractive agent in the liquid/liquid extraction step and in the extractive distillation step. The complete set of steps is shown in the flowsheet in Fig. 40.

We now need to put in the proposed recycle flows to see if the structure discovered is possible when they are present. Rigorous simulation gives the results shown in Fig. 41. It is noteworthy that, despite the complexity of the nonideal mixture behavior, it has been possible to obtain all species as highly pure single-species products using only water which is already present as the separating agent.

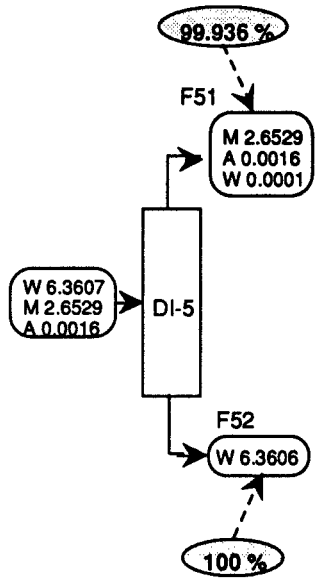

FIG. 39. Water/methanol separation.

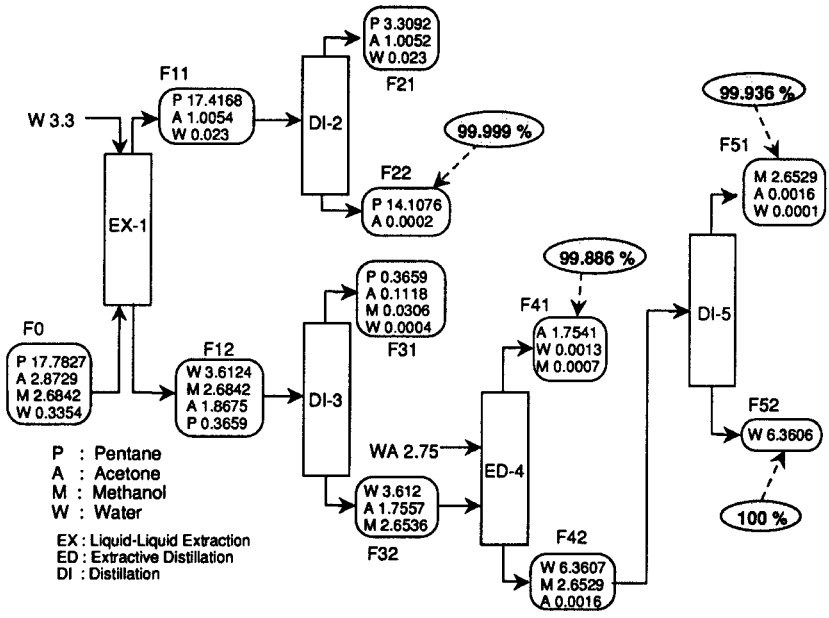

FIG. 40. Total process flowsheet before adding recycle streams.

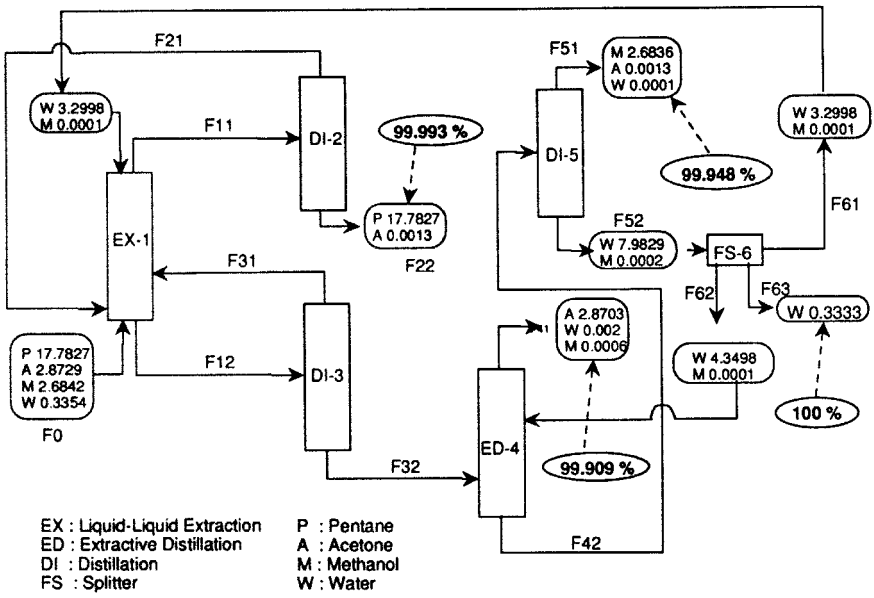

FIG. 41. Total flowsheet after including recycles.

We note that the liquid/liquid extraction step accomplishes separations across three relatively azeotropic compositions: namely, that between acetone and pentane, that between methanol and pentane, and that between water and pentane. It should also be noted that, since the extractor does not have to perform sharp separations, it requires an overall optimization to determine how many stages should be used. In principle, a single stage or, in other words, a simple decanter should suffice to make the process feasible.

The comparison between the simulation results for the original steps while they were being proposed and the final process with the recycles included shows that it is indeed possible to maintain the separation functionality of a sequence, and even to slightly improve the achievable purities—one of the essential premises of the sequential synthesis approach being advocated here.

Alternatives to this process are generated by returning to those steps where we made decisions and checking to see if alternatives decisions might exist. For example, we could look for a different extraction agent in the liquid/liquid extractor. We eliminated one obvious alternative when we discovered that adding more water to the liquid/liquid extractor did not allow us to remove all the acetone from the top product stream even though there is a good separation factor suggesting this alternative.

Sargent (1994) presents a related approach to the synthesis of distillation processes. His goal is to generate a superstructure of interconnected columns from a "state/task" network. The superstructure contains all the process alter-

natives as substructures. For ideally behaving species, he reproduces the superstructure proposed earlier by Sargent and Gaminibandara (1976).

For nonideal systems, Sargent first determines all the distillation regions. He then labels the pure species and all the azeotropes as pseudo-species in the system, giving the label A to the most volatile, B to the next, and so forth. For example, he would label the diagram in Fig. 25 for acetone, chloroform, and benzene with A for acetone, B for chloroform, C for the maximum-boiling azeotrope between acetone and chloroform, and D for benzene. The region on the left side of the distillation boundary has the species A, C and D, while the region to the right has the species B, C, and D. He then uses the "bow-tie" analysis we discussed earlier (and which we shall discuss in more detail in Section IX.B) to identify the reachable products for each of the regions. For example, in the left region, a first column can produce A, AC, CD, and D as products—where CD is a product along the distillation boundary. The product CD can be split in a second column. If the distillation boundary were straight, the distillate would be C (azeotrope) and the bottoms would be D (benzene). Here, however, the boundary is curved, indicating a mixture of B and C (azeotrope and chloroform) as the distillate product and D as the bottoms.

Sargent gives heuristic rules to suggest where to place recycle streams. Also, when two different columns give rise to the same product, he merges the products in the superstructure. By eliminating parts of the superstructure to form a substructure that produces all the products of interest, one generates a design alternative. Dropping different parts generates different alternatives.

To find the best substructure for a given feed, the idea is to optimize this superstructure to find the optimal substructure. Two potential difficulties arise: (1) It is difficult enough to solve the model equations for a single column displaying azeotropic behavior, much less optimize a superstructure containing several such columns with numerous recycles; (2) the superstructure almost certainly has local optima, requiring the use of much more costly approaches to find global optima. Although we shall overcome these restrictions in the next few years, they are currently serious difficulties.

IX. More Advanced Pre-analysis Methods

We re-examine how to assess species and equipment behavior when dealing with highly nonideal mixtures—this time in much more detail.

A. Species Behavior

In this section, we discuss advanced methods of finding azeotropes and determining if a mixture displays liquid/liquid behavior.

1. Finding Azeotropes

If a mixture forms an azeotropic composition, the vapor and liquid compositions at equilibrium are identical to each other. The following equations define this situation:

$$y_i = K_i x_i \qquad \text{for } i = 1,2, \ldots, n_C$$

$$K_i = K_i(T,P, \text{ all } x_i, \text{ all } y_i)$$

$$\sum_{i=1}^{n_C} y_i = 1$$

$$\sum_{i=1}^{n_C} x_i = 1$$

$$y_i = x_i \qquad \text{for } i = 1,2, \ldots, n_C - 1$$

There are $3n_C + 2$ variables (x_i, y_i, and K_i for all species, temperature T, and pressure P) in these $3n_C + 1$ equations. If we fix pressure, the model is completely fixed. Solving, we will determine the bubble-point temperature for the azeotrope as well as its composition. We note, therefore, that an azeotropic composition for a mixture is, as we already knew, pressure-dependent.

Suppose we have a mixture of water, pyridine, and toluene. We set the pressure to 1 atm and attempt to solve the above equations. Lacking any further insight, we set all the vapor and liquid compositions equal to 0.33333 and then attempt a solution using a Newton-based method. The problem with finding azeotropes becomes immediately evident. There are six solutions to these equations: the three binary azeotropes and the three pure species. There is no ternary azeotrope. To find all azeotropes for a mixture, we must find all solutions to the above equations. Finding multiple solutions to a set of highly nonlinear equations like these is usually a very difficult task.

We can attack this problem in two ways: (1) try to find a numerical procedure that will find all roots to a set of nonlinear equations, or (2) try to develop a method that uses physical insights to find all the roots.

We know of no numerical procedures that will guarantee finding all the solutions to an arbitrary set of nonlinear equations. "Continuation" methods are often capable of finding more than one solution if several exist. Fidkowski *et al.* (1993) propose using such a method along with discovering bifurcation points to compute all the azeotropic compositions for a mixture. Their homotopy function

$$\tilde{y} = \left[(1 - t) + t \frac{\gamma_i}{\phi_i}\right] \frac{P_i^{\text{sat}}}{P} x_i$$

causes the K-values for the species to move from those Raoult's law predicts to their nonideal values as the homotopy parameter t moves from 0 to 1. Except for very close-boiling species, there will be no azeotropes assuming Raoult's law. Thus, we know that only the pure species will satisfy these equations when the continuation parameter is 0. Their algorithm starts by solving these equations for $t = 0$ at each of the pure species. As the continuation parameter increases, these equations can become singular at one or more of the pure species' starting points. If they do, the singularity indicates the solution trajectory plotted versus the continuation parameter branches, one branch staying at the pure species (always a solution) and the other heading to the composition of a binary azeotrope along one of the adjacent binary edges of the composition diagram. An eigenvector analysis of the local linearized behavior of these equations indicates the direction for the bifurcating solution. The temperature along these branches increases for a maximum-boiling azeotrope and decreases for a minimum-boiling azeotrope. The solution along one of these branches may itself become singular, indicating a further bifurcation. Fidkowski and colleagues conjecture—and their computational experience suggests—that one will discover all azeotropes in the system by tracing all these solution trajectories starting from all pure species.

Wahnschafft (1994) has developed and tested extensively an interesting alternative method of finding all the azeotropes. The slight change that Wahnschafft makes has a significant impact on how to find azeotropes. He replaces the third and last of the equations above (i.e., $\sum_{i=1}^{n_C} y_i = 1$ and $y_i = x_i$ for $i = 1,2, ..., n_C - 1$) with

$$K_i = 1 \qquad \text{for } i = 1,2, ..., n_C$$

This alternative set of equations is generally satisfied only at azeotropic points involving all n_C species. Assuming for the moment that each n_C species system has only one azeotrope—i.e., that a binary mixture has only one binary azeotrope, a ternary system has at most one ternary azeotrope, and so forth—the advantage of the above formulation is that there are no longer multiple solutions to the same set of equations, but rather a different set of equations to find each of the azeotropic points. In particular, the pure species generally do not satisfy the azeotrope condition for any set of $K_i = 1$ involving more than just one species. The latter could happen only if an azeotrope occurred exactly at a pure species point—we would be talking about the special situation of a tangent pinch.

In principle, we could use any root-finding method for solving problems involving the equations $K_i = 1$ for combinations of species representing different tuples, such as all binary combinations, all ternary combinations, quaternary,

and so on, up to the one system of equation involving all n_C species. However, the root-finding methods may still suffer from convergence problems. Wahnschafft found that it is more robust to devise a continuation method that can lead up to the solution at the azeotropic points one wants to find.

Wahnschafft based his continuation method on a relaxation of the azeotropy condition for a given n_C species system. At an azeotropic point, all n_C K-values equal unity, which is a special situation of the condition that they are equal. In the surroundings of an azeotrope involving n_C species, the K-values are no longer equal to unity, but subsets of them will be equal to each other; in other words, the relative volatility between species pairs will still be unity at certain points close to an n_C species azeotrope.

Consider Fig. 42, where we plot three trajectories for a ternary system that involves three binary and one ternary azeotropes. At a binary azeotrope, the relative volatility between the two species involved, i.e., their K-value ratio, equals unity. We can seek out the trajectory emanating from this azeotrope into the three species region along which the relative volatility of these two species remains equal (i.e., along which their K-values remain equal). The K-value for the third species will generally be different. However, we find that, owing to the existence of the ternary azeotrope, there will be one specific composition along this trajectory where the K-value of the third species becomes the same as the other two; moreover that situation occurs as all three K-values become equal to unity. We can find the same point by tracing along another curve starting at either of the other binary azeotropes.

The trajectories along which two (or more) species have the same volatility have been called *isovolatility curves*. Based on the ability to trace out such curves in the composition space, we can outline a simple algorithm to robustly determine all azeotropic points that are predicted for a multispecies mixture:

(1) Fix the pressure at the value desired.

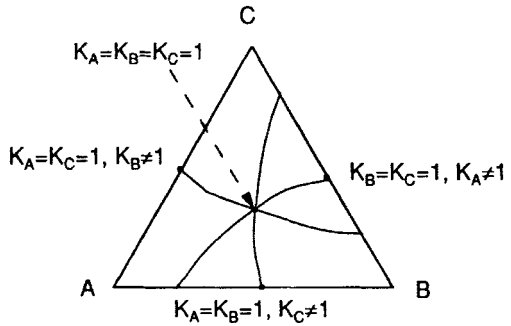

FIG. 42. Trajectories having subsets of all K-values equal to unity.

(2) Compute the infinite-dilution K-values for all pairs of species, as we did earlier to check for the existence of binary azeotropes. For this example, we would find that all three binary pairs display an azeotrope.
(3) Where a binary azeotrope exists (e.g., along the AB axis), use a Newton-based method to find the point along that axis where the two K-values are unity.
(4) At that azeotrope, compute the infinite-dilution K-value for one of the missing species.
(5) Increase the composition for that missing species—here, species C—monitoring its K-value. Solve the equations, keeping the K-values for the other two species equal to each other. Monitor the K-value of the newly introduced species (here, species C) to determine if its value gets close to unity (e.g., by checking for changing from values larger than 1 to values less than 1 or vice versa, and by checking the derivative of the K-value along the curve to see if it passes through a minimum or maximum). In either of these cases, we have approached a ternary azeotrope. Switch to solving the equations for the azeotrope (where all K-values are unity) using a Newton based method. If the trajectory hits the side of the composition space, stop searching along it.
(6) Given a ternary azeotrope and a fourth species in the mixture, compute its infinite-dilution K-value at this ternary azeotrope. Increase the amount of the fourth species, keeping the K-values for the other three equal to each other. Stop where the fourth K-value passes near 1 or shows a minimum or maximum along the trajectory being traced out. Solve directly for the four-species azeotrope. Stop searching this trajectory when it hits a side of the composition space.
(7) Repeat the second step above to find the remaining binary azeotropes. If more than a single binary, ternary, or higher-order azeotrope is suspected, march away from each of lower-order azeotropes toward it, as is done in the third and fourth steps above.
(8) And so forth.

The algorithm stops looking for azeotropes involving $n + 1$ species when there are no azeotropes involving n species. When applying this algorithm, we have to solve the equivalent of several flash unit calculations for each trajectory we trace. This algorithm very efficiently finds all azeotropes predicted by the physical property models being used for a multicomponent mixture. It does not require an eigenvalue/eigenvector analysis to spot bifurcations. Finally, it can be made to take advantage of the topological constraint that Zharov and Serafimov (1975) developed (see Section VII.A.1.c).

Doherty and Perkins (1979) examined the possibility of the existence of ternary azeotropes if there are no binary azeotropes. They show that the infinite-

dilution K-value for one of other species must be exactly unity at a pure species node, which is equivalent to saying that the isovolatility trajectory starts at a point which is a pure species and a binary azeotrope at the same time. Obviously such situations will be extremely unlikely, but the proposed algorithm would not present any difficulty in moving to a ternary azeotrope for this case.

We are aware of no papers that prove this type of result for azeotropes involving more than three species; but, assuming such results do exist, the above algorithms should find all azeotropes.

a. Example: Ethanol and Water. We first detect the existence of the azeotrope by carrying out two bubble-point calculations, each at near-infinite dilution—the first with molar compositions of 0.9999 and 0.0001 and the second with 0.0001 and 0.9999 of ethanol in water. The desired K-value for each calculation is the ratio of the vapor composition, y, to the liquid composition, x, for the trace species; we get 1.29 (the K-value of water for a trace of water in ethanol) and 14.6 (the K-value of ethanol for a trace of ethanol in water), respectively. As discussed earlier, these numbers indicate a minimum-boiling azeotrope exists, very likely for an ethanol-rich composition.

We next search over the range of compositions from 0 to 1 for ethanol in water, computing a bubble point for each. At low ethanol composition, ethanol is more volatile. For a mixture that is nearly pure ethanol, the reverse is true. We are looking for the point where the K-value for ethanol changes from above unity to below. Near this point, we switch from a bubble-point computation to that for the equations above where we set the two K-values to unity. A Newton-based convergence algorithm converges easily to the desired azeotropic composition, $y_{\text{ethanol}} = 0.868$ (using Unifac) if we start the calculation close to the answer.

b. Example: Ethanol, Water, and Toluene. For a ternary mixture, we first discover one or more of the binary azeotropes, as we propose to use one of these azeotropes to start the search for a ternary azeotrope. We just discussed finding the ethanol/water azeotrope; we can also quickly discover the ethanol/toluene azeotrope.

In looking for a water/toluene azeotrope, we run into the problem that these two species generally form two liquid phases, a water-rich one and a toluene-rich one. We cannot ignore this two-liquid phase behavior, lest we get nonsensical answers. An azeotrope occurs when the composition for the combined liquid phases equals that for the vapor phase. Having K-values for a species set to unity, as we discussed above, means that the composition for that species for the combined liquid phases matches that for the vapor phase. Whether allowing for two liquid phases or not, water and toluene form a binary azeotrope for a

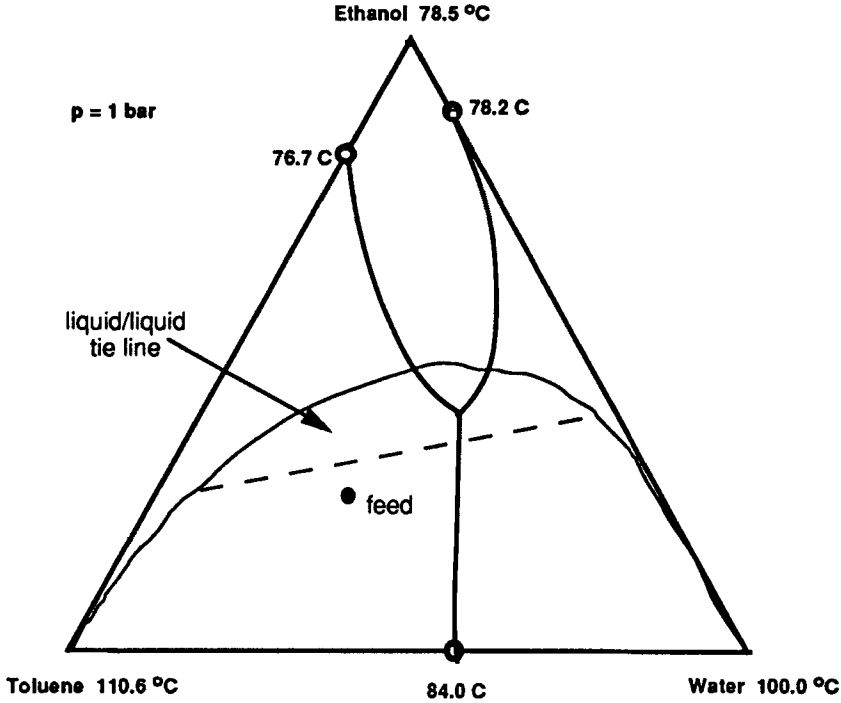

FIG. 43. Ternary diagram for water, ethanol, and toluene.

mixture that is somewhat more than 50% water. When allowing for two liquid phases, the temperature is, as shown below, at 84°C. If we do not permit two-liquid phase behavior, the temperature is much lower, namely, 65.6°C, a result that does not match at all with experimental data.

Figure 43 shows these azeotropes as well as a ternary one we now wish to find. Starting at the ethanol/water binary azeotrope, the infinite-dilution K-value for toluene is 2.78. Allowing for two liquid phases, the above algorithm locates the ternary azeotrope without difficulty. If we do not allow for two liquid phases, computations indicate there is no ternary azeotrope.

2. *Discovering Liquid/Liquid(/Liquid) Behavior*

Wasylkiewicz *et al.* (1993) present a method to find regions where mixtures partition in two or more liquid phases. They base it on the Gibbs tangent plane test (Michelsen, 1982, 1993) to decide if a current composition resides in a single- or a multiple-liquid phase region.

We shall first illustrate, using Fig. 44, why a mixture will split into two or more liquid phases by examining the shape of the Gibbs free energy for a binary

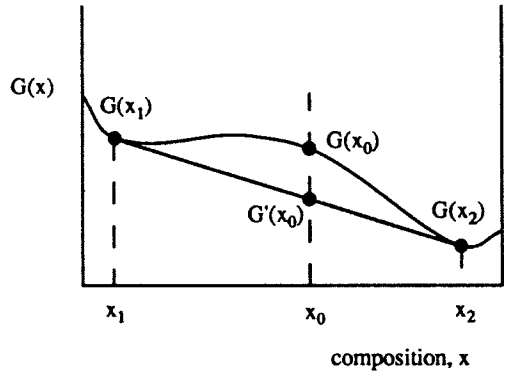

FIG. 44. Gibbs free energy for binary mixture that breaks into two liquid phases at any composition between x_1 and x_2.

mixture versus composition. We examine in particular the composition x_0. Its single-phase Gibbs free energy is above the tangent plane that supports the Gibbs free energy function at points x_1 and x_2. The single phase can reduce its Gibbs free energy by splitting into two phases having the two compositions x_1 and x_2. The total Gibbs free energy for the two phases is

$$G'(x_0) = \frac{x_2 - x_0}{x_2 - x_1} G(x_1) + \frac{x_0 - x_1}{x_2 - x_1} G(x_2)$$

a value that lies, as illustrated, on the tangent plane below $G(x_0)$.

Based on this insight, we place a plane that is tangent to $G(x)$ at the composition of interest. If that plane lies entirely below $G(x)$ for all x, then the given mixture will remain as a single-liquid phase at equilibrium; otherwise, it will split into multiple-liquid phases. Figure 45 illustrates for the point x_0. The tan-

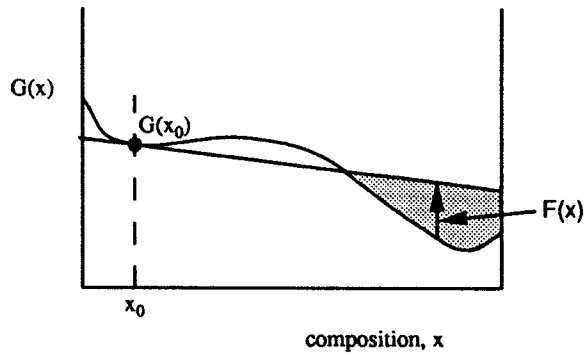

FIG. 45. Tangent plane supporting $G(x)$ at x_0. If $G(x)$ lies above this plane anywhere, the mixture at x_0 will break into multiple liquid phases.

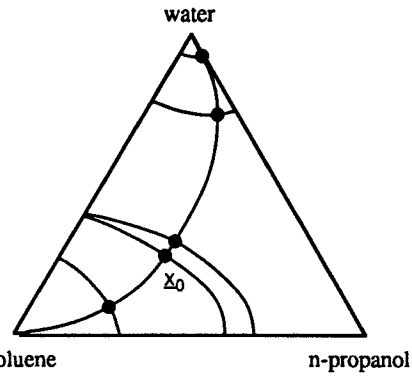

FIG. 46. Stationary points in the modified Gibbs free energy function over the composition space for multispecies mixtures. Diagram is approximate.

gent plane that supports $G(x)$ at x_0 lies partially above $G(x)$ on the right-hand side of the figure. This mixture lies between compositions x_1 and x_2 on the previous figure and will split into these two liquid phases. But how do we carry out this test? It would appear we have to cover the composition space with test points and hope that no regions are missed.

Wasylkiewicz *et al.* (1993) presented a method to carry out this test for general multispecies mixtures. They pick a point to test and create a tangent plane for it. The distance between the tangent plane and the Gibbs free energy surface defines a nonlinear surface above the composition triangle. The starting point is on a ridge in this surface. These authors propose tracing all ridges starting from this point to find all extreme point along these ridges in the surface (as opposed to searching the entire composition space). These paths can bifurcate. Figure 46 illustrates a typical path that their algorithm will trace. Only the extreme points need to be checked to discover if the tangent plane goes above the Gibbs free energy surface, thus indicating liquid/liquid behavior. The extreme points are good guesses for the phase compositions when they detect liquid/liquid behavior. Ridge-following and bifurcation detection involve evaluating eigenvectors and eigenvalues.

To test a single composition is a considerable amount of work. To develop a phase diagram for a mixture, we have to place compositions strategically over all of the composition space, detecting tie-regions (as lines, triangles, etc.). Fortunately, a tie-region covers all the compositions in it which no longer have to be explored. Figure 47, based on a figure in Wasylkiewicz *et al.* (1993), illustrates a completed phase diagram.

McDonald and Floudas (1994) and Michelsen (1994) also present methods to find the phase conditions for a given mixture. Both methods discover the number of phases and the compositions of these phases. McDonald and Floudas globally minimize the Gibbs free energy of the mixture using a computer pack-

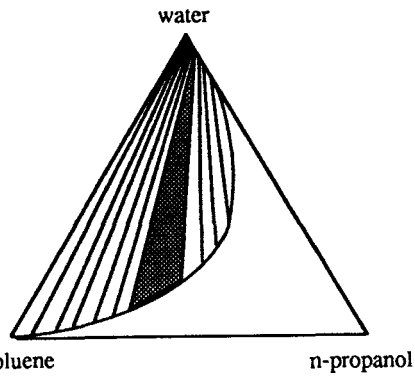

FIG. 47. Resulting liquid/liquid phase diagram. Diagram is approximate.

age they call GLOPEQ. Michelsen formulates the problem as a two-level problem. The outer level computes phase fugacity coefficients for all the possible phases. They show how to formulate the inner problem as a convex continuous-variable minimization problem.

B. LIMITING SIMPLE DISTILLATION COLUMN BEHAVIOR

We shall determine the limiting behavior for simple distillation columns by discovering all the products of such a column, regardless of the number of stages it has or the reflux ratio used in operating it. We present and extend here the ideas advanced in Wahnschafft (1992) and Wahnschafft *et al.* (1992).

1. Reachable Regions

To develop the alternative process configurations needed to separate a given feed mixture into a set of specified products, we need to know just what distillate and bottoms product compositions we can reach when using a conventional distillation column. We shall start by examining this problem for ideally behaving mixtures. We shall then look at the much harder problem in which the mixtures do not behave ideally.

a. The Material Balance Constraint. The following constraint holds for any number of species (see Treybal, 1968):

Material Balance Constraint: *For a conventional single-feed, two-product distillation column operating at steady state, the feed composition must lie on a straight line between the compositions for the distillate and bottoms products.*

b. Infinite Reflux. There are two convenient ways to imagine having infinite reflux conditions in a column. First we can consider having a real column where we turn off the feed and the product flows while maintaining a finite flow for the internal liquid and vapor, L and V. We get an infinite reflux ratio by having a zero denominator in the equation

$$R = \frac{L}{D}$$

The second extreme we can imagine is to maintain finite flows for the feed and products but increase the internal flows for L and V to infinite values. This second case cannot really occur, as we would need a column with an infinite diameter. It is a limiting case. Both ways to think of infinite reflux are useful. In the latter case the column is still thought of as producing its products.

At infinite reflux we can add a second constraint that must hold for the compositions of the two products:

Infinite Reflux Constraint: *The compositions for the distillate and bottoms products must both lie on the same distillation curve.*

This constraint follows from the definition of a distillation curve. Each point along a distillation curve represents both the vapor and the liquid compositions just above (or below) any tray, including those at the ends of the column where products would normally be withdrawn. This constraint, together with the material balance constraint, completely defines the reachable products for a column at total reflux.

Figure 48 illustrates some possible pairs of product compositions we might obtain for a given feed. It is for a relatively ideal three-species mixture, H/I/L.

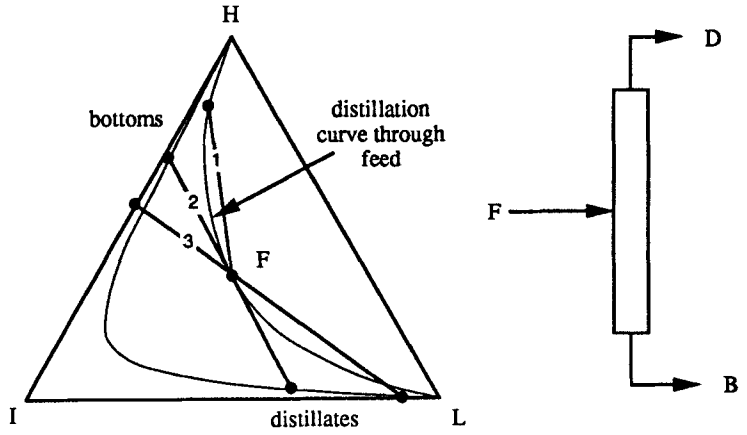

FIG. 48. Examples of reachable products for a column operating at infinite reflux.

The line marked with a 1 is one of two extreme situations we can see for this example. It has a bottoms composition on the distillation curve passing through the feed and a distillate composition which is exactly the feed. It is the limit of maintaining a finite feed while reducing the bottoms product flow to zero. If we take one drop of bottoms and the rest as distillate product, the distillate will have the same composition as the feed. The bottoms product is along the distillation curve at a point corresponding to the number of trays in the bottom of the column. Allowing for fractional trays, we can reach any point along this line.

Line 3 illustrates the other extreme—which is to connect a bottoms composition lying on the IH edge to one lying on the LI edge. There is a limiting distillation curve that passes from L to I to H on which these two points lie. Line 2 connects two points lying on a distillation curve that is between these other two extreme distillation curves for this example.

By plotting all such points, we create the shaded reachable region shown on Fig. 49. The straight edge from F to the LI edge occurs because any point along that edge can be a distillate if pure H is the bottoms product. All distillation curves passing through that edge will ultimately reach H, given an infinite number of trays.

If we bypass some of the feed and then mix what we bypass with either the distillate product or with the bottoms product, we can fill all the bow-tie area between the straight line passing from L through F to the IH edge and the line passing from H through F to the LI edge. The point marked a in Fig. 49 illus-

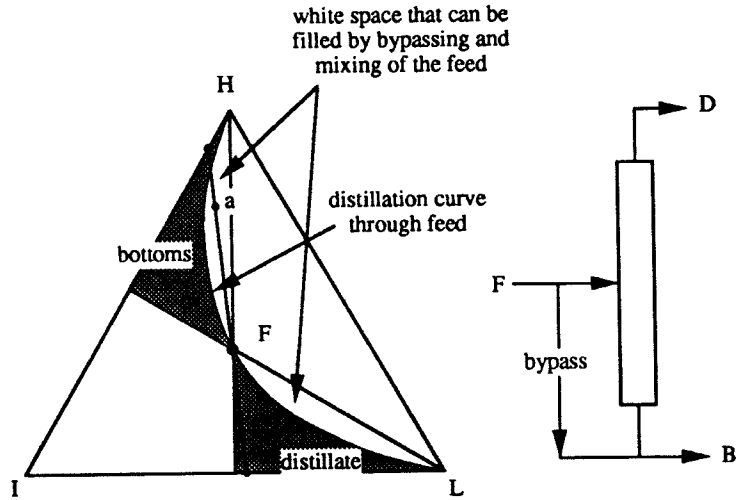

FIG. 49. All reachable products for a simple distillation column separating a nearly ideal mixture with the given feed composition F.

trates. This composition is reached by producing the two products at the extreme ends of the line as these are on the same distillation curve. Then by mixing the bypassed feed with the bottoms, we reach point *a*.

c. Finite Reflux (Petlyuk, 1978; Petlyuk et al., *1981; Wahnschafft, 1992; Wahnschafft* et al., *1992; Poellmann and Blass, 1994).* To understand what we can reach by reducing the reflux, we can write a material balance around the top of a column (as shown in Fig. 50):

$$V_{n+1} = L_n + D$$

This material balance says that the composition for V_{n+1} will lie between the compositions for L_n and D on the straight line connecting them.

We can imagine being on a composition diagram and stepping down the column starting at the top tray. Figure 51 illustrates the case when we have a total condenser and withdraw a liquid distillate product. (We leave it to the reader to discover that essentially the same analysis holds if we withdraw a vapor distillate product. If the distillate is a two-phase equilibrium mixture, the point D lies on the straight line joining the distillate's vapor and liquid compositions.) At the top of the column for a total condenser, the vapor leaving the top tray, V_1, condenses to form the distillate, D, and then refluxes back to the column, L_0. Therefore, they all have the same composition. We step along a distillation curve from that point to the composition for L_1, which is in equilibrium with that for V_1. It is exactly one stage along this curve. From the argument above, the composition for V_2 must lie on the straight line connecting L_1 to D. We step along the distillation curve, passing through V_2 one stage to L_2. We find V_3 along the straight line connecting L_2 to D.

We can keep on stepping along in this manner until we run into a situation where the compositions start to repeat—the characteristic of a pinch point for the column. Here, we see V_n leading to L_n. For a pinch situation, we find both V_n and V_{n+1} along the same straight line back to D from L_n, and these points coincide. Then L_{n+1} coincides with L_n, ad infinitum. Note that we are talking

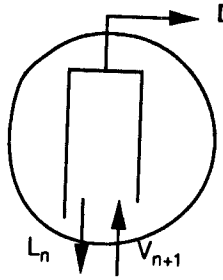

FIG. 50. Flow in the top of a column.

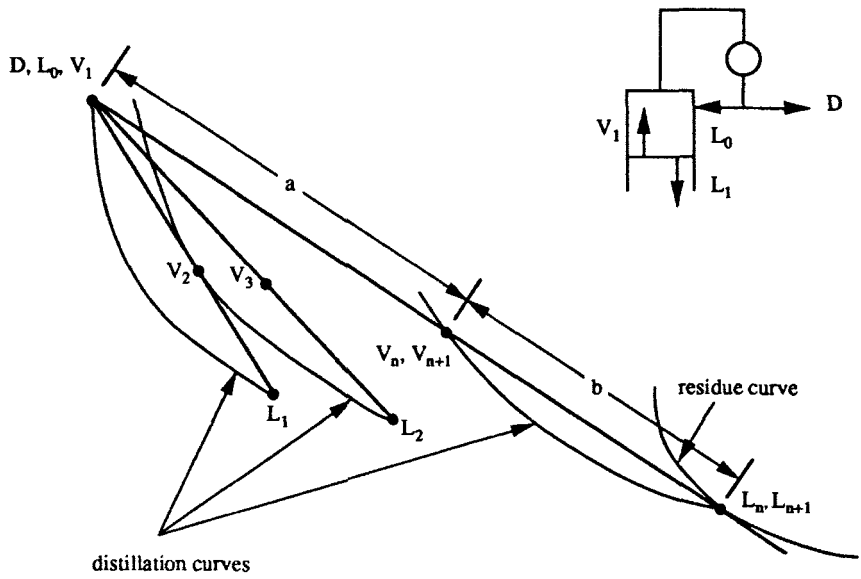

FIG. 51. Stepping down a column from the top.

about the same pinch points we discussed earlier. Thus we have already talked about how we might find such points by carrying out a computation similar to a flash computation.

There is a lot of interesting geometry in this diagram. First, we can look at where V_{n+1} is placed along the line relative to the positioning of L_n and D. From the level rule, we write

$$\frac{L_n}{D} = \frac{a}{b} = R_n$$

where a and b are the lengths shown in the diagram. This equation says that the reflux ratio defined in terms of the liquid flow leaving the nth stage divided by the distillate top product flowrate is the ratio of the line lengths a to b. If the reflux ratio does not change much, then this ratio does not change, and V_{k+1} is always about the same fraction of the distance along the line from L_k back to D. Figure 51 shows all the vapor compositions (V_2, V_3, and finally V_n) positioned in this manner.

Next we remember the equations that define a residue curve:

$$\frac{dx_i}{d\theta} = x_i - y_i$$

These equations have an interesting geometric interpretation. They say that the vapor composition V_n in equilibrium with the liquid composition L_n lies along

a line that is tangent to the residue curve passing through the composition L_n. If that line also passes through D, then V_{n+1} is on the same line. It is possible to prove also that V_n and V_{n+1} must be coincident and therefore so are L_n and L_{n+1}. The proof follows from observing that if V_n and V_{n+1} are on the same line back to D, then L_{n-1} and L_n must also be coincident. If L_{n-1} and L_n are not coincident, then there must be at least two points where residue curves are tangent to that line. The proof takes some effort, but ultimately it demonstrates that these points are coincident.

Finally, from the results of these observations, we can prove that *a pinch point is any point where a line emanating from the distillate composition is tangent to a residue curve.* The vapor composition in equilibrium is on that same line. The reflux ratio to reach that pinch point is the ratio *a/b.*

Figure 52 illustrates stepping to a pinch point from a liquid distillate composition on a triangular diagram. This diagram is also rich in geometric interpretation. Starting at the distillate composition with a particular reflux ratio for the column, we step down the column as shown, finally ending at a pinch point. If we choose a slightly larger reflux ratio, we reach another pinch point farther

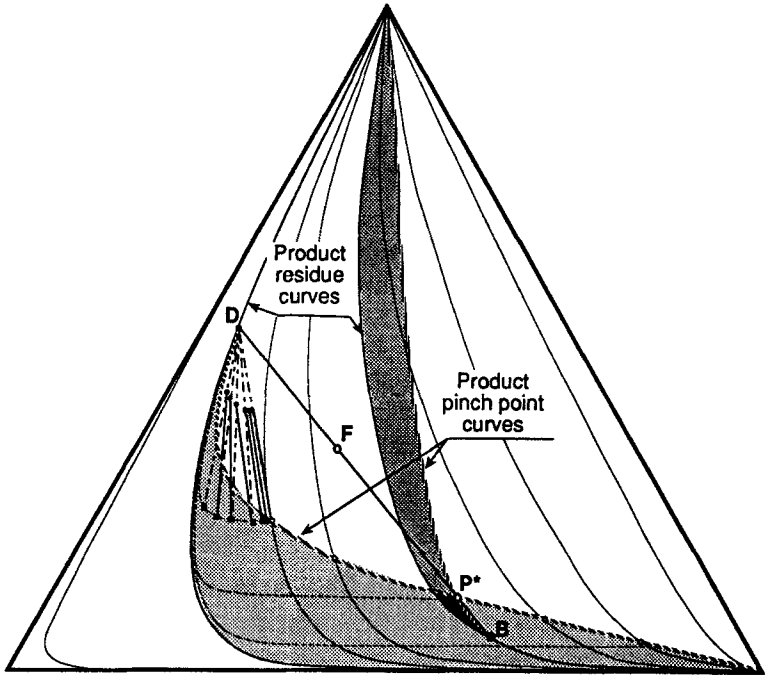

FIG. 52. All compositions that can be reached for both finite and infinite reflux conditions from the distillate D and bottoms B compositions by stepping away from them using a tray-by-tray calculation.

away from D. In this manner, we can construct a curve made up of pinch points. Which pinch point we will reach in a column depends on the reflux ratio; thus, this curve is parametric in the reflux ratio. We saw this parametric behavior earlier when we discussed pinch points just before developing insights into Underwood's method for estimating minimum reflux.

Any point between the distillation curve passing through the distillate and its corresponding pinch point curve is *reachable* from the distillate using tray-by-tray computations (allowing fractional trays). Here, for example, we could reach the bottoms product labeled B by choosing a reflux ratio that leads to a curve that traverses at first very close to the distillation curve through D until the tray-by-tray computations bend inward toward the pinch curve. We stop at B by choosing a finite number of trays (it takes an infinite number to reach the pinch curve) along that curve. We define the gray region as the *reachable region* for D. We can repeat a similar construction for the bottoms product, producing a pinch point curve and then a reachable region for B.

If the shaded regions do not overlap, no conventional column can produce these two products at the same time. We need to argue that the converse is true; namely, if the regions overlap, a column exists that can produce these two products. We would have no trouble making that statement for this particular column as B is reachable from D directly using tray-by-tray computations. We would feed the bottom tray in this column (very likely not the best way to run a column to get these two products).

There is a point P^* that resides on both pinch point curves in Fig. 52. We can make the following argument concerning P^*:

- By construction, P^* is simultaneously on both pinch point curves.
- As it is on the pinch point curve for D, the residue curve passing through P^* is tangent to the line from P^* to D.
- As it is on the pinch point curve for B, the residue curve passing through P^* is tangent to the line from P^* to B.
- Thus the line must be the same straight line (both pass through P^* and both have the same slope).
- By overall material balance for the column, the feed point F is on a straight line between D and B.
- Thus the point P^* must be on that line.
- Thus the point P^* must be a pinch point for F, too.

We therefore conclude that P^* is a pinch point for all three points: D, B and F.

For a reasonable topology for the residue map, we next can discover that the points between P^* and F may not be products from any column for which F is a feed. The construction in Fig. 53 illustrates. This figure corresponds either to a total condenser with a liquid top product or to a partial condenser with a vapor top product. If the top product is two-phase, the distillation curve passes through

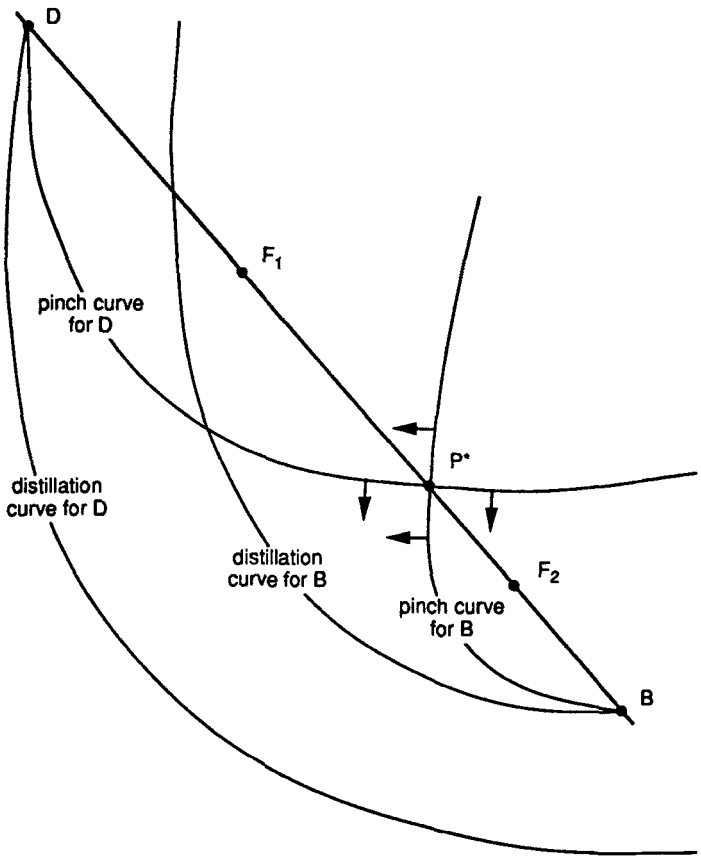

FIG. 53. Topology of the point P^*, the intersection point for a liquid distillate and bottom product pinch point curves.

both the vapor and liquid compositions for the distillate—they are in equilibrium with each other—while the distillate pinch point curve passes through D.

First, the column feed F must lie on the line between the products D and B. Both points F_1 and F_2 are possible feeds that could lead to the product D and B.

If the feed is F_1, a point lying between D and P^*, then the pinch curve through D lies entirely to one side of the point F_1 and curves back to cross at P^*. The corresponding distillation curve lies even farther away to the same side (the pinch point curve turns more sharply than the distillation curve). The reachable region for D excludes all points between D and P^*. Thus the points between F_1 and P^* are unreachable by the top part of the column. As D could move to be coincident with F_1, points beyond F_1 are not excluded.

If the feed is F_2, the pinch curve for B excludes all points between B and P^* by a similar argument. Again, the points between F_2 and P^* are unreachable. We have proved our assertion.

We now should understand the meaning of a reasonable topology. It is where the distillation curves turn in only one direction over the region of interest, a property they will have for ideally behaving species. We shall look in a moment at a case where the topology is more complex.

The region between F and P^* is a function only of F, the feed to the column, as we can find P^* by finding the pinch point curve for F from the arguments above. We have subtly turned our attention from D and B to F. Thus, we can map out this unreachable region by knowing only the column feed.

Excluding the option of bypassing and remixing any of the feed with either of the products, the diagram for an ideally behaving set of species in Fig. 54 maps out the entire set of reachable products for a given feed—for any reflux conditions from minimum to infinite. We can reach the lightly shaded region using total reflux. We can extend the region with the dark gray areas by using finite reflux.

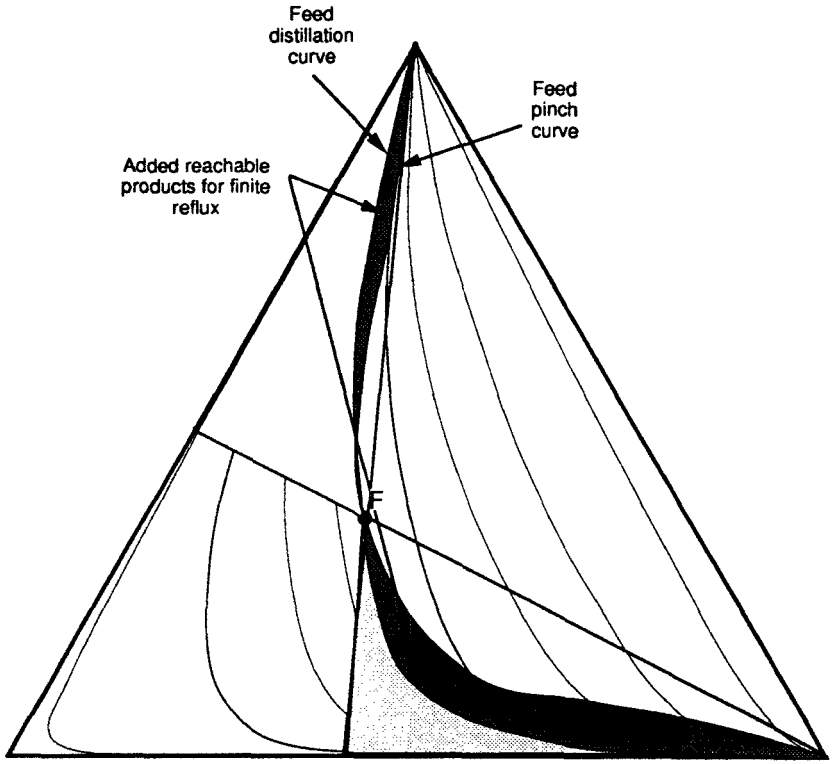

FIG. 54. Reachable products for a column separating ideally behaving species.

i. S-shaped residue and distillation curves. For nonideally behaving species, some of the residue and distillation curves take on a more complex shape. We shall examine the situation when some of them are S-shaped as in Fig. 55. S-Shaped residue curves appear to the left of the maximum-boiling azeotrope along the lower edge. They are also present in the residue diagram for acetone, chloroform, and benzene (Fig. 25), appearing just to the right of the maximum-boiling azeotrope along the lower edge. With little difficulty, we can demonstrate that this shape is quite common. We now examine its implications for finding reachable products for a column.

Figure 56 shows a region with S-shaped distillation curves, where the feed lies somewhere near the inflection point for one of these curves. We note some very interesting differences from what we have discussed so far. We know from earlier discussion that we can reach any products at total reflux when both lie at opposite ends of a straight line passing through F while also lying on the same distillation curve. B_1 and D_1 are such a pair. Interestingly, B_2 corresponds to two different distillate products, D_2' and D_2''. We see that the total reflux products are outside the region bounded by the lines passing to the minimum and maximum temperatures for the region (total reflux products were wholly inside this region before).

The shaded regions between the two S-shaped bounding curves are the reachable product regions for total reflux for the feed F. To see how we construct these two bounding curves, consider the two points marked a lying simultaneously on the same straight line passing through F and on the same distillation curve. The one to the left and below the feed lies where the straight line just brushes a distillation curve. If we rotate this straight line counterclockwise, it will no longer intersect this distillation curve. Thus, a column at total reflux cannot reach points to the left of the upper point a where this straight line intersects this same distillation curve. We create one segment of these bounding

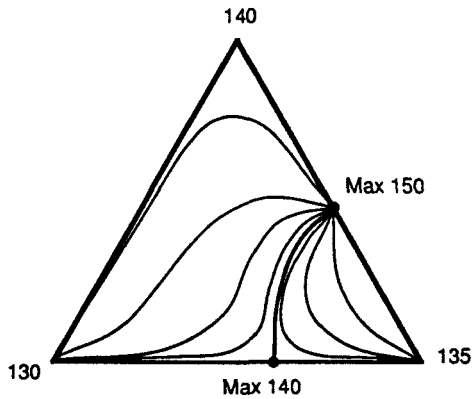

FIG. 55. Composition diagram featuring S-shaped distillation/residue curves.

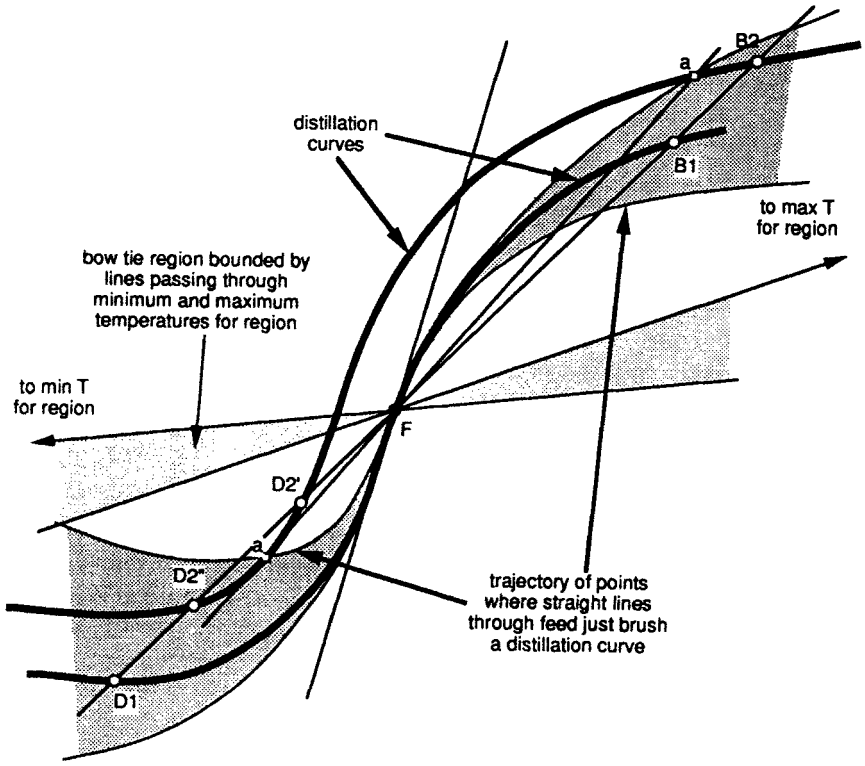

FIG. 56. Reachable products (shaded area between two S-shaped bounding curves) at total reflux for S-shaped distillation curves.

lines by finding the trajectory of points where a straight line passing through the feed just brushes a distillation curve and the other segment by locating the corresponding point on the other side of the feed where this line intersects the same distillation curve.

We find the same complexity for mapping out reachable products for finite reflux—see Fig. 57. We ask if we can distill the feed F into the distillate product D and bottoms product B. The shaded regions indicate the reachable regions for these two products. They overlap, suggesting we can reach them. We see there are two feed pinch points, P_1^* and P_2^*, along the straight line joining B, F, and D, whereas we saw only one before. In a manner similar to that used earlier, we can develop an argument that says that, if B lies between P_1^* and F, then D cannot lie between P_2^* and F. Similarly, if D lies between P_2^* and F, then B cannot lie between P_1^* and F. These segments between P_1^* and F and between P_2^* and F are reachable (in contrast to earlier findings), but they are not simultaneously reachable in the same column.

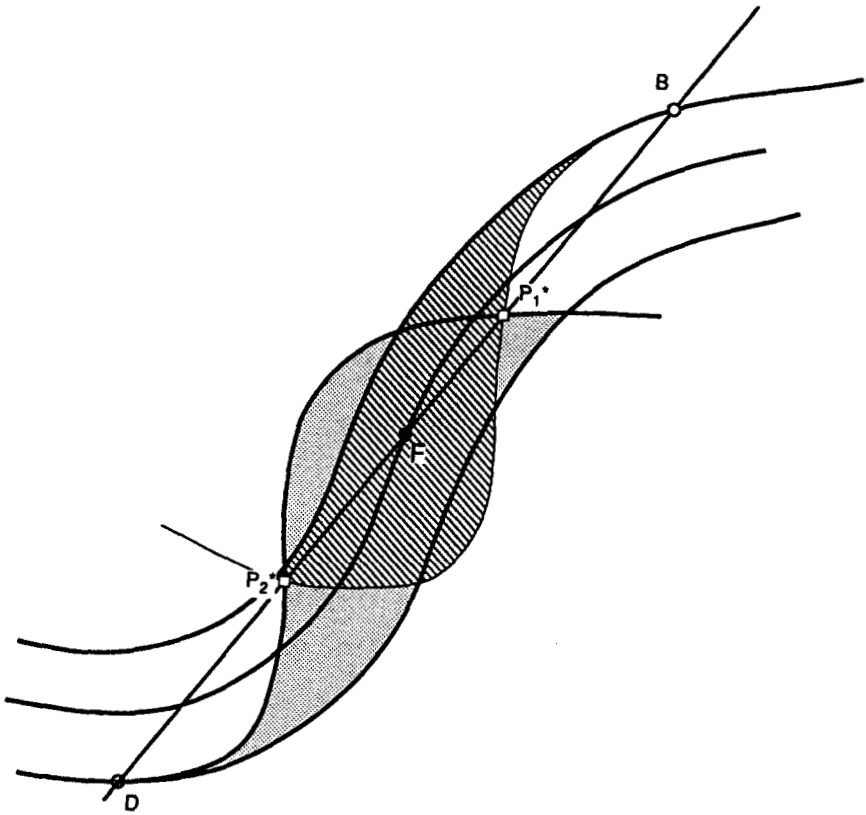

FIG. 57. Reachable products for finite reflux for an S-shaped region.

We see that the S-shaped region makes the process of discovering reachable regions more difficult (but not impossible).

ii. Crossing residue curve boundaries (Wahnschafft, 1992; Wahnschafft, *et al.*, 1992). Nikolaev *et al.* (1979) and Van Dongen (1983), among others, demonstrate by column simulations that one can cross residue curve boundaries when operating a column at finite reflux. Consider Fig. 58, which shows the distillation curves for acetone, chloroform, and benzene. We are going to be very particular and note that this plot features a *distillation* curve boundary as opposed to residue curve boundary. No column operating at total reflux can produce a distillate and bottoms product on opposite sides of this boundary because the two products must reside on the same distillation curve. However, this restriction does not hold for finite reflux. As we have shown above, we can step to a product by carrying out plate-by-plate computations from any com-

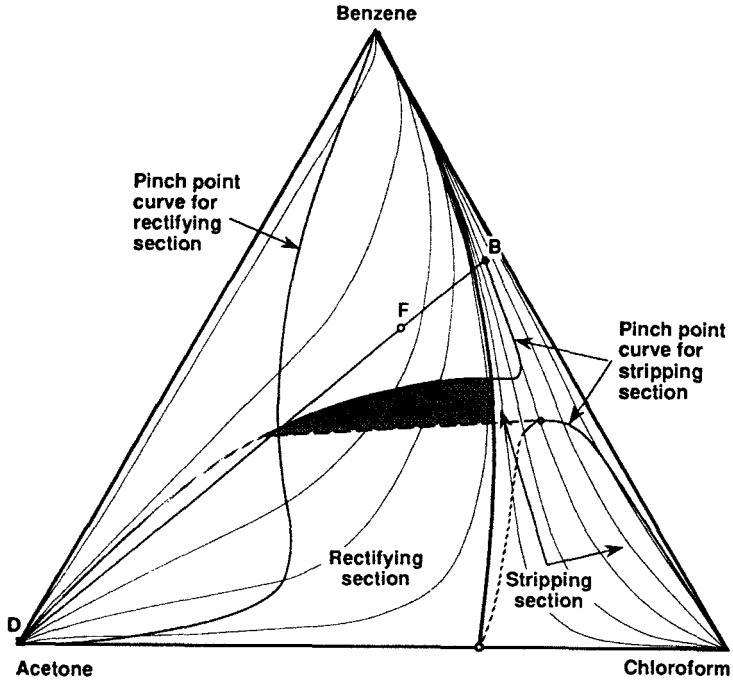

FIG. 58. Bifurcation of the pinch curve trajectory when a product is in another distillation region.

position residing between the distillation curve passing through a product and the pinch curve emanating from that product. We propose here a bottoms product in the right-hand-side region and a distillate product in the left-hand-side region, with the feed between as shown. Is this possible?

Examining Fig. 58, we see that there are two pinch point curves corresponding to B (i.e., to the stripping section of the column). Mentally treating the distillation curves shown as residue curves (they will be similar in shape), we see that a pinch point occurs where a straight line passing through the bottoms product composition is just tangent to a residue curve. The pinch curve passing through B, crossing into the left-hand-side region, and ending at the acetone node satisfies this requirement. However, so does a totally disjoint pinch curve starting at the maximum-boiling azeotrope, heading upward into the right-hand-side region, and ending at the chloroform node. For a small enough reboil ratio, we will quickly move from the distillation curve passing through B toward the pinch curve emanating from B. At total reflux, we will stay on the distillation curve, and, for an infinite number of stages, we will end up at the chloroform node which is on the disjoint pinch curve. Somewhere in between, we must jump from the one pinch curve to the other.

Figure 59 illustrates the process of stepping up the column away from the bottoms product end. This figure reminds us of the geometry involved. First, we note that L_n must lie on a straight line between B and V_{n+1}. Next, we remember that the residue curve passing through L_n points at the vapor composition in equilibrium with the composition corresponding to L_n. We consider three cases. (1) If the residue curve passing through the liquid composition points as shown, the composition in equilibrium with L_n will be down and to the right of L_n. In this case, the column compositions will move to the right as we step away from B, causing us to move toward the disjoint pinch trajectory. (2) If the tangent to the residue curve points straight at B, then L_n is a pinch point, and we would stop moving. (3) If it points to the left as we move away, the trajectory moves to the left. Thus we move to the disjoint pinch trajectory only if the composition of the liquid steps across the lower pinch curve, i.e., passes from case (3) through case (2) to case (1).

Associated with every pinch point is a vapor composition in equilibrium with it, a composition we already have from computing the pinch point itself. We are reminded by Fig. 59 of the geometry for computing the reboil ratio to reach a given pinch point. It is the ratio of the distance from B to L_n (b on the figure) divided by the distance from L_n to V_{n+1} (a on the figure). We can label each pinch point on both trajectories with a corresponding reboil ratio. The point B itself corresponds to a reboil ratio of zero. The reboil ratio increases to infinity along the pinch trajectory emanating from B as it passes to the pure acetone node. To see that it goes to infinity, we note that the distance b gets larger as

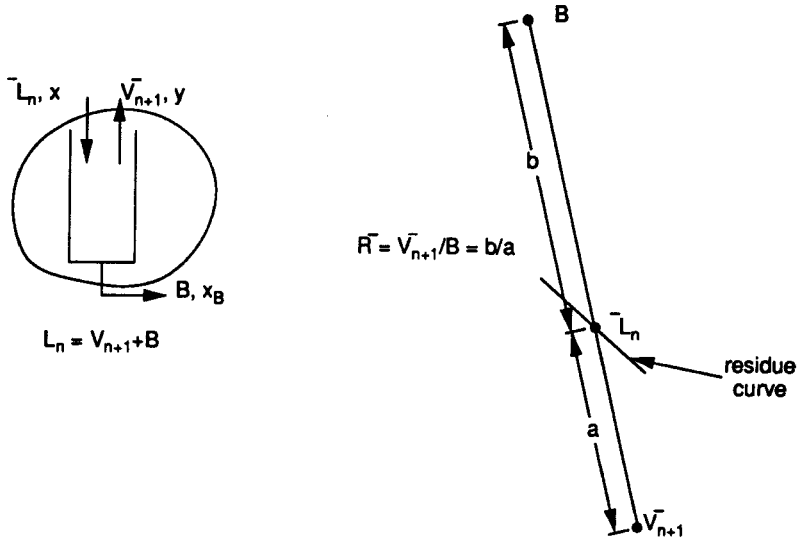

FIG. 59. Stepping up the column from the bottoms product.

we move away from B while the distance a must go to zero as we approach acetone.

Using a similar argument, we recognize that the reboil ratio for the disjoint pinch trajectory passes from infinity at the azeotrope to a finite but positive number and back to infinity as we approach the chloroform node. If we keep the reboil ratio less that the smallest reboil ratio along the disjoint trajectory, we cannot reach this trajectory. So, again, we see that we need to use small reboil ratios to cross a boundary.

iii. Bottoms compositions that permit crossing of a boundary. We are now in a position to map out those bottoms compositions that have a reachable products region that crosses the distillation boundary. Place a bottoms composition somewhere in the lower right of the composition diagram Fig. 58 for acetone, chloroform and benzene. If it is close enough to the chloroform node, two pinch point trajectories will again appear, but they will be qualitatively different from before. The one starting at the bottoms composition will end at the chloroform node. The second will move from the acetone node and end at the azeotrope. In this case, the reachable region for B will stay entirely in the right-hand-side region, lying between the distillation curve passing through B to chloroform and the pinch point curve emanating from B and passing to chloroform.

There must be one or more compositions somewhere between this one and the one shown Fig. 58, where the trajectories switch from the one shape to the other. We can imagine the two trajectories just touching and then trading branches. Let's explore where this will happen.

Examine Fig. 60. We show the residue curves that have the same S-shape as those in the lower left part of the right-hand-side region for acetone, chloroform, and benzene. Each curve is convex to the left at the top (curves toward the left) and convex to the right at the bottom, and each switches the direction it curves at its inflection point. Point a is such an inflection point on one of these residue curves. Draw a straight line through point a such that it has the same slope as the residue curve. Above the inflection point, this straight line is entirely to the right of the residue curve, and below it is entirely to the left.

Next, pick a bottoms product, B, that lies on this straight line above the inflection point. The pinch point curve emanating from B will move to the left initially because of the curvature of the local residue curves. It will move left until it encounters point a which, by construction, is a pinch point for B. It cannot cross this residue curve, however, because any residue curve an infinitesimal bit to its left can have no pinch point with B. On the other hand, a curve just to the right will have two pinch points with B, one just before a and one just after. The pinch point trajectory thus "reflects" off this residue curve. After encountering point a, it heads to the lower right and ultimately to the chloroform node.

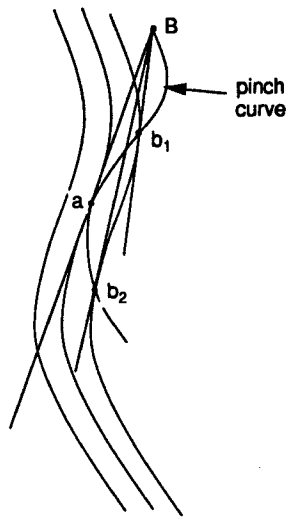

FIG. 60. The pinch point trajectory emanating from the bottoms product "reflects" off a pinch point that occurs at an inflection point of a residue curve.

Thus, any point B that lies on a line passing through an inflection point of a residue curve with the same slope as the residue curve cannot have a pinch point trajectory emanating from it that crosses the distillation boundary. We draw a family of lines through every such inflection point. To the left of all these lines are the bottoms products, *B*, that can be bottoms products with a top product in the left-hand-side region. Points on and to the right of these lines are not candidates.

Finally, we note with a similar set of arguments that no product in the left-hand-side region can have a pinch point curve that crosses the distillation boundary, thereby justifying the statement appearing in the literature that one cannot cross such boundaries from the "convex" side.

2. *Thoughts on the Geometry for Two and Four or More Species*

All the above insights are for three species. How do these insights extend to mixtures with two species and with four or more species. If we extrapolate the two-dimensional (planar) triangular diagram for three species down to two, we get a composition line. Each edge of a triangular diagram is such a line. For a four-species mixture, we need a three-dimensional tetrahedron such that each of its four sides is a three-species triangular diagram. Five species require four dimensions, one more than we can comfortably visualize, so we almost certainly must abandon visualization for five or more species. But we can attempt to describe the geometry of expressing equilibrium, distillation, and residue curves; operating "lines"; and, finally, pinch point trajectories.

Vapor–liquid equilibrium is a mapping from a liquid composition to a vapor composition. It can be done by including tie lines from one to the other for all compositions. On a line, such a mapping is very difficult to visualize, so we typically use a second dimension where we can plot vapor composition versus liquid composition as in a McCabe–Thiele plot or as in a temperature versus composition diagram. For three or four species, showing tie lines is fairly direct. The important point is that equilibrium is not a line (as we might think because of our familiarity with McCabe–Thiele plots) but a mapping.

Distillation and residue lines that we have plotted for three species on a planar triangular diagram remain as lines for all dimensional spaces. Each corresponds to a trajectory of composition points. A distillation curve corresponds to the curve we pass through the liquid compositions that occur on the trays of a distillation column operating at total reflux. A residue curve is the trajectory we get when we solve the differential equations

$$\frac{dx_i}{d\theta} = x_i - y_i$$

Each curve is "pinned" down by requiring it to pass through a particular composition.

For a fixed reflux ratio for a column, the operating line remains a line in higher-dimension composition space, as it too is a line passing through the sequence of liquid compositions appearing on the trays as we move up or down a column.

One line we have to think more carefully about is the pinch point line as we move to other dimensions. Each point on the line is the end point of a operating line for a distillation column operating with a fixed distillate (or bottoms) product, varying parametrically with the reflux ratio we use to define that operating line. Thus, a pinch point curve emanating from a fixed distillate composition is a sequence of points. It remains a line. It may bifurcate, as we have shown above, but it remains a line.

The compositions from which we can reach a distillate or bottoms product are those lying along a distillation curve if we operate at total reflux. If we operate with a finite reflux ratio, these trajectories move off this line and toward the pinch point trajectory emanating from that product, ending on it if we have an infinite number of stages. Thus, the reachable compositions should look like a ribbon moving through higher-dimension space. Almost certainly, this ribbon has bulges in it, but it should be a bounded two-dimensional surface between these two lines. However, this geometry is for reaching a particular product composition.

Thinking about all reachable products for a given feed is more difficult problem, particularly for four or more species. We still require the material balance constraint to hold. Thus, the points must line up on a straight line in whatever

dimension space we examine. At total reflux, the points must also lie on the same distillation line. On a triangular diagram, all distillation lines lie in a planar surface, so we have little difficulty in seeing that these two constraints map out a two-dimensional portion of that diagram. But if four species are represented in a three-dimensional tetrahedron, do these same two constraints map out a three-dimensional portion or only a two-dimensional portion of that tetrahedron? Even if we answer this question, are we prepared to discover the shape of this space for each problem we face, and would we find it useful if we did? It was for this reason that we have proposed a different strategy to discover the reachable products for separating a mixture of four and more species: namely, the plotting of separation ranges as in Fig. 27. This representation does not provide the complete picture for three species, but it does give us one approach for such mixtures that neither grows combinatorially with the number of species nor defies our ability to visualize the results.

C. Extractive Distillation

Many researchers have contributed to the literature on extractive distillation, including Benedict and Rubin (1945), Hoffman (1964), Tanaka and Yamada (1965), Berg and Yeh (1985), Hunek *et al.* (1989), Pham *et al.* (1989), Ryan and Doherty (1989), Pham and Doherty (1990), Wahnschafft (1992), and Wahnschafft and Westerberg (1993). We shall base much of our discussion here on the last two references.

1. Difference Point

Suppose we would like to separate water (normal boiling point 100°C) from isopropanol (nbp 82°C). Isopropanol and water form a minimum-boiling azeotrope (nbp 80°C) at about 72% isopropanol and cannot be separated into pure products by ordinary distillation. We discover by computing infinite-dilution K-values that, in the presence of sufficient ethylene glycol (nbp 197°C), isopropanol is more volatile than water, and the two can be separated completely. We need to operate a distillation column such that, whenever isopropanol and water are together in the column, there is sufficient ethylene glycol present to make the isopropanol more volatile. Suppose we feed relatively pure ethylene glycol (the extractive solvent E) as a separate feed a few trays from the top of a column, as shown in Fig. 61. Being a high-boiling material, it will largely head straight down the column in the liquid phase. The feed (where A is the isopropanol and B is the water) enters several trays below the solvent. The section of the column between the two feeds washes out B. Just below the solvent feed, it must be essentially completely removed, or else it will end up in the distillate product.

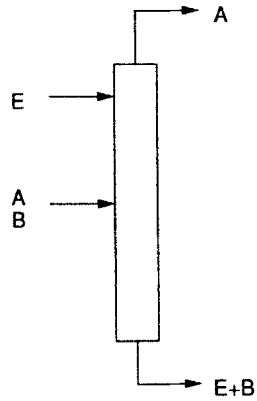

FIG. 61. Typical extractive distillation column.

The bottom section of the column is to remove species A. Species A heads down the column but is removed more and more until, just before the bottom tray, it is more or less completely depleted. The top few trays above the solvent feed are to separate A from E. As ethylene glycol is a very high-boiling material relative to isopropanol, two trays will remove it.

We can determine the reachable products for this type of column by extending the concepts developed for an ordinary column. We again develop our insights for a three-species mixture using a ternary composition diagram.

We start by writing a material balance for the section of the column between the two feeds, as shown in Fig. 62.

$$\hat{V}_{n+1} = \hat{L}_n + D - S$$

This equations looks just like a material balance for a normal column, except that we have replaced D by $D - S$.

Let us define Δ as a difference point (Hoffman, 1964)

$$\Delta = D - S$$

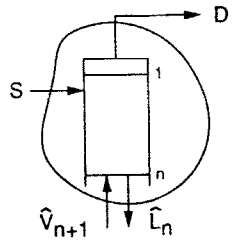

FIG. 62. Intermediate section of extractive distillation column.

and let it play the role of D in a normal column. Thus, Δ is the constant difference that we will see between the total (and species) vapor and liquid flows in this section of the column. For a normal column, the operating line must pass through the composition point for D. For the intermediate section of this column, the operating line must pass through the composition point for Δ, given by

$$x_{\Delta,i} = \frac{x_{D,i}D - x_{S,i}S}{D - S} = \frac{x_{D,i}D - x_{S,i}S}{\Delta}$$

Let us look again at the case of separating isopropanol from water using ethylene glycol. If we assume the solvent is essentially pure ethylene glycol and the top product essentially pure isopropanol, then

$$x_{\Delta,E} = \frac{0D - 1.0S}{D - S} = \frac{-S}{D - S}; \qquad x_{\Delta,A} = \frac{1.0D - 0S}{D - S} = \frac{D}{D - S}; \qquad x_{\Delta,B} = 0$$

For D > S, the first composition is negative and the second is greater than 1. The third (for water), being 0, says that this composition lies on the edge of the triangle opposite the node for pure water (B). A negative composition for the solvent E and a composition greater than unity for species A says the Δ point lies outside the normal composition triangle. Figure 63 shows where Δ will lie for the case of pure solvent feed and pure distillate top product. As noted, when $D > S$, $x_{\Delta,E}$ is negative which must be past the A/B edge. Composition $x_{\Delta,A}$ is greater than unity, which must be above the vertex for A. In

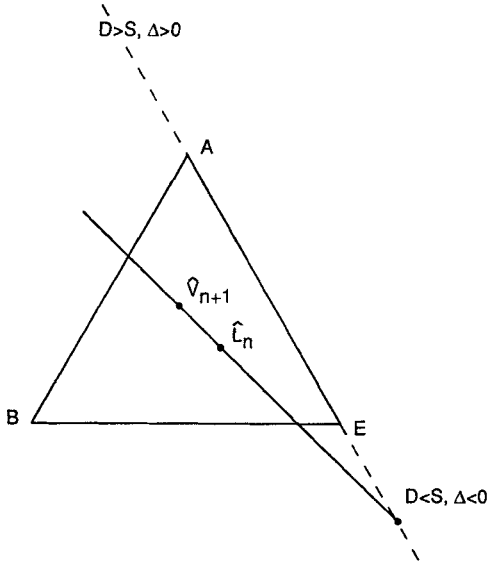

FIG. 63. Location of Δ point and corresponding material balance line for extractive distillation.

other words, the point must lie along the A/E edge extending above and to the left of the vertex for pure A.

If D = S, the Δ point is at infinity along this line. As S starts to exceed D, Δ jumps to negative infinity along this same edge. It moves toward the point E as S gets larger and larger relative to D. This makes sense. When $S = 0$, the Δ point should be at the distillate composition, here pure A. Adding solvent moves it upward along the line, extending the A/E edge. It should ultimately approach pure solvent as S becomes very large relative to D.

If $\Delta = D - S$ is positive, the material balance constraint says the vapor composition for $\hat{V}_{n+1}$ is a mixture of the liquid composition for $\hat{L}_n$ and the composition for Δ. Thus the point for $\hat{V}_{n+1}$ will lie between $\hat{L}_n$ and Δ. This puts $\hat{V}_{n+1}$ above and to the left of $\hat{L}_n$ in Fig. 63. If $\Delta = D - S$ is negative, then the same material balance equation says $\hat{L}_n$ is a mixture of the vapor composition for $\hat{V}_{n+1}$ and the composition for Δ, which now lies below and to the right (as we have sketched it in Fig. 63). In this case, $\hat{V}_{n+1}$ is again above that for $\hat{L}_n$ along the line passing through Δ. Therefore, while Δ jumps from plus infinity to minus infinity, the relative positions for $\hat{V}_{n+1}$ and $\hat{L}_n$ stay the same, and their positions move smoothly even as Δ jumps.

We stated above that isopropanol (A) is more volatile than water (B) in the presence of lots of ethylene glycol (E). Figure 64 is a sketch of how the residue curves appear for this mixture on a triangular composition diagram. Cover the upper left part of the diagram, leaving only the node for E showing—i.e., where we circle the node for E. This part of the diagram looks just like that for an ideal mixture where A is the most volatile species and B the intermediate. As

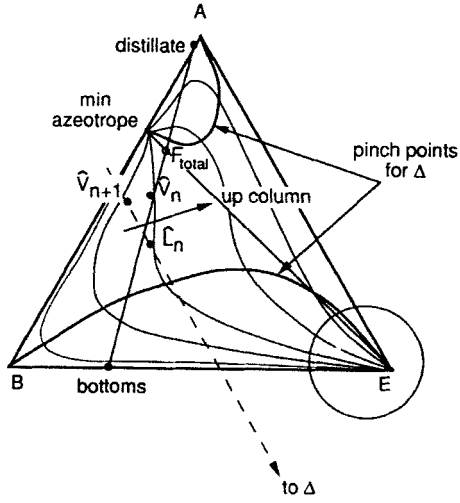

FIG. 64. Stepping up the middle section of an extractive distillation column.

one passes along a residue curve toward species A, the system becomes "aware" that A is not the lightest species around, but rather the minimum-boiling azeotrope is. The curves turn and head for it instead, terminating at A. They pick up a distinct S shape to them, as shown.

Let us assume we need to separate an azeotropic mixture of A and B. Since a conventional distillation column cannot carry out this separation, we plan to use solvent E as an extractive agent. We perform an analysis to see if it will work. The total feed, F_{total}, to the column is the sum of the azeotropic mixture and the solvent E. Its composition will lie along the line joining the compositions for the azeotrope and E. We want relatively pure A for the distillate (possibly contaminated with a small amount of B); so we sketch in about where we wish to find our desired distillate product composition. The bottoms product will be a mixture of species B and E. We place the products on our diagram, noting that both must lie on a straight line passing through the total feed composition.

If we sketch the compositions that can reach the distillate product in a conventional column, we find them limited to being near the A/E edge. To see this, follow the residue curve passing through the distillate product toward higher and higher temperatures. The pinch point trajectory emanating from the distillate product is a bit to the inside of this residue curve, but never too far from it here. All compositions that can reach the distillate are bounded by this pinch point trajectory and the distillation curves (close to the residue curve) passing through the distillate composition point. Similarly, we see that the compositions that can reach the bottoms are roughly those between the bottoms and the azeotrope. Not surprisingly, the two regions do not intersect, and thus we know we cannot separate the total feed mixture (azeotrope mixed with solvent E) in a conventional single-feed column.

Our intention is to use an extractive distillation column. The extractive agent is to be fed separately near the top of the column. We wish to see if this section has a composition trajectory that steps between a pair of compositions that the top and bottom sections can each reach from their respective product compositions.

Let us set the solvent feed initially equal to that of the distillate, which puts the Δ point at infinity. We choose this point initially only because it is easy to sketch the lines passing through it: they are parallel to the A/E edge. $\hat{V}_{n+1}$ and $\hat{L}_n$ for the column section between the two feeds will lie on such a line, as shown. Let us then locate $\hat{V}_n$, given $\hat{L}_n$. The slope of the residue curve passing through $\hat{L}_n$ points at $\hat{V}_n$. We see that $\hat{V}_n$ is thus to the right of $\hat{V}_{n+1}$. We sketch in a possible point. We note then that we move up the column when the tray number decreases from $n+1$ to n. Thus, $\hat{V}_n$ moves toward the A/E edge relative to $\hat{V}_{n+1}$. This is the exact direction in which we must move to connect the compositions reachable from the bottoms product to those reachable by the distillate. (If there were no extractive agent present, the Δ point would be located

at pure A. For this case, $\hat{V}_{n+1}$ and $\hat{L}_n$ would be on a line passing through the node for A instead, and we would find ourselves moving toward the node for B rather than toward the A/E edge as we move up the column. That is incompatible with our intentions for this column.) With solvent fed as in an extractive column, we move from compositions we can reach from the bottoms product toward those along the A/E edge, from which we can step to the desired distillate product just a few trays above the solvent feed.

We moved toward the A/E edge because of the relative slopes of the material balance line passing through the Δ point and the residue curve passing through $\hat{L}_n$. Imagine that we have an $\hat{L}_n$ that lies much closer to the node for E, where the relative slopes are the reverse. Here, the column does not function as desired. The limit point for the desired behavior is where the slope of the line passing through Δ and the slope of the residue curve coincide. That is precisely *a pinch point* for Δ. With Δ at infinity, this occurs where a residue curve has a slope parallel to the A/E edge. We have plotted a trajectory of pinch points for the Δ point. It starts at the node for B and ends at the node for E here. Above this line, we move from left to right (the desired direction) in the section of the column between the feeds; below, we move in the other direction.

The S shape of the residue curves gives us another pinch point curve for Δ. It starts at the azeotrope and ends at the node for A. Above this curve, movement is again in the wrong direction. Thus, we have only the region between these two curves in which we can correctly operate the section of the column between the two feeds.

What does it mean to have two pinch point curves for Δ? To operate as we wish, we need to keep the composition of the liquid on the trays between these two curves for the section of the column between the feeds. We shall now show that one of the curves dictates a minimum reflux ratio and the other a maximum reflux ratio that must be used to operate the column for a fixed solvent ratio. We shall then show that there is a minimum solvent ratio we can use—one where the pinch point trajectories just touch. We will also show that larger ratios move the pinch curves apart, making it easier to effect the separation.

2. *The Impact of Reflux Ratio for Fixed Solvent Ratio*

The reflux ratio, R, for a column is the ratio of the liquid we reflux back to the column at the top stage relative to the distillate product flow; i.e., $R = L/D$, where L is the liquid flow in the top section of our column. Suppose we operate our column with a fixed solvent-to-distillate ratio; i.e., $R_s = S/D = \text{constant}$. If R_s and D are fixed, the location of the Δ point is fixed because

$$\Delta = D - S = D - R_S D = (1 - R_S)D$$

With Δ fixed, we can find its pinch point trajectories, as we show in Fig. 65. When $\hat{L}_n$ sits exactly on such a trajectory, the compositions for $\hat{V}_{n+1}$ and $\hat{V}_n$

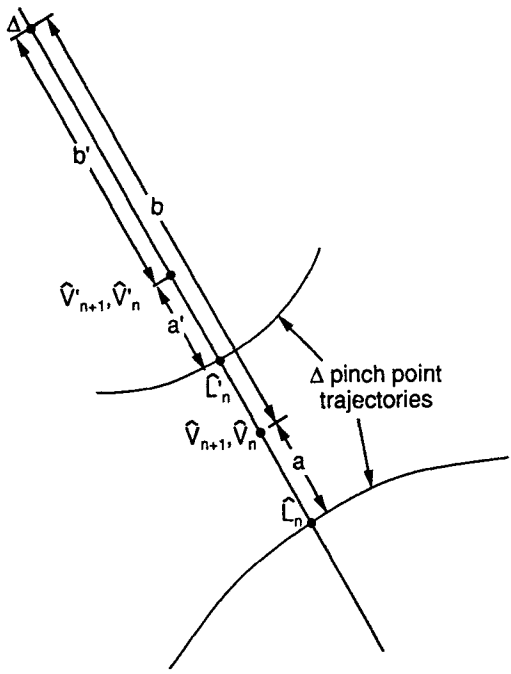

FIG. 65. Geometry to explain minimum and maximum reflux ratios for an extractive distillation column.

coincide because the line through the Δ point and the residue curve passing through $\hat{L}_n$ have the same slope at such a pinch point. The former points at $\hat{V}_{n+1}$, while the latter points at $\hat{V}_n$. We show the point $\hat{L}_n$ sitting on the lower curve and a second case in which $\hat{L}'_n$ sits precisely on the upper curve.

Let us first examine the point $\hat{L}_n$ sitting on the lower curve. We remember that a material balance for the section of the column between the feeds is

$$\hat{V}_{n+1} = \hat{L}_n + D - S = \hat{L}_n + \Delta$$

where we show the Δ point in Fig. 65 for the case in which Δ is positive ($R_S < 1$). Using the lever rule, we can write

$$\frac{b}{a} = \frac{\hat{L}}{\Delta} = \frac{L + q_S S}{D - S} = \frac{RD + q_S R_S D}{(1 - R_S)D} = \frac{R + q_S R_S}{(1 - R_S)}$$

where L is the liquid flow above the solvent feed and q_S characterizes the thermal condition of the solvent (typically the solvent will be subcooled with a q_S greater than unity). Thus the column reflux ratio is given by

$$R = \frac{b}{a}(1 - R_S) - q_S R_S$$

We can determine R for each pinch point by computing the distances a and b. $\hat{L}_n$ cannot actually sit on the pinch curve as shown because that requires a column with an infinite number of trays. We must place it between the two pinch curves at a point where b is smaller, which, by the above, requires R to decrease, assuming that the distance a does not change much with such a move. We argue, therefore, that the reflux ratio for a real column must be less than any R we see along this pinch point trajectory. This curve therefore defines a *maximum* allowed reflux ratio for operating the column.

From the geometry we see here, the maximum value of R along the pinch point trajectory is likely where the distance b is a maximum (but it may not be if a changes as we move along the trajectory).

The upper pinch curve produces the above equations, only this time in terms of the prime variables we show on Fig. 65. This time we must increase b, increasing R, to keep the liquid compositions inside the region between the two pinch curves. We must have R larger than the least value produced by all the points along this pinch curve.

We see that we have both an upper bound and a lower bound on the column reflux ratio. Does having an upper bound make intuitive sense? We have set the solvent flow proportional to the distillate product flow; i.e., $S = R_S D$. As we increase the reflux ratio R, the ratio of solvent feed flow, $R_S D$, to reflux flow, RD, decreases. This decreases the solvent concentration throughout the column, thus reducing its impact on the liquid activity coefficients that we are using to separate A from B. With an infinite reflux ratio, the solvent flow reduces to zero, and we have a normal column operating at total reflux which we know cannot separate A from B.

A similar set of arguments gives us the same results as above when the solvent rate exceeds the distillate rate, i.e., when the Δ point is to the lower right in Fig. 65. Again, the lower curve defines a maximum reflux ratio, and the upper a minimum.

There are other restrictions on the minimum value for the column reflux ratio. Both the bottom section (below the bottom feed) and top section above the solvent feed must be able to reach compositions that join with the trajectory traced by the middle section for a given reflux ratio. These must not restrict R to be outside the limits we just discovered, or else the column cannot operate.

3. The Impact of Solvent Ratio

In the previous section, we fixed the solvent ratio. Here we shall allow it to vary. We noted above that, as the solvent ratio increases, the Δ point moves away from the distillate composition toward infinity, jumps to negative infinity, and then moves toward the solvent composition, always along the line that

passes through these two compositions. As we decrease the solvent ratio, the two pinch curves shown in Fig. 64 move closer together until they just coincide. Decreasing the solvent ratio below this value precludes the existence of a path for the composition trajectory for the column section between the feeds. Thus the column cannot function. Increasing the solvent ratio moves the two pinch point curves away from each other, giving an even larger region for the composition trajectory to pass for the section between the feeds.

We argue that the two pinch trajectories coincide at an inflection point for one (or more) of the residue curves. See Fig. 66. The line marked 1 in this figure has the same slope as the residue curve at its inflection point. For this line, Δ would be quite close to the pure A node (implying a small amount of solvent). If we move Δ away from A, there are two points, one to each side of the inflection point, which would point at the same Δ point (see the two lines marked 2). Only at the inflection point is there a single pinch point for the corresponding Δ point.

To find the minimum solvent rate, we draw all lines passing through all inflection points for the residue curves and project them to the line on which the Δ point must exist, i.e., the line passing through the composition points for the distillate and the solvent. The Δ point must be no closer to the distillate composition point than the most distant such intersection point to keep the Δ

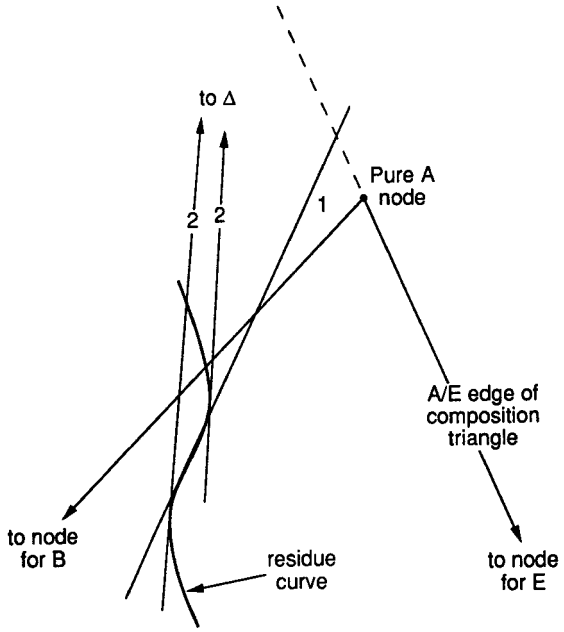

FIG. 66. Locating the Δ point that gives the minimum solvent flow.

pinch points for the corresponding residue curve from coinciding. This construction defines the minimum solvent ratio needed for the column.

X. Post-analysis Methods: Column Design Calculations

Column design represents the third major analysis activity in analysis-driven synthesis. However, our discussion here is short as column design is not the theme of this paper.

Once one has proposed alternative configurations for systems of separation devices to effect a desired separation, one must then design these devices so the various alternatives may be compared. For a distillation column, the first set of design decisions is to choose the number of trays, the feed tray location, and the reflux ratio at which to operate it. For a binary separation, the McCabe–Thiele diagram (or the concepts behind it) is an indispensable aid in making these decisions.

An approach to setting the reflux ratio often involves computing a minimum reflux ratio, a topic we have discussed several times in this article with respect to pinch points. Considerable work has been done on computing minimum reflux ratios for columns. Koehler (1991) reviews this work. As a rule of thumb, one sets the reflux ratio to be 20–100% or so above the minimum, a number that experience shows trades off the number of trays with column diameter in a near cost-optimal way.

With the reflux ratio fixed, one can step off the number of trays for a binary column using a McCabe–Thiele diagram or, if one wishes to account for heat effects, a Ponchon–Savarit diagram (Treybal, 1968), establishing the number of trays needed and where to feed the column.

For more than two species and a reflux ratio set to 1.2 times the minimum, a rule of thumb is to compute the total number of trays required for a total reflux column to produce the separation desired and then double this number as a first guess (Douglas, 1988). The next decision is select the tray on which to feed the column. For multispecies columns, the placement is not obvious. Typically, one must search by placing it on any one of a range of trays using a tray-by-tray simulation, thereby discovering which tray location requires the least reflux to effect the desired separation.

Using collocation models, which we mentioned earlier (Huss and Westerberg, 1994), one can formulate the design problem as a continuous-variable optimization problem with present worth as the objective function. The optimization problem will select the number of trays needed in both the top and bottom sections along with the reflux ratio—all of which are continuous variables in such a model.

Acknowledgments

The National Science Foundation, through its grant to the Engineering Design Research Center, and Eastman Chemical Co., through its support of the Computer Aided Process Design Consortium at Carnegie Mellon University, provided support for this work.

References

Andrecovich, M. J., and Westerberg, A. W. "A Simple Synthesis Method Based on Utility Bounding for Heat Integrated Distillation Sequences," *AIChE J.* **31,** p. 363 (1985).

Barnicki, S. D. and Fair, J. R. "Separation System Synthesis: A Knowledge-Based Approach. 1. Liquid Mixture Separations," *Ind. Eng. Chem. Res.* **29,** 421–432 (1990).

Bekiaris, N., Meski, G. A., Radu, C. M., and Morari, M. "Multiple Steady States in Homogeneous Azeotropic Distillation Columns," *Ind. Eng. Chem. Res.* **29,** 421–432 (1993).

Benedict, M., and Rubin, L. C. "Extractive and Azeotropic Distillation. 1. Theoretical Aspects." *Trans. Am. Inst. Chem. Eng.,* **41,** 353–370 (1945).

Berg, L. "Selecting the Agent for Distillation," *Chem. Eng. Prog.* **65,** (9), 52–57 (1969).

Berg, L., and Yeh, A. 1985. "The Unusual Behavior of Extractive Distillation—Reversing the Volatility of the Acetone—Isopropyl Ether System," *AIChE J.* **31,** (3), 504–506 (1985).

Bossen, B. S., Jorgensen, S. B., and Gani, R. "Simulation, Design, and Analysis of Azeotropic Distillation Operations," *Ind. Eng. Chem. Res.,* **32,** 620–633 (1993).

Cho, Y. S., and Joseph, B. "Reduced-Order Steady-State and Dynamic Models for Separation Processes," *AIChE J,* **29,** 261–269, 270–276 (1983).

Doherty, M. F. "The Presynthesis Problem for Homogeneous Azeotropic Distillations has a Unique Explicit Solution," *Chem. Eng. Sci.* **40,** 1885–1889 (1985).

Doherty, M. F., and Caldarola, G. A. "Design and Synthesis of Homogeneous Azeotropic Distillations. 3. The Sequencing of Columns for Azeotropic and Extractive Distillations," *Ind. Eng. Chem. Fundam.* **24,** 474–485 (1985).

Doherty, M. F., and Perkins, J. D. "On the Dynamics of Distillation Processes. I. The Simple Distillation of Multicomponent Non-Reacting Homogeneous Liquid Mixtures," *Chem. Eng. Sci.* **33,** 281–301 (1978).

Doherty, M. F., and Perkins, J.D. "On the Dynamics of Distillation Processes. III. The Topological Structure of Ternary Residue Curve Maps," *Chem. Eng. Sci.* **34,** 1401–1414 (1979).

Douglas, J. M. "Conceptual Design of Chemical Processes." McGraw-Hill, New York, 1988.

Ewell, R. H., and Welch, L. M. "Rectification in Ternary Systems Containing Binary Azeotropes," *Ind. Eng. Chem.* **37,** 1224–1231 (1945).

Fidkowski, Z. T., Malone, M. F., and Doherty, M. F. "Computing Azeotropes in Multicomponent Mixtures," *Comput. Chem. Eng.* **17**(12), 1141–1155 (1993).

Fien, G. A. F., and Liu, Y. A. "Heuristic Synthesis and Shortcut Design of Separation Processes Using Residue Curve Maps: A Review," *Ind. Eng. Chem. Res.* **33,** 2505–2522 (1994).

Foucher, E. R., Doherty, M. F., and Malone, M. F. "Automatic Screening of Entrainers for Homogeneous Azeotropic Distillation," *Ind. Eng. Chem. Res.* **30,** 760–772 (1991).

Hendry, J. E., Rudd, D. F., and Seader, J. D. "Synthesis in the Design of Chemical Processes," *AIChE J.* **19**(1), 1–15 (1973).

Henley, E. J., and Seader, J. D. "Equilibrium-State Separation Operations in Chemical Engineering," Wiley, New York, 1981.

Hlavacek, V. "Synthesis in the Design of Chemical Processes," *Comput. Chem. Eng.* **2,** 67–75 (1978).

Hoffman E. J. "Azeotropic and Extractive Distillation." Wiley (Interscience), New York, 1964.

Holland, C. D. "Fundamentals of Multicomponent Distillation." McGraw-Hill, New York, 1981.

Horsley, L. H. "Azeotropic Data III," Adv. Chem. Ser. No. 116. American Chemical Society, Washington, DC, 1973.

Hunek, J., Gal, S., Posel, F., and Gavic, P. "Separation of an Azeotropic Mixture by Reverse Extractive Distillation," *AIChE J.* **35**(7), 1207–1210 (1989).

Huss, R. S., and Westerberg, A. W. "Collocation Methods for Distillation Design," Paper 131c, Annual AIChE Meeting, San Francisco (1994).

Julka, V., and Doherty, M. F. "Geometric Behavior and Minimum Flows for Nonideal Multicomponent Distillation," *Chem. Eng. Sci.* **45,** 1801–1822 (1990).

King, C. J. "Separation Processes," 2nd ed. McGraw-Hill, New York, 1980.

Knight, J. R., and Doherty, M. F. "Optimal Design and Synthesis of Homogeneous Azeotropic Distillation Sequences," *Ind. Eng. Chem. Res.* **28,** 564–572 (1989).

Koehler, J. W., "Struktursynthese und minimaler Energiebedarf Nichtidealer Bektifikationen," Ph.D. Dissertation, Technical University of Munich (1991).

Laroche, L., Andersen, H. W., and Morari, M. "Homogeneous Azeotropic Distillation: Comparing Entrainers," *Can. J. Chem. Eng.* **69,** 1302–1319 (1991).

Levy, S. G., Van Dongen, D. B., and Doherty, M. F. "Design and Synthesis of Homogeneous Azeotropic Distillations. 2. Minimum Reflux Calculations for Nonideal and Azeotropic Columns," *Ind. Eng. Chem. Fundam.* **24,** 463–473 (1985).

Matsuyama, H. "Synthesis of Azeotropic Distillation Systems," Paper presented at the Japan-U.S. Joint Seminar, Kyoto, Japan (1975).

McCabe, W. L., and Smith, J. C. "Unit Operations of Chemical Engineering," 3rd ed. McGraw-Hill, New York, 1976.

McDonald, C.M., and Floudas, C. A. "Global Solutions for the Phase and Chemical Equilibrium Problem," Paper 220c, AIChE Annual Meeting, San Francisco (1994).

Michelsen, M. L. "The Isothermal Flash Problem. Part I: Stability," *Fluid Phase Equilib.* **9,** 1–19 (1982).

Michelsen, M. L. "Phase Equilibrium Calculations. What is Easy and What is Difficult," *Comput. Chem. Eng.* **17**(5/6), 431–439 (1993).

Michelsen, M. L. "Calculation of Multiphase Equilibrium," *Comput. Chem. Eng.* **18**(7), 545–550 (1994).

Modi, A. K. and Westerberg, A. W. "Distillation Column Sequencing Using Marginal Price," *Ind. Eng. Chem. Res.* **31,** 839–848 (1992).

Nikolaev, N. S., Kiva, V. N., Mozzhukhin, A. S., Serafimov, L. A., and Goloborodkin, S. I. "Utilization of Functional Operators for Determining the Regions of Continuous Rectification," *Theor. Found. Chem. Eng. (Engl. Transl.)* **13,** 418–423 (1979).

Nishida, N., Stephanopoulos, G., and Westerberg, A. W. "A Review of Process Synthesis," *AIChE J.* **27,** 321 (1981).

Perry, J. H. "Chemical Engineers' Handbook," 3rd ed. McGraw-Hill, New York, 1950.

Petlyuk, F. B. "Rectification of Zeotropic, Azeotropic, and Continuous Mixtures in Simple and Complex Infinite Columns with Finite Reflux," *Theor. Found. Chem. Eng. (Engl. Transl.)* **12,** 671–678 (1978).

Petlyuk, F. B., Serafimov, L. A., Avet'yan, V. S., and Vinogradova, E. I. "Trajectories of Reversible Rectification when One of the Components Completely Disappears in Each Section," *Theor. Found. Chem. Eng. (Engl. Transl.)* **15,** 185–192 (1981).

Pham, H. N., and Doherty, M. F. "Design and Synthesis of Heterogeneous Azeotropic Distillations. III. Column Sequences," *Chem. Eng. Sci.* **45,** 1844–1854 (1990).

Pham, H. N., Ryan, P. J., and Doherty, M. F. "Design and Minimum Reflux for Heterogeneous Azeotropic Distillation Columns," *AIChE J.* **35,**(10), 1585–1591 (1989).

Poellmann, P., and Blass, E. "Best Products of Homogeneous Azeotropic Distillations," *Gas Separ. Purif.* **8**(4), 194–228 (1994).

Rathore, R. N. S., VanWormer, K. A., and Powers, G. J. "Synthesis Strategies for Multicomponent Separation Systems with Energy Integration," *AIChE J.* **20,**491 (1974).

Reid, R. C., Prausnitz, J. M., and Poling, B. E. "The Properties of Gases and Liquids," 4th ed. McGraw-Hill, New York, 1987.

Ryan, P. J., and Doherty, M. F. "Design/Optimization of Ternary Heterogeneous Azeotropic Distillation Sequences," *AIChE J.* **35,**(10), 1592–1601 (1989).

Sargent, R. W. S. H. "A Functional Approach to Process Synthesis and its Application to Distillation Systems," Tech. Rep. Centre for Process Systems Engineering, Imperial College, London, 1994.

Sargent, R. W. S. H., and Gaminibandara, K. "Optimum Design of Plate Distillation Columns," *in* "Optimization in Action" (L. W. C. Dixon, ed.), 267–314. Academic Press, London, 1976.

Seferlis, P., and Hrymak, A. N. Optimization of Distillation Units Using Collocation Models, *AIChE J.*, **40,** 813–825 (1994).

Serafimov, L. A. "Thermodynamic Topological Analysis and the Separation of Multicomponent Polyazeotropic Mixtures," *Theor. Found. Chem. Eng. (Engl. Transl.)* **21,** 44–54 (1987) (translated from *Teor. Osn. Khim. Tekhnol.* **21**(1), 74–85, (1987)).

Smith, J. M., and Van Ness, H. C. "Introduction to Chemical Engineering Thermodynamics," 4th ed. McGraw-Hill, New York, 1987.

Stewart, W. E., Levien, K. L., and Morari, M. "Collocation Methods in Distillation," *in* "Foundations Computer-Aided Process Design (FOCAPD'83)" (A. W. Westerberg and H. H. Chien, eds.), pp. 539–569. Cache Corp., Ann Arbor, MI, 1984.

Stichlmair, J., Fair, J. R., and Bravo, J. L. "Separation of Azeotropic Mixtures via Enhanced Distillation," *Chem. Eng. Prog.* **85,**(1), 63–69 (1989).

Tanaka, S., and Yamada, J. "Graphical Solution of Operating Region in Extractive Distillation," *Kagaku Kogaku* (Abr. E. *Engl.*) **3,**(1), 40–43, (1965).

Terranova, B. E., and Westerberg, A. W. "Temperature-Heat Diagrams for Complex Columns. 1. Intercooled/Interheated Distillation Columns," *Ind. Eng. Chem. Res.* **28,** 1374–1379 (1989).

Thompson, R. W., and King, C. J. "Systematic Synthesis of Separation Schemes," *AIChE J.* **18,** 941–948 (1972).

Treybal, R.E. Mass-Transfer Operations, 2nd ed. p. 297. McGraw-Hill, New York, 1968.

Underwood, A. J. V. "Fractional Distillation of Multicomponent Mixtures—Calculation of Minimum Reflux Ratio," *J. Inst. Petrol.* **32,** 614 (1946).

Van Dongen, D. B. "Distillation of Azeotropic Mixtures. The Application of Simple-Distillation Theory to the Design of Continuous Processes," Ph.D. Dissertation, University of Massachusetts, Amherst (1983).

Van Dongen, D. B., and Doherty, M. F. "Design and Synthesis of Homogeneous Azeotropic Distillations. 1. Problem Formulation for a Single Column," *Ind. Eng. Chem. Fundam.* **24,** 454–463 (1985).

Wahnschafft, O. M. "Synthesis of Separation Systems for Azeotropic Mixtures with an Emphasis on Distillation-Based Methods," Ph.D. Dissertation, University of Munich, Munich, Germany (1992).

Wahnschafft, O. M. "A Simple and Robust Continuation Method for Determining All Azeotropes Predicted by a Multicomponent Vapor-Liquid Equilibrium Model," in preparation (1994).

Wahnschafft, O. M., and Westerberg, A. W. "The Product Composition Regions Azeotropic Distillation Columns. 2. Separability in Two-Feed Columns and Entrainer Selection." *Ind. Eng. Chem. Res.* **32,** 1108–1120 (1993).

Wahnschafft, O. M., Koehler, J., Blass, E., and Westerberg, A. W. "The Product Composition Regions of Single Feed Azeotropic Distillation Columns," *Ind. Eng. Chem. Res.* **21,** 2345–2362 (1992).

Wasylkiewicz, S., Sridher, L., Malone, M. F., and Doherty, M. F. "Gibbs Tangent Plane Anaylsis for Complex Liquid Mixtures: A Global Algorithm," Paper 151a, Annual Meeting AIChE, St. Louis, MO (1993).

Westerberg, A. W. "A Review of Process Synthesis, in Computer Applications to Chemical Engineering Process Design and Simulation," *ACS Symp. Ser.* **124,** 54–87 (1980).

Westerberg, A. W. "The Synthesis of Distillation-Based Separation Systems," *Comput. Chem. Eng.* **9,**(5), 421–429 (1985).

Zharov, W. T., and Serafimov, L. A. "Physicochemical Fundamentals of Distillations and Rectifications (in Russian)." Khimiya, Leningrad, 1975.